EFFECTS OF HIGH HYDROSTATIC PRESSURE AND IMMOBILIZATION ON GLUCOSE OXIDASE AND ALCOHOL OXIDASE FOR BIOSENSOR FABRICATION

by

DAOYUAN YANG

(Under the Direction of José I. Reyes-De-Corcuera)

ABSTRACT

Enzymes have been widely used in the food industries as biocatalysts and enzyme biosensors. However, many industrial applications of enzymes are hindered by their low stability or activity. Immobilization is a common method to stabilize enzymes. High hydrostatic pressure (HHP), normally used to kill microorganisms and inactivate enzymes in food processing, is reported to be able to stabilize and activate enzymes as well. Previously, our laboratory reported the stabilizing effect of HHP on the stability of glucose oxidase (GOx) and alcohol oxidase (AOx). We also reported the activating effect of HHP on GOx. In this study, the effect of HHP combined with immobilization in electrochemically generated poly-*o*-phenylenediamine (PoPD) nano-films on the stability of GOx or AOx biosensors is reported. The effect of HHP on the activity of AOx is also reported. Immobilized GOx inactivated at 70 °C and 180 MPa was 87.6 times more stable than GOx in solution inactivated at 70 °C and atmospheric pressure. Alcohol oxidase from *P. pastoris* has two enzyme fractions, the labile (L) fraction and the resistant (R) fraction. The R fraction is of more interest because it is ~150 times more stable than the L fraction. The reaction rate of the R fraction AOx at 50 °C was 17.9 ± 3.6 or 17.7 ± 0.8 μM min^{-1} at 80 or 160 MPa, respectively. It was approximately 6 times relative to the reaction rate of 3.2 ± 0.2 μM min^{-1} at 25

°C and atmospheric pressure. The increase in the activity of the R fraction AOx attributed to the stabilizing effect of HHP. The effect of HHP on the stability of the AOx biosensors in terms of the stability of AOx could not be determined. The pseudo-first-order rate constant of response loss of the immobilized AOx was higher than the pseudo-first-order rate constant of inactivation of the R fraction AOx in solution, suggesting the decrease in the effective amperometric response was caused by enzyme leaching out of the immobilization matrix. Indeed, the thickness of PoPD is similar to the diameter of AOx. Therefore, electrochemically generated PoPD is not an adequate immobilization material for AOx.

INDEX WORDS: High hydrostatic pressure, glucose oxidase, alcohol oxidase, enzyme biosensor, electropolymerization, enzyme stabilization

EFFECTS OF HIGH HYDROSTATIC PRESSURE AND IMMOBILIZATION ON GLUCOSE OXIDASE AND ALCOHOL OXIDASE FOR BIOSENSOR FABRICATION

by

DAOYUAN YANG

B.E., Ocean University of China, China, 2013

M.S., University of Georgia, 2015

A Dissertation Submitted to the Graduate Faculty of The University of Georgia in Partial Fulfillment of the Requirements for the Degree

DOCTOR OF PHILOSOPHY

ATHENS, GEORGIA

2020

EFFECTS OF HIGH HYDROSTATIC PRESSURE AND IMMOBILIZATION ON GLUCOSE OXIDASE AND ALCOHOL OXIDASE FOR BIOSENSOR FABRICATION

by

DAOYUAN YANG

Major Professor:	José I. Reyes-De-Corcuera
Committee:	Fanbin Kong
	Derek R. Dee
	Ramaraja Ramasamy

Electronic Version Approved:

Ron Walcott
Interim Dean of the Graduate School
The University of Georgia
May 2020

DEDICATION

For my beloved parents Ming Yang and Yinqiu Lu, and my wife Zirui Huang.

ACKNOWLEDGEMENTS

I would like to thank my major advisor, Dr. José I. Reyes-De-Corcuera, for his guidance and support along my way to pursue the degree and finish the dissertation. It has been a good time to work with him since 2013. The many trainings and opportunities provided by him not only improved my research techniques but also my personalities and skills in many fields. I also acknowledge and appreciate the assistance and funding from Dr. Reyes, the department of food science and technology, and the USDA-NIFA-AFRI grant. I am also grateful for my committee members, Dr. Fanbin Kong, Dr. Derek Dee, and Dr. Ramaraja Ramasamy, for their guidance, support, and contributions. I would also like to thank my friends for their help and encouragement. At last, I want to thank my parents, Yinqiu Lu and Ming Yang, my wife, Zirui Huang, and my parents-in-law, Yongzheng Huang and Juan Li. It was their love and support that made it possible for me to get this far.

TABLE OF CONTENTS

Page

LIST OF TABLES

Page

LIST OF FIGURES

Page

CHAPTER 1

INTRODUCTION AND LITERATURE REVIEW

1.1. Introduction

Enzymes are proteins with catalytic activity, that is, they can accelerate the rate of reaction by lowering the activation energy of biochemical reactions. Some RNA molecules have similar catalytic activities named as ribozymes (Doherty and Doudna 2001). Enzymes are produced by all the living organisms. One living organism may generate only one enzyme for a specific reaction, or two or more different enzymes for the same reaction where the enzymes are named as isozymes (Pariza and Foster 1983). The enzyme activity is affected by many environmental factors and is the highest at optimal pH and temperature. An Enzyme Commission (EC) was created by the International Union of Biochemistry and Molecular Biology and the International Union for Pure and Applied Chemistry to systematically name the enzymes. The EC classified enzymes into six classes based on the type of reactions, including oxidoreductase, transferase, hydrolase, lyases, isomerase, and ligase (Singh et al. 2016).

Enzymes have been widely used in multiple industries, including food (Chandrasekaran et al. 2015), pharmaceutical (Rasor and Voss 2001), fine chemicals (Yadav et al. 2007), and pulp and paper (Bajpai 1999). The advantages of using enzymes instead of chemical catalysts include high yield, reduced or eliminated toxic by-products, low costs, and better process control (Raveendran et al. 2018). The two most important industrial applications of enzymes are as biocatalysts and enzyme biosensors. In the food industry, enzymes can be applied in a various of fields, including dairy and cheese manufacturing (Fox and Stepaniak 1993), bakery (Miguel et al. 2013), juice

processing (Ribeiro et al. 2010), brewing (Bamforth 2009), starch processing (Nigam and Singh 1995), and flavor (Christen and López-Munguía 1994). Enzymes used in the food industry are manufactured from plants, animals, or nonpathogenic and nontoxigenic microorganisms (Pariza and Foster 1983). Among those, microbial enzymes are more widely used than the other two because of their stability, activity, and ease of production (Singh et al. 2016). In the food industry, the use of enzymes can be classified as manufacturing aids or food additives. Most of the enzymes are manufacturing aids used during the processing and do not have a function in the final food products (Chandrasekaran et al. 2015). For example, β-galactosidase is used to hydrolyze lactose in milk and milk by-products for lactose intolerance consumers (Xavier et al. 2018). Pectinases have been commercially used since 1930s and play a key role in the juice industry by degrading the pectin to increase the extraction yield, to clarify the juice after maceration, and to stabilize the color during storage (Ribeiro et al. 2010). Few enzymes are added directly to the food products as food additives, i.e., adding papain or bromelain to aid in digestion (Chandrasekaran et al. 2015).

However, the poor stability and lack of specificity of some enzymes hamper their industrial applications either as biocatalyst (Choi et al. 2015) or as enzyme biosensors (Reyes-De-Corcuera JI et al. 2018). Compared to the other catalysts, enzymes degrade at high temperatures, at surfaces, or in the presence of denaturants, and can be chemically modified or hydrolyzed in certain conditions (Brady 2013). The most commonly used method to stabilize and recover enzymes for reuse is immobilization (Sheldon and van Pelt 2013). A less known approach to stabilize enzymes is the application of high hydrostatic pressure (HHP), which has been normally used to kill microbes and inactivate enzymes in food processing. However, at moderate levels, HHP stabilizes and activates some enzymes (Eisenmenger and Reyes-De-Corcuera 2009b). In this chapter, the applications of enzymes as biocatalysts and enzyme biosensors, and the methods of immobilization

and HHP to stabilize and/or activate enzymes are reviewed. Particular emphases are placed on glucose oxidase (GOx) and alcohol oxidase (AOx), and on the biosensors made with these enzymes, which are the focus of this research.

1.2. The application of enzymes as biocatalysts in the food industry

1.2.1. Overview of commercial enzymes as biocatalysts

In recent years, the number of applications of enzyme biocatalysts in various industries has increased dramatically, owing to the advantages of enzyme biocatalyst and the development of protein engineering. The global industrial enzyme market was estimated to be USD 6.30 billion by 2022 (Binod et al. 2017), and the food enzyme market was proposed to reach USD 2.94 billion by 2021 (Sutay Kocabaş and Grumet 2019). The commercial food enzymes were reported to be the second-largest segment of the market about two decades ago, which accounted for approximately 25 % of the market (Cherry and Fidantsef 2003). However, the food and feed enzymes were recently reported to account for 55 – 60 % of the global enzyme market, with an annual increase of 6 – 8 % (Guerrand 2018). The increasing applications of enzymes in the food industry is one of the main factors driving the growth of the enzyme market (Sutay Kocabaş and Grumet 2019). The eco-friendly features of enzymes are in accordance with the needs for alternative sources of raw materials from the industries and the demand for green technologies from the public (Choi et al. 2015). The applications of enzymes in the food industry have been well-reviewed (Raveendran et al. 2018). Detailed summaries of the applications of each enzyme in different food and beverage industries can be found from Li S et al. (2012) and Chandrasekaran et al. (2015). Many of the enzymes are used to aid in processing. For example, glucose isomerase is used to process corn syrup to convert glucose into fructose while making high-fructose corn syrup. α-amylase is widely used in baking, brewing, starch processing, and juice clarification

(Raveendran et al. 2018). Enzyme biocatalysts can also find applications in the active food packaging. Enzymes have been immobilized in biopolymers or nanostructured materials (Fernández et al. 2008). Lysozyme is known for its antimicrobial property against Gram-positive bacteria (Barbiroli et al. 2016; Benelhadj et al. 2016). Glucose oxidase with catalase is commonly used in food packaging as an oxygen scavenger where glucose is present (Dey and Neogi 2019).

1.2.2. Factors that hamper the applications of enzymes as biocatalysts

The limitations of enzymes include high cost, low activity, poor stability, narrow scope of substrates, and narrow range of working pH (Schoemaker et al. 2003; Fernandes 2010). Protein engineering, in particular recombinant DNA and screening techniques, have been used to overcome the shortcomings of enzymes (Dalby 2011; Patel AK et al. 2016). The development of protein engineering made it possible to produce enzymes with high activity and stability in a large scale and at an acceptable price (Illanes et al. 2012). Direct evolution and rational design are the two most commonly used methods in protein engineering. Direct evolution is to modify genes through random mutagenesis and mimic the natural evolutionary processes in the laboratory to acquire the expected properties of enzymes just in weeks or months (Dalby 2011). Rational design is to engineer enzymes through site-directed mutagenesis based on the understanding of the enzyme structures, and it is often combined with computational modeling and simulation (Illanes et al. 2012). An example is the improvement of the secretion and enzyme activity of *Rhizopus oryzae* lipase through rational design of the N-glycosylation site which could enable its application to the edible oil and fat industries (Yu X-W et al. 2017). During the last two decades, the development of protein engineering techniques improved the properties of enzymes, and the use of immobilization enables enzymes to work under harsh industrial environments, which made many enzymes commercially available as biocatalysts (Sheldon and Brady 2018). Examples of

using protein engineering or immobilization to improve thermostability, activity, pH-activity, or substrate specificity of some enzymes applied in the food or feed industries were listed by Fernandes (2010) and Patel AK et al. (2016). Enzymes genetically modified intend for better characteristics such as purity, yield, specificity, catalytic activity, stability, and cost-effective properties for food processing were reviewed by Zhang et al. (2019), including carbohydrases/glycosidases, proteases/peptidases, and lipases. Nevertheless, many enzymes with the potential to be applied in the food industry remain hindered by limitations mentioned above. One of the most important limitations is often their low stability (Illanes et al. 2012).

1.2.3. Enzymes have potential industrial applications to foods but with low stability

Some examples of the efforts to stabilize enzymes with potential applications to the food industry reported over the last decade are summarized in this section. β-glucosidases enhance aromas in wines (Baffi et al. 2013), tea beverages (Su et al. 2010), and other food or beverage products by hydrolyzing the glucoside precursors such as β-D-glucosides and β-D-glucopyranosides to release aromatic compounds. The low stability and high cost of β-glucosidases are the main factors hindering the commercial application in the industries (Agrawal R et al. 2016). β-amylases catalyze the release of maltose from polyglucans, where maltose is used in bakery, winemaking, brewing, and in the production of maltose syrup which is used for confectionary (Pyeshkova et al. 2009; Srivastava and Kayastha 2014). The lack of reusability, low thermostability, and operational instability constrain the industrial application of β-amylases (Das R et al. 2017; Agrawal DC et al. 2020). Xylanase degrades xylan and can be used in improving sensory properties in bakery, juice clarification, and optimizing the process of ethanol (dos Santos et al. 2018). Insufficient stability limits the enzyme in the use of many processes (Kumar et al. 2017). L-asparaginases catalyze the reaction of L-asparagine to L-aspartate and ammonia, where

L-asparagine is one of the precursors of acrylamide. Acrylamide formed in fried, roasted, or baked foods is a potential carcinogen to humans (Monajati et al. 2018). In order to reduce the acrylamide formation in the food industry, L-asparaginases need to be functional in a wide range of processing temperatures and a higher thermostability is needed to broaden the application (Zuo et al. 2015; Li X et al. 2018). β-glucanases catalyze the hydrolysis of β-glucans and have the potential to be used in the brewing industry to help degrade β-glucans during the barley malting process to prevent any increase in the viscosity and turbidity of brewer mash (Celestino et al. 2006). However, many β-glucanases have low stability against thermal treatments (You et al. 2016). The enzymes mentioned above and the examples of the strategies used to improve their stabilities such as immobilization and protein engineering are summarized in Table 1.1.

In our laboratory, we are interested in a series of oxidases, including glucose oxidase (GOx), alcohol oxidase (AOx), xanthine oxidase (XOx), pyruvate oxidase (POx), and galactose oxidase (GaOx). The enzymes are dimer, octamer, dimer, tetramer, and monomer, respectively. Glucose oxidase (EC 1.1.2.3.4) catalyzes the oxidation of β-D-glucose by oxygen to D-glucono-1,5-lactone and hydrogen peroxide, and has been used in foods and beverages to remove glucose and oxygen (Bankar et al. 2009). Glucose oxidase will be further discussed in section 1.5.1. Alcohol oxidase (EC 1.1.3.13) catalyzes the oxidation of alcohols into the corresponding carbonyl groups, which produce flavor and fragrance compounds (Kakoti et al. 2012; Goswami et al. 2013). Unlike GOx and AOx, GaOx, XOx, and POx do not have applications in the food industry as biocatalysts. Galactose oxidase (EC 1.1.3.9) catalyzes the oxidation of primary or secondary alcohols into the corresponding aldehydes or ketones, respectively, and it is mainly applied to modify polysaccharides or to synthesize aldehydes or ketones (Toftgaard Pedersen et al. 2015). Xanthine oxidase (EC 1.17.3.2) catalyzes the oxidation of xanthine into uric acid, and the enzyme

is involved in the metabolism of xenobiotics and drugs (Rashidi et al. 2009). Pyruvate oxidase (EC 1.2.3.3) catalyzes the oxidation of pyruvate to acetate and carbon dioxide (Abdel-Hamid et al. 2001). Nevertheless, all these oxidases can be employed for enzyme biosensors used in the food industry. However, except for glucose oxidase, the other oxidases have not been industrially used, mainly due to the high cost and low stability. The unit price of each oxidase retrieved from Sigma-Aldrich website can be found in Table 1.2.

1.3. The application of enzymes to the fabrication of electrochemical enzyme biosensors

1.3.1. Introduction to biosensors

A biosensor is a device made of a biological element in intimate contact with a transducer, which in turn connected to an electronic indicator. As an analytical device, the biosensor converts the biological response from the interaction of the analyte of interest and the biological component that is immobilized on the transducer into a signal (electrical, optical, or thermal) that can be quantitively measured by the transducer (Nguyen HH et al. 2019). Biosensors can be classified by the biological elements, including enzymes, microorganisms, and bio-affinity groups such as antibodies and nucleic acids, or the methods of transduction such as the electrochemical, optical, and mass-based (Mehrotra 2016).

The demand for highly efficient analytical methods to assess the composition of samples is driven by the needs of industrial processing and the legislation of governments agencies such as Food and Drug Administration and Environmental Protection Agency (Monteiro and Almeida 2019). The analytes are typically determined using the methods such as chromatographic or electrophoretic separations followed by spectrophotometric or electrochemical detections (Barthelmebs et al. 2010). However, these methods often have long sample analysis time and high complexity which require external laboratory to perform and cannot be applied to the non-

laboratory settings (Reyes-De-Corcuera JI and Cavalieri 2003). Biosensors overcome these shortcomings and have advantages of low cost, high selectivity, high specificity, and the ability to be made into simple, portable, and automated equipment suitable for laboratory or field applications (Barthelmebs et al. 2010).

Enzyme biosensors using enzymes as the biological element are among the most extensively studied biosensors because of the advantages of using enzymes such as high specificity and high reaction rate (Nguyen HH et al. 2019). Enzyme biosensors have existing and potential applications in the medical diagnostic, plant biology, food industry, and marine applications (Mehrotra 2016). The most successfully commercialized enzyme biosensors are GOx biosensors used to detect glucose for patients with diabetes (Bahadır and Sezgintürk 2015). Enzymes commonly used for enzyme biosensors are oxidoreductases, polyphenol oxidases, peroxidases, and aminooxidases (Mehrotra 2016). The most commonly used enzymes in enzyme biosensors for detecting substrates are oxidoreductases, such as oxidases, peroxidases, or dehydrogenases, where the signals recognized by the transducer are from the reactions of oxygen to hydrogen peroxide, hydrogen peroxide to water, or the reduced form to oxidized form of nicotinamide adenine dinucleotide (FAD), respectively (Rotariu et al. 2016). Electrochemical enzyme biosensors transform the signals generated from the redox reactions on the electrode to current, potential, or impedance. Electrochemical biosensors have advantages of making simple, rapid, low cost, and highly sensitive devices (Nguyen HH et al. 2019). Based on the output signals, electrochemical biosensors can be classified as amperometric, potentiometric, conductometric, or impedimetric biosensors (Ronkainen et al. 2010). Among those, the amperometric biosensors are the most commonly used, in which a constant potential is maintained and the current generated from the redox reaction is monitored (Ronkainen et al. 2010). The concentration of the substrate of the

reaction can then be determined because it is proportional to the current monitored (Ronkainen et al. 2010). Historically, amperometric biosensors have been grouped into three generations. The first-generation biosensors are the simplest by measuring the electroactive compounds such as H_2O_2 generated from the redox reactions of oxidoreductases; the second-generation biosensors monitor the current changes through synthetic or natural redox mediators; and the third-generation biosensors rely on the direct electron transfers between the enzymes and electrodes (Monteiro and Almeida 2019).

1.3.2. Commercial biosensors

Biosensors were first introduced in the 1960s, and the first commercial biosensor was a glucose biosensor by Yellow Springs Instruments in 1973. The global market of biosensors is expected to reach USD 31.5 billion by 2024, with the compound annual growth rate of 8.3 % (Marketsandmarkets 2019). The global market of electrochemical biosensors is estimated to be USD 30.9 billion by 2025, with the compound annual growth rate of 10.5 % (Marketresearchfuture 2019). Among the commercial biosensors, the majority of the market is for glucose determination, which is expected to reach over USD 17.7 billion by 2025 (Researchandmarkets 2020). Biosensors for blood glucose testing mainly for diabetes patients accounted for 85 % of the total biosensor market in 2012 (Vashist 2012). In the food industry, only a few biosensors are commercially available and are primarily used to determine glucose and lactic acid (Barthelmebs et al. 2010). The commercial biosensors applied in the food and other industries have been extensively reviewed (Bahadır and Sezgintürk 2015).

1.3.3. Recent research on enzyme biosensors for food

In the food industry, biosensors can be used to detect food components, pathogens, and food contaminants (Narsaiah et al. 2012; Reyes-De-Corcuera J 2015). The biosensors developed

to detect different components in various foods or beverages, such as glucose, fructose, sucrose, lactose, lactic, ethanol, and amino acids, were reviewed by Monosik et al. (2012). Electrochemical biosensors for the detection of *Salmonella* for food safety assessment were reviewed by Silva et al. (2018). The electrochemical biosensors to detect food contaminants for food quality control were reviewed by Rotariu et al. (2016). Potentially, some biosensors can also be integrated into food packaging (Vanderroost et al. 2014).

Among the oxidoreductases, oxidases have been extensively used for enzyme biosensors (Rotariu et al. 2016). As mentioned in section 1.2.3, the oxidases of interest in our laboratory have various applications in the food industries as enzyme biosensors. Glucose oxidase is the most widely used oxidase enzyme for glucose determination, because of its high activity and stability (Barthelmebs et al. 2010). Glucose oxidase biosensors will be discussed in section 1.5.1. Alcohol oxidase biosensors are extensively applied to determine ethanol or methanol in food products during fermentation, or in beer, wine, and liquor (Barthelmebs et al. 2010; Cinti et al. 2017). A dual-enzyme biosensor consisting of carboxyl esterase and AOx can be used for the determination of aspartame in soft drinks and sweeteners (Odacı et al. 2004). Alcohol oxidase and GOx can also be used together to develop a biosensor that can be used to determine ethanol and glucose simultaneously. The biosensor can be made by either immobilizing the two enzymes onto the same electrode (Asav and Akyilmaz 2010) or onto two separate electrodes (Mentana et al. 2013). Galactose oxidase biosensors have applications in determining the lactose which is an important component in the dairy products. Low lactose concentration in milk can be an indicator of cows suffering from mastitis (Conzuelo et al. 2010). The biosensor is typically a bienzyme biosensor consisting the GaOx and the β-galactosidase. Lactose is first hydrolyzed by β-galactosidase into galactose and glucose, and the galactose is further oxidized to galacto-hexodialdose (Monosik et

al. 2012; Gursoy et al. 2018). Xanthine oxidase biosensors can be used to evaluate the freshness of fish meat by determining the concentration of hypoxanthine, which is the product of the decomposition of fish and can be oxidized into uric acid by XOx (Nakatani et al. 2005). An xanthine oxidase biosensor was also developed for determining the antioxidant capacity in the Amazonian fruits (graviola, bacuri, and murici), based on the principle that the antioxidants such as gallic acid decreased the concentration H_2O_2 produced by the oxidation of hypoxanthine and thereby decreasing the electrochemical signal (Becker et al. 2019). Pyruvate oxidase biosensors can be used to determine the pyruvate responsible for the pungent taste in garlic and onion products (Pundir et al. 2019). A pyruvate oxidase-lactate oxidase or dehydrogenase bienzyme biosensor was reported for the determination of lactate which is important to control the lactic fermentation in the dairy industry or to assess the malate-lactate fermentation in the wine industry (Chan et al. 2017). A trienzyme biosensor consisting of pyruvate oxidase, kinase, and pyruvate kinase was able to determine the acetic acid in food samples, where the acetic acid affects the taste and flavor of fermented products such as wines, vinegar, and soy sauces (Mizutani et al. 2001).

1.3.4. Enzyme biosensors research for increased stability

Almost six decades have passed since the development of the first enzyme biosensor. However, only a few enzyme biosensors are commercially available compared to the huge number of published research articles (~23,000 articles till 2018) documenting the biosensors using enzymes as the biological elements (Reyes-De-Corcuera JI et al. 2018). One of the main limitations that greatly hinders the development of practical enzyme biosensors is their low storage stability or short operational life which is due to the poor stability of enzymes (Reyes-De-Corcuera JI et al. 2018; Klos-Witkowska et al. 2019). A commonly used method to stabilize enzymes is immobilization (Mateo et al. 2007; Dwevedi 2016). The selected research articles from 1996 to

2017 related to the immobilization methods and the stability performance of GOx biosensors, AOx, and XOx have been well summarized (Reyes-De-Corcuera JI et al. 2018). The immobilization methods and the stability of POx biosensors have also been summarized recently (Kucherenko I. S. et al. 2019; Malik et al. 2019; Pundir et al. 2019). Tables 1.3-1.7 summarize the immobilization methods and the stability performance of the most recently reported GOx biosensors, AOx biosensors, XOx biosensors, POx biosensors, and GaOx biosensors.

1.3.4.1. Immobilization

The methods of enzyme immobilization have been extensively reviewed (Sirisha et al. 2016; Nguyen HH and Kim 2017). The methods can be classified as irreversible and reversible immobilization. The irreversible immobilization methods such as covalent bonding, entrapment, and cross-linking prevent the enzymes from detaching once attached to the support unless the enzyme or the support is destroyed, while the reversible methods such as absorption or disulfide bonding often allow enzyme leaching (Brena et al. 2013). Both the irreversible and reversible methods have been used to fabricate enzyme biosensors. The common method of absorption used in enzyme biosensors is the electrostatic binding such as layer-by-layer assembly and electrochemical deposition where the enzymes with positive or negative surfaces are immobilized onto the electrode with opposite charges through ionic and polar intonations (Nguyen HH and Kim 2017). However, the irreversible immobilization methods are often preferred to develop stable enzyme biosensors. Brief introductions of two most commonly used irreversible immobilization methods are reviewed below.

1.3.4.1.1. Covalent binding

Covalent binding mainly involves the formation of covalent bonds between the functional groups of enzymes and the supporting material. The functional groups in enzymes used for

covalent binding must have no or little effect on the enzyme activity and the common groups used include amino, carboxylic, phenolic, hydroxyl, thiol, imidazole, indole, and sulfhydryl (Novick and Rozzell 2005). To protect the functional groups essential for the enzymatic activity, strategies such as adding substrates or competitive inhibitors have been used (Das S 2014). The binding process usually starts with activating the surface of support materials with linker molecules such as glutaraldehyde and N-hydroxy succinimide and then coupling the enzymes to the activated supports (Nguyen HH and Kim 2017). Some examples of the activated support surfaces and the corresponding covalent bindings can be found from Das S (2014). The covalent bonds can also be formed directly without the linker molecules (coupling agents or spacers). For example, the GaOx was immobilized onto the poly(N-glycidylpyrrole-co-pyrrole) film through direct covalent binding without any coupling agents (Şenel et al. 2011). Covalent binding has the potential to be used for enzyme stabilization by forming strong bindings and having little leakage of enzymes (Brena et al. 2013; Nguyen HH and Kim 2017). The multi-point attachment where the covalent bonds were formed at various points of the enzyme and support was reported to be effective in stabilizing enzymes against denaturation in aqueous or organic solutions (Mozhaev V et al. 1990; Wang P et al. 2001). For example, the carrier material Eupergit C has high density of oxirane groups that can be covalently bound to anime groups at multiple points of the enzyme (Katchalski-Katzir and Kraemer 2000). However, covalent binding also has risks of losing enzyme activity and sometimes resulting in unusable support when the enzyme is deactivated (Brena et al. 2013; Sheldon and van Pelt 2013).

Cross-linking is a subgroup of covalent binding that forms covalent bonds between or within enzyme molecules named as inter- or intramolecular cross-linking. Cross-linkers are used to connect to the functional groups of enzymes and the most commonly used cross-linker is

glutaraldehyde which reacts to the primary amino groups (Barbosa et al. 2014). Cross-linking is an irreversible immobilization method that stabilizes the enzymes (Brena et al. 2013; Nguyen HH and Kim 2017). However, the enzyme activity decrease may occur (Das S 2014).

1.3.4.1.2. Entrapment

Entrapment is to cage the enzymes within a polymeric network which allows the substrates and products to go through while the enzymes are retained. The enzymes are typically physically retained in the network and have no chemical interactions with the entrapping polymer (Nguyen HH and Kim 2017). Entrapment stabilizes the enzymes by trapping the enzymes in the polymer and has no chemical changes on enzymes thereby no changes in enzyme activity (Das S 2014). However, entrapment results in a diffusion barrier that limits the mass transfer and it also suffers from the enzyme leaching (Brena et al. 2013; Das S 2014). Common methods of entrapment include electropolymerization, photopolymerization, sol-gel process, and microencapsulation.

In electropolymerization a polymeric network is formed by applying a potential or current to the mixture of enzymes and monomers to trigger the redox reactions of monomers. It is an easy, one-step method to form homogeneous polymer films. In photopolymerization the polymerization is initiated by exposing photopolymers to UV or visible light (Nguyen HH and Kim 2017). Sol-gel is a process that forms a porous gel to entrap enzymes through the hydrolysis of alkoxide precursors followed by condensation and polycondensation. The sol-gel entrapment can retain a large amount of water which helps stabilize enzymes (Kandimalla et al. 2006). In micro-encapsulation enzymes are entrapped in semi-permeable membranes with the pore size smaller than the enzymes but bigger than the substrates and products (Hassan et al. 2016).

1.4. Effects of high hydrostatic pressure on the stability and activity of enzymes

High hydrostatic pressure (HHP) has been used to kill microbes and inactivate enzymes in food processing. However, it can also stabilize and activate some enzymes at moderate pressures (Eisenmenger and Reyes-De-Corcuera 2009b). The activating and stabilizing effects of HHP on various enzymes have been extensively reported. The enhancing effects of HHP on the activity and stability of enzymes involved in the beer processing were reviewed by Santos et al. (2017). The improved enzymatic hydrolysis of food proteins with activated enzymes by HHP was reviewed by Marciniak et al. (2018). The enhancements of HHP on enzymes grouped as oxidoreductases, transferases, hydrolases, and lyases were reviewed by Eisenmenger and Reyes-De-Corcuera (2009b). In our laboratory, we reported the effects of HHP on lipase B, pectinases, GOx, AOx, XOx, and POx. The activity of lipase was increased up to 10-fold at 200 MPa and 40 or 80 °C (Eisenmenger and Reyes-De-Corcuera 2010). The stability of lipase (Eisenmenger and Reyes-De-Corcuera 2009a), GOx (Halalipour et al. 2017b), AOx (Buchholz-Afari et al. 2019), XOx (Halalipour et al. 2017a), or POx (Wallace 2017) was increased at selected temperatures and pressures. Among those, the best stabilizing effect was the stability of GOx that was increased up to 50 times at 240 MPa and 74.5 °C compared to the GOx inactivated at 0.1 MPa and 74.5 °C (Halalipour et al. 2017b). The stabilizing or activating effects of HHP on the enzymes reported from 2009 have been summarized in Table 1.8.

1.4.1. Stabilization effect of HHP

The stabilizing effect of HHP enables enzymes to work at temperatures that would normally be inactivated and thereby resulting in a faster reaction rate (Li Y et al. 2015b). The stabilization by HHP becomes apparent at temperatures above 50 °C and pressures below 400 MPa (Mozhaev VV et al. 1996). Despite the many reports and some hypotheses, the mechanism of

enzyme stabilization by HHP remains unclear. Proteins are only reversibly changed by moderate HHP but are denatured at pressures in excess of 400-500 MPa. The quaternary structure of proteins is affected by pressures below 150-300 MPa, while the tertiary structures are changed by pressures above 200 MPa (Furtado et al. 2012). High pressure decreases the volume of proteins and compresses non-rigid internal voids through the displacement of helices (Collins et al. 2007). At moderate pressures, the protein is stabilized by increased Van der Waals forces resulting from compressed cavities (Boonyaratanakornkit et al. 2002). At high pressures, the volume decrease is mainly from the penetration of water molecules into the cavities which causes the inactivation of proteins by weakening the electrostatic and hydrophobic interactions and disturbing the tertiary structures (Hummer et al. 1998; Degraeve et al. 2002; Roche et al. 2017). An antagonistic effect of pressure and temperature on the inactivation of enzymes is often observed, and the native state of enzymes is retained at high temperatures and moderately high pressures (Degraeve et al. 2002; Eisenmenger and Reyes-De-Corcuera 2009b). This was because the pressures typically below 300 MPa can counteract the unfolding of proteins caused by high temperature to increase the thermal stability of enzymes. High temperature can cause the disruption of the highly ordered structure of electrostricted water, resulting in the essential water loss when the thermal inactivation starts, which will lead to structural rearrangement and protein denaturation. High pressure, on the other hand, can strengthen the hydration of charged and non-polar groups, compress the protein hydration shell, and counteract the process from high temperature (Mozhaev VV et al. 1996; Degraeve et al. 2002; Eisenmenger and Reyes-De-Corcuera 2009b; Terefe et al. 2013). High temperature weakens the intermolecular oxygen-hydrogen interactions, resulting in a softened hydrogen bond network. On the contrary, HHP strengthens the intermolecular oxygen-hydrogen interactions by shortening the distance between hydrogen bonds and thereby stabilizing them

(Eisenmenger and Reyes-De-Corcuera 2009b; Li Y et al. 2015b). High pressure also strengthens the ion pairs which further stabilizes the tertiary and quaternary structures of enzymes (Li Y et al. 2015b). High pressure can also introduce disulfide bonds to stabilize the enzyme conformation through the movement of the flexible thiol groups under high pressure (Li Y et al. 2015b). For multi-domain enzymes, pressure can affect the orientation of the inter-domains which is potentially related to the enzyme stability (Medvedev et al. 2018).

1.4.2. Activation effects of HHP

The activation of enzymes by HHP is also widely reported. To give a few examples, the activity of polyphenol oxidase from apple juice (Buckow et al. 2009), blueberry (Terefe et al. 2015), apricot nectar (Huang Wenshu et al. 2013), garlic (Eroman Unni et al. 2014), or Pacific white shrimp (Huang Wanyou et al. 2014) was increased up to 65 %, 6.1 times, 41.5 %, 20 %, or 57.61 % at certain pressures, respectively. The activity of peroxidase from feijoa puree (Ortuño et al. 2013) or apricot nectar (Huang Wenshu et al. 2013) was increased up to 140 % or 47 % at certain pressures, respectively. The activity of lipase from *Yarrowia lipolytica* was increased at most 209 % after being treated at 450 MPa and 40 °C for 10 min (Yang et al. 2016). Similar to the stabilization of enzymes by HHP, the mechanism of activation of enzymes by HHP remains unclear. The rate of enzyme-catalyzed reactions can be changed by HHP through changing the protein structure, changing the rate-limiting step, or changing the substrate or solvent (Low and Somero 1975; Eisenmenger and Reyes-De-Corcuera 2009b). According to Le Chatelier principle, a system at equilibrium will counteract itself to restore the equilibrium state when the high pressure is applied, which results in the decrease in the overall volume of the system. In transition-state theory, the effect of HHP on the reaction rate can be described using the Eyring's equation (Eq. 1).

$$\left(\frac{\partial \ln k}{\partial p}\right)_T = -\frac{\Delta V^{\neq}}{RT} \quad (1)$$

$\Delta V^{\neq}$ is the activation volume, which is the difference of the molar volume between the reactants (enzyme-substrate complex) and the transition state. k is the rate constant, p is the pressure, T is the temperature (K), R is the gas constant (8.314 cm^3 MPa K^{-1} mol^{-1}). When the reaction rate is increased by HHP, the energy barrier for the reaction is lowered and the activation volume is negative (Li Y et al. 2015a). In contrast, the activation volume is positive when the enzymatic reaction is suppressed by HHP (Ohmae et al. 2007). The volume changes induced by HHP can be attributed to the reactants themselves or the result of the interactions between the reactants and the solvents (Boonyaratanakornkit et al. 2002). Eq. 1 can be transformed into a linear form which is often used for graphical analysis (Eq. 2).

$$\text{Ln } k_p = -\frac{\Delta V^{\neq}}{RT} + \text{Ln } k_0 \quad (2)$$

Negative activation volumes indicate that HHP accelerates the reactions, in other words, HHP increases the enzyme activity, i.e., α-chymotrypsin (Mozhaev VV et al. 1996; Luong and Winter 2015; Schuabb et al. 2016) and naringinase (Vila-Real et al. 2010). The negative activation volume may result from the destruction of the electrostatic interactions when forming the transition state, which strengthens the hydration caused by the interaction of water with charged and polar amino acid exposed by HHP (Mozhaev VV et al. 1996; Luong and Winter 2015). Volume changes of proteins are often associated with the changes of enzyme conformation. Since the moderately HHP can alter the tertiary or quaternary structure of protein without denaturation, the changes in enzyme activity is related to the conformation changes of proteins (Nguyen LM and Roche 2017). The active site of enzymes and the enzyme flexibility may also be modified by HHP to result in the increase in the rate of reaction. The molecular dynamics simulation of lipase activated at high pressure (> 100 MPa) revealed the channel access to the active site was opened through a

conformation change induced by HHP (Johnson et al. 2016). In order to better understand the protein conformation change, the protein structure is needed to be analyzed by fluorescence, nuclear magnetic resonance (NMR) spectroscopy, or Fourier-transform infrared spectroscopy. The development of NMR spectroscopy or X-ray crystallography at HHP makes the investigation possible (Cioni and Gabellieri 2011).

1.5. Enzymes relevant to this research

1.5.1. Glucose oxidase and glucose oxidase biosensors

Glucose oxidase (GOx) (EC 1.1.3.4) catalyzes the oxidation of β-D-glucose by oxygen to D-glucono-1,5-lactone and hydrogen peroxide. It is a flavin-dependent homodimer of approximately 160 kDa. Glucose oxidase has been widely used in industries including clinical, food, chemical, and biotechnology, and it is mainly used to remove glucose and oxygen in foods and beverages (Bankar et al. 2009). It has been used as the oxidizing agent in breadmaking, as the glucose remover while making the dry egg powder, as the food preservative or oxygen scavenger for food products such as high-fat foods, wine, and beer, as the sugar reducer to manufacture reduced alcohol wine, as the catalyst for gluconic acid production, and as the enzyme used in glucose biosensors (Wong et al. 2008).

Glucose biosensors that use immobilized GOx have been extensively researched and used in the clinical industry for the last four decades (Rahman et al. 2010). Glucose oxidase biosensors can be used to determine the concentration of glucose in fruit juice or the liquors under fermentation, and can also be used to form multi-enzyme biosensors for the detection of other analytes (Terry et al. 2005; Barthelmebs et al. 2010). Glucose oxidase and acid phosphatase (AP) were immobilized together to determine the organophosphorus and carbamic acid type pesticides, through the inhibition effect of pesticides on AP. In that dual-enzyme biosensor, GOx catalyzed

the oxidation of glucose generated from the catalytic reaction of glucose-6-phosphate by AP (Mazzei et al. 1996). A three-enzyme biosensor, including glucose oxidase, invertase, and mutarotase, was designed to determine the sucrose in the food industry, where the sucrose was decomposed by the three enzymes and the changes in conductivity were measured (Soldatkin et al. 2008). Glucose oxidase biosensors can also be used to determine heavy metals due to the reversible inhibition effects of metal ions on GOx; and a number of heavy metals on GOx have been researched such as Hg^{2+}, Ag^{2+}, Cu^{2+}, Cd^{2+}, Cd^{2+}, and Pb^{2+} (Malitesta and Guascito 2005; Guascito et al. 2008).

Among all glucose biosensors, electrochemical glucose biosensors are the most frequently researched and are further classified as potentiometric, amperometric, or impedimetric/conductometric biosensors based on their transduction signal (Rahman et al. 2010). In first-generation amperometric glucose biosensors, glucose oxidase is immobilized on the surface of an electrode. As glucose diffuses into the immobilized GOx layer, it is oxidized into gluconic acid and hydrogen peroxide. Then, at the surface of the metal electrode, hydrogen peroxide is oxidized exchanging two electrons and producing an electrical current that is a function of the concentration of glucose in the sample. Glucose oxidase biosensors have been widely developed into commercial biosensors (Bahadır and Sezgintürk 2015).

The stability performances of the selected GOx biosensors published from 2018 are summarized in Table 1.3. The storage stability of GOx biosensors was from retaining 50 % to 95 % residual activity after a month with different immobilization methods. For example, the GOx biosensors immobilized through absorption of the mixture of enzymes and core shell Fe_3O_4@Au nanoparticles onto carbon paste electrodes with the aid of an external magnetic field retained 50 % response after 30 days (Samphao et al. 2018). The GOx biosensors immobilized through

adsorption by layer-by-layer deposition onto gold electrodes retained 65 % response after a month (David et al. 2018). The GOx biosensors immobilized through covalent binding to poly (pyrrole-2-carboxylic acid) particles on the graphite rod electrode combined with cross-linking retained 95.3 % response after storing at 4 °C for a month (Kausaite-Minkstimiene et al. 2018). The GOx biosensors immobilized through entrapment by electropolymerization with poly(sulfobetaine-3,4-ethylenedioxythiophene) retained 95 % response after 7 days (Wu et al. 2018). The GOx biosensors immobilized through encapsulation in chitosan/κ-carrageenan polyelectrolyte complex combined with the addition of glutaraldehyde had no change in response after storing for 3 weeks (Rassas et al. 2019). Therefore, the GOx biosensors were able to have good stability with certain immobilization methods such as covalent binding or entrapment. However, a better stability performance is always preferred for commercial applications.

1.5.2. Alcohol oxidase and alcohol oxidase biosensors

Alcohol oxidase (AOx; EC. 1.1.3.13) catalyzes the oxidation of alcohols into the corresponding carbonyl compound and hydrogen peroxide. It is an octamer of approximately 600 kDa and each subunit has a flavin adenine dinucleotide cofactor (Ozimek et al. 2005). It can be categorized into four groups based on the substrate specificity, including short chain alcohol oxidase, long chain alcohol oxidase, aromatic alcohol oxidase, and secondary alcohol oxidase (Goswami et al. 2013). Most of the AOx are from yeasts such as *Pichia pastoris*, *Pichia angusta*, *Candida boidinii* and filamentous fungi such as *Penicillium chrysogenum*, *Cladosporium fulvum*; the genes encoding the AOx protein were summarized by Ozimek et al. (2005). Particularly, the AOx from *Pichia pastoris* is encoded by two genes, AOx1 and AOx2 (Cregg et al. 1989).

Alcohol oxidase is an important enzyme used to detect and quantify alcohols. It is used in the clinical and forensic tests to analyze the human fluids such as blood, urine, and serum; it can

also be used for the quality control in the food, beverage, and pulp industries and to monitor the progress of alcoholic fermentation (Patel NG et al. 2001). To overcome some shortcomings of the chemical methods, e.g. titration, colorimetric, chromatographic, or spectroscopic methods, alcohol oxidase biosensors have been extensively researched (Azevedo et al. 2005). Alcohol oxidase can also be used to synthesize carbonyl compounds that are important as solvents, pharmaceuticals, or the ingredients in fragrances and flavors, e.g., n-heptanal, which is the starting material of many aroma and flavor compounds with high yield in synthesis (Kakoti et al. 2012). The conversion of alcohols to the corresponding carbonyl products that can be selectively catalyzed by AOx without producing undesirable harmful by-products have been summarized by Kakoti et al. (2012).

Alcohol oxidase biosensors are extensively applied to determine ethanol or methanol in food products during fermentation, or in beer, wine, and liquor (Barthelmebs et al. 2010; Cinti et al. 2017). A dual-enzyme biosensor consisting of carboxyl esterase and alcohol oxidase has been proposed for the determination of aspartame in soft drinks and sweeteners (Odacı et al. 2004). Electrochemical alcohol oxidase biosensors monitor either the consumption of O_2 or the formation of H_2O_2. The most common way to measure O_2 is using the Clark-type O_2 electrode. However, due to many disadvantages when monitoring O_2 such as low accuracy, low reproducibility, high detecting limit, H_2O_2 is a good alternative method commonly used (Azevedo et al. 2005). For the first and second generation amperometric AOx biosensors, the alcohol is oxidized by the immobilized AOx into the corresponding carbonyl compound and the cofactor FAD is reduced to $FADH_2$. $FADH_2$ then reacts with O_2 to FAD and H_2O_2. The electrons generated through the oxidation of H_2O_2 (1^{st} generation) or relayed by a mediator (2^{nd} generation) are then collected by the transducer (Azevedo et al. 2005). For the 3^{rd} generation biosensor, the direct electron transfer

between the AOx and electrode is established (Das M and Goswami 2013). The current response is proportional to the concentration of alcohols in the sample.

Different from GOx biosensors, the stability of AOx biosensors is usually low. Actually, the application of AOx and AOx biosensors into practical instruments is mainly hampered by the poor stability of the enzyme (Goswami et al. 2013). The stability performances of AOx biosensors published from 1996-2017 were summarized by Reyes-De-Corcuera JI et al. (2018) and the AOx biosensors published from 2018 were summarized in Table 1.4. For example, the AOx biosensors immobilized through adsorption onto the bimetallic PtRu nanoparticle covered graphite electrode and then covered by polymers retained 20 % response after 14 days and had a half-life time 10 days (Stasyuk et al. 2019). The AOx biosensors immobilized through adsorption onto green synthesized nanoparticle modified graphite electrodes and then covered by the mixture of chitosan and polyethyleneimine retained ~50 % response after 3 days (Gayda et al. 2019). The AOx biosensors immobilized through cross-linking with glutaraldehyde onto printed carbon nanotube electrodes completely lost the response after 5 days (Yu H et al. 2018). Most immobilization methods were not able to increase the stability of AOx and AOx biosensors to meet the requirements for long-term industrial applications such as monitoring the alcohols during fermentation. Therefore, the immobilization methods are worth trying to combine with other techniques such as HHP to further increase the stability.

1.6. Hypotheses and objectives

We and others have studied the enhancement effect of high pressure on the stability of enzymes (Table 1.8). However, to the best of our knowledge, HHP has not been applied to increase the stability of enzyme biosensors. Immobilization alone sometimes is not sufficient to fabricate an enzyme biosensor that is stable enough to be commercially used, such as AOx biosensor.

Therefore, HHP combined with immobilization is worth trying to further increase the stability. To the best of our knowledge, the effects of HHP applied during enzyme immobilization or inactivation of immobilized enzymes have not been studied. A well-studied and relative stable enzyme GOx and an instable enzyme AOx are chosen in this study to determine the effects of HHP on the stability of enzyme biosensors. The hypotheses for this research are 1) combining HHP with electropolymerization of *o*-phenylenediamine (oPD) or cross-linking improves the stability of GOx or AOx biosensors, 2) the stabilizing effect of HHP can be retained after depressurization through immobilization.

We and others have also studied the enhancement effect of high pressure on the activity of GOx (Halalipour et al. 2020) and other enzymes (Table 1.8). To the best of our knowledge, high pressure has not been used to improve the activity of AOx. We studied the stabilizing effect of HHP on AOx at high temperatures (Buchholz-Afari et al. 2019). To better understand the effects of HHP on the oxidases mentioned in section 1.2.3, it is worth studying both the stability and the activity of the oxidases at HHP. Besides, the increase in the activity of AOx is beneficial to the industrial applications in terms of higher efficiency and economic saving. Therefore, it is reasonable to hypothesize that the activity of AOx would increase at HHP.

Therefore, the objectives of this study were 1) to assess the effect of HHP on the activity of AOx at selected temperatures, 2) to assess the effect of HHP during electropolymerization on the thermal stability of GOx and AOx biosensors, 3) to combine HHP and cross-linking with GA to enhance the stability of GOx biosensors, and 4) to assess the effect of HHP during thermal inactivation on the stability of immobilized GOx and AOx.

1.7. References

Abdel-Hamid AM, Attwood MM, Guest JR. 2001. Pyruvate oxidase contributes to the aerobic growth efficiency of *Escherichia coli*. Microbiology. 147(6):1483-1498.

Agrawal DC, Yadav A, Singh VK, Srivastava A, Kayastha AM. 2020. Immobilization of fenugreek β-amylase onto functionalized tungsten disulfide nanoparticles using response surface methodology: Its characterization and interaction with maltose and sucrose. Colloids and Surfaces B: Biointerfaces. 185:110600.

Agrawal R, Verma AK, Satlewal A. 2016. Application of nanoparticle-immobilized thermostable β-glucosidase for improving the sugarcane juice properties. Innovative Food Science & Emerging Technologies. 33:472-482.

Apichartsrangkoon A, Srisajjalertwaja S, Chaikham P, Hirun S. 2013. Physical and chemical properties of Nam Prig Noom, a Thai green-chili paste, following ultra-high pressure and thermal processes. High Pressure Research. 33(1):83-95.

Asav E, Akyilmaz E. 2010. Preparation and optimization of a bienzymic biosensor based on self-assembled monolayer modified gold electrode for alcohol and glucose detection. Biosensors and Bioelectronics. 25(5):1014-1018.

Atchudan R, Muthuchamy N, Edison TNJI, Perumal S, Vinodh R, Park KH, Lee YR. 2019. An ultrasensitive photoelectrochemical biosensor for glucose based on bio-derived nitrogen-doped carbon sheets wrapped titanium dioxide nanoparticles. Biosensors and Bioelectronics. 126:160-169.

Azevedo AM, Prazeres DMF, Cabral JMS, Fonseca LP. 2005. Ethanol biosensors based on alcohol oxidase. Biosensors and Bioelectronics. 21(2):235-247.

Baffi MA, Tobal T, Lago JHG, Boscolo M, Gomes E, Da-Silva R. 2013. Wine aroma improvement using a β-glucosidase preparation from *Aureobasidium pullulans*. Applied Biochemistry and Biotechnology. 169(2):493-501.

Bahadır EB, Sezgintürk MK. 2015. Applications of commercial biosensors in clinical, food, environmental, and biothreat/biowarfare analyses. Analytical Biochemistry. 478:107-120.

Bajpai P. 1999. Application of enzymes in the pulp and paper industry. Biotechnology Progress. 15(2):147-157.

Bamforth CW. 2009. Current perspectives on the role of enzymes in brewing. Journal of Cereal Science. 50(3):353-357.

Bankar SB, Bule MV, Singhal RS, Ananthanarayan L. 2009. Glucose oxidase-an overview. Biotechnology Advances. 27(4):489-501.

Barbiroli A, Farris S, Rollini M. 2016. Combinational approaches for antimicrobial packaging: lysozyme and lactoferrin. Antimicrobial Food Packaging. Elsevier; p. 589-597.

Barbosa O, Ortiz C, Berenguer-Murcia Á, Torres R, Rodrigues RC, Fernandez-Lafuente R. 2014. Glutaraldehyde in bio-catalysts design: a useful crosslinker and a versatile tool in enzyme immobilization. Rsc Advances. 4(4):1583-1600.

Barthelmebs L, Calas-Blanchard C, Istamboulie G, Marty J-L, Noguer T. 2010. Biosensors as analytical tools in food fermentation industry. Bio-Farms for Nutraceuticals. Springer; p. 293-307.

Bashari M, Abdelhai MH, Abbas S, Eibaid A, Xu X, Jin Z. 2014. Effect of ultrasound and high hydrostatic pressure (US/HHP) on the degradation of dextran catalyzed by dextranase. Ultrasonics Sonochemistry. 21(1):76-83.

Becker MM, Ribeiro EB, de Oliveira Marques PRB, Marty J-L, Nunes GS, Catanante G. 2019. Development of a highly sensitive xanthine oxidase-based biosensor for the determination of antioxidant capacity in Amazonian fruit samples. Talanta. 204:626-632.

Ben Messaoud N, Ghica ME, Dridi C, Ben Ali M, Brett CMA. 2018. A novel amperometric enzyme inhibition biosensor based on xanthine oxidase immobilised onto glassy carbon electrodes for bisphenol A determination. Talanta. 184:388-393.

Benelhadj S, Fejji N, Degraeve P, Attia H, Ghorbel D, Gharsallaoui A. 2016. Properties of lysozyme/*Arthrospira platensis (Spirulina)* protein complexes for antimicrobial edible food packaging. Algal Research. 15:43-49.

Binod P, Sindhu R, Madhavan A, Abraham A, Mathew AK, Beevi US, Sukumaran RK, Singh SP, Pandey A. 2017. Recent developments in l-glutaminase production and applications-An overview. Bioresource Technology. 245:1766-1774.

Bleoanca I, Neagu C, Turtoi M, Borda D. 2018. Mild-thermal and high pressure processing inactivation kinetics of polyphenol oxidase from peach puree. Journal of Food Process Engineering. 41(7):e12871.

Boonyaratanakornkit BB, Park CB, Clark DS. 2002. Pressure effects on intra- and intermolecular interactions within proteins. Biochimica et Biophysica Acta - Protein Structure and Molecular Enzymology. 1595(1):235-249.

Boulekou SS, Katsaros GJ, Taoukis PS. 2010. Inactivation kinetics of peach pulp pectin methylesterase as a function of high hydrostatic pressure and temperature process conditions. Food and Bioprocess Technology. 3(5):699-706.

Brady JW. 2013. Introductory food chemistry. Comstock.

Brena B, González-Pombo P, Batista-Viera F. 2013. Immobilization of enzymes: a literature survey. Immobilization of enzymes and cells. Springer; p. 15-31.

Bruins ME, Creusot N, Gruppen H, Janssen AE, Boom RM. 2009. Pressure-aided proteolysis of β-casein. Journal of Agricultural and Food Chemistry. 57(12):5529-5534.

Bruins ME, Meersman F, Janssen AE, Heremans K, Boom RM. 2008. Increased susceptibility of b-glucosidase from the hyperthermophile *Pyrococcus furiosus* to thermal inactivation at higher pressures.

Buchholz-Afari MI, Halalipour A, Yang D, Reyes-De-Corcuera JI. 2019. Increased stability of alcohol oxidase under high hydrostatic pressure. Journal of Food Engineering. 246:95-101.

Buckow R, Weiss U, Knorr D. 2009. Inactivation kinetics of apple polyphenol oxidase in different pressure–temperature domains. Innovative Food Science & Emerging Technologies. 10(4):441-448.

Buk V, Pemble ME, Twomey K. 2019. Fabrication and evaluation of a carbon quantum dot/gold nanoparticle nanohybrid material integrated onto planar micro gold electrodes for potential bioelectrochemical sensing applications. Electrochimica Acta. 293:307-317.

Cao X, Zhang Y, Zhang F, Wang Y, Yi J, Liao X. 2011. Effects of high hydrostatic pressure on enzymes, phenolic compounds, anthocyanins, polymeric color and color of strawberry pulps. Journal of the Science of Food and Agriculture. 91(5):877-885.

Celestino KRS, Cunha RB, Felix CR. 2006. Characterization of a β-glucanase produced by *Rhizopus microsporus* var. *microsporus*, and its potential for application in the brewing industry. BMC Biochemistry. 7(1):23.

Çevik E, Şenel M, Fatih Abasıyanık M. 2010. Construction of biosensor for determination of galactose with galactose oxidase immobilized on polymeric mediator contains ferrocene. Current Applied Physics. 10(5):1313-1316.

Chakraborty S, Rao PS, Mishra HN. 2015. Kinetic modeling of polyphenoloxidase and peroxidase inactivation in pineapple (*Ananas comosus L.*) puree during high-pressure and thermal treatments. Innovative Food Science & Emerging Technologies. 27:57-68.

Chan D, Barsan MM, Korpan Y, Brett CMA. 2017. L-lactate selective impedimetric bienzymatic biosensor based on lactate dehydrogenase and pyruvate oxidase. Electrochimica Acta. 231:209-215.

Chandrasekaran M, Basheer SM, Chellappan S, Krishna JG, Beena P. 2015. Enzymes in food and beverage production: an overview. Enzymes in Food and Beverage Processing. CRC Press; p. 133-154.

Charmantray F, Touisni N, Hecquet L, Mousty C. 2013. Amperometric biosensor based on galactose oxidase immobilized in clay matrix. Electroanalysis. 25(3):630-635.

Chen G, Miao M, Jiang B, Jin J, Campanella OH, Feng B. 2017. Effects of high hydrostatic pressure on lipase from *Rhizopus chinensis*: I. Conformational changes. Innovative Food Science & Emerging Technologies. 41:267-276.

Cherry JR, Fidantsef AL. 2003. Directed evolution of industrial enzymes: an update. Current Opinion in Biotechnology. 14(4):438-443.

Choi J-M, Han S-S, Kim H-S. 2015. Industrial applications of enzyme biocatalysis: Current status and future aspects. Biotechnology Advances. 33(7):1443-1454.

Christen P, López-Munguía A. 1994. Enzymes and food flavor-a review. Food Biotechnology. 8(2-3):167-190.

Cinti S, Basso M, Moscone D, Arduini F. 2017. A paper-based nanomodified electrochemical biosensor for ethanol detection in beers. Analytica Chimica Acta. 960:123-130.

Cioni P, Gabellieri E. 2011. Protein dynamics and pressure: What can high pressure tell us about protein structural flexibility? Biochimica et Biophysica Acta - Proteins and Proteomics. 1814(8):934-941.

Collins MD, Quillin ML, Hummer G, Matthews BW, Gruner SM. 2007. Structural rigidity of a large cavity-containing protein revealed by high-pressure crystallography. Journal of Molecular Biology. 367(3):752-763.

Conzuelo F, Gamella M, Campuzano S, Ruiz M, Reviejo A, Pingarron J. 2010. An integrated amperometric biosensor for the determination of lactose in milk and dairy products. Journal of Agricultural and Food Chemistry. 58(12):7141-7148.

Cregg JM, Madden KR, Barringer KJ, Thill GP, Stillman CA. 1989. Functional characterization of the two alcohol oxidase genes from the yeast *Pichia pastoris*. Molecular and Cellular Biology. 9(3):1316.

Dalby PA. 2011. Strategy and success for the directed evolution of enzymes. Current Opinion in Structural Biology. 21(4):473-480.

Dalkıran B, Erden PE, Kılıç E. 2016. Electrochemical biosensing of galactose based on carbon materials: graphene versus multi-walled carbon nanotubes. Analytical and Bioanalytical Chemistry. 408(16):4329-4339.

Das M, Goswami P. 2013. Direct electrochemistry of alcohol oxidase using multiwalled carbon nanotube as electroactive matrix for biosensor application. Bioelectrochemistry. 89:19-25.

Das R, Mishra H, Srivastava A, Kayastha AM. 2017. Covalent immobilization of β-amylase onto functionalized molybdenum sulfide nanosheets, its kinetics and stability studies: A gateway to boost enzyme application. Chemical Engineering Journal. 328:215-227.

Das S. 2014. Microbial biodegradation and bioremediation. Elsevier.

David M, Barsan MM, Brett CMA, Florescu M. 2018. Improved glucose label-free biosensor with layer-by-layer architecture and conducting polymer poly(3,4-ethylenedioxythiophene). Sensors and Actuators B: Chemical. 255:3227-3234.

Degraeve P, Rubens P, Lemay P, Heremans K. 2002. In situ observation of pressure-induced increased thermostability of two β-galactosidases with FT-IR spectroscopy in the diamond anvil cell. Enzyme and Microbial Technology. 31(5):673-684.

Dey A, Neogi S. 2019. Oxygen scavengers for food packaging applications: A Review. Trends in Food Science & Technology.

Doherty EA, Doudna JA. 2001. Ribozyme structures and mechanisms. Annual Review of Biophysics and Biomolecular Structure. 30(1):457-475.

dos Santos JP, Zavareze EdR, Dias ARG, Vanier NL. 2018. Immobilization of xylanase and xylanase–β-cyclodextrin complex in polyvinyl alcohol via electrospinning improves enzyme activity at a wide pH and temperature range. International Journal of Biological Macromolecules. 118:1676-1684.

Dwevedi A. 2016. Basics of enzyme immobilization. Enzyme immobilization. Springer; p. 21-44.

Eisenmenger MJ, Reyes-De-Corcuera JI. 2009a. High hydrostatic pressure increased stability and activity of immobilized lipase in hexane. Enzyme and Microbial Technology. 45(2):118-125.

Eisenmenger MJ, Reyes-De-Corcuera JI. 2009b. High pressure enhancement of enzymes: a review. Enzyme and Microbial Technology. 45(5):331-347.

Eisenmenger MJ, Reyes-De-Corcuera JI. 2010. Kinetics of lipase catalyzed isoamyl acetate synthesis at high hydrostatic pressure in hexane. Biotechnology Letters. 32(9):1287-1291.

Eroman Unni L, Chauhan OP, Raju PS. 2014. High pressure processing of garlic paste: Effect on the quality attributes. International Journal of Food Science & Technology. 49(6):1579-1585.

Fathollahzadeh M, Hosseini M, Norouzi M, Ebrahimi A, Fathipour M, Kolahdouz M, Haghighi B. 2018. Immobilization of glucose oxidase on ZnO nanorods decorated electrolyte-gated field effect transistor for glucose detection. Journal of Solid State Electrochemistry. 22(1):61-67.

Fernandes P. 2010. Enzymes in food processing: a condensed overview on strategies for better biocatalysts. Enzyme Research. 2010.

Fernández A, Cava D, Ocio MJ, Lagarón JM. 2008. Perspectives for biocatalysts in food packaging. Trends in Food Science & Technology. 19(4):198-206.

Fidalgo LG, Saraiva JA, Aubourg SP, Vázquez M, Torres JA. 2014. High pressure effects on the activities of cathepsins B and D of mackerel and horse mackerel muscle.

Fox PF, Stepaniak L. 1993. Enzymes in cheese technology. International Dairy Journal. 3(4):509-530.

Furtado A, Rosário PM, Calado AR, Alfaia AJ, Ribeiro MH. 2012. High pressure studies on hesperitin production with hesperidinase free and immobilized in calcium alginate beads. High Pressure Research. 32(1):128-137.

Gayda GZ, Demkiv OM, Stasyuk NY, Serkiz RY, Lootsik MD, Errachid A, Gonchar MV, Nisnevitch M. 2019. Metallic nanoparticles obtained via "green" synthesis as a platform for biosensor construction. Applied Sciences. 9(4):720.

Giannoglou M, Alexandrakis Z, Stavros P, Katsaros G, Katapodis P, Nounesis G, Taoukis P. 2018. Effect of high pressure on structural modifications and enzymatic activity of a purified X-prolyl dipeptidyl aminopeptidase from Streptococcus thermophilus. Food Chemistry. 248:304-311.

Goswami P, Chinnadayyala SSR, Chakraborty M, Kumar AK, Kakoti A. 2013. An overview on alcohol oxidases and their potential applications. Applied Microbiology and Biotechnology. 97(10):4259-4275.

Grauwet T, Van der Plancken I, Vervoort L, Hendrickx ME, Loey AV. 2009. Investigating the potential of *Bacillus subtilis* α-amylase as a pressure-temperature-time indicator for high hydrostatic pressure pasteurization processes. Biotechnology Progress. 25(4):1184-1193.

Grossi A, Gkarane V, Otte JA, Ertbjerg P, Orlien V. 2012. High pressure treatment of brine enhanced pork affects endopeptidase activity, protein solubility, and peptide formation. Food Chemistry. 134(3):1556-1563.

Guan H, Gong D, Song Y, Han B, Zhang N. 2019. Biosensor composed of integrated glucose oxidase with liposome microreactors/chitosan nanocomposite for amperometric glucose sensing. Colloids and Surfaces A: Physicochemical and Engineering Aspects. 574:260-267.

Guascito MR, Malitesta C, Mazzotta E, Turco A. 2008. Inhibitive determination of metal ions by an amperometric glucose oxidase biosensor: Study of the effect of hydrogen peroxide decomposition. Sensors and Actuators B: Chemical. 131(2):394-402.

Guerrand D. 2018. Chapter 26 - Economics of food and feed enzymes: Status and prospectives. In: Nunes CS, Kumar V, editors. Enzymes in Human and Animal Nutrition. Academic Press; p. 487-514.

Gursoy O, Sen Gursoy S, Cogal S, Celik Cogal G. 2018. Development of a new two-enzyme biosensor based on poly (pyrrole-co-3, 4-ethylenedioxythiophene) for lactose determination in milk. Polymer Engineering & Science. 58(6):839-848.

Halalipour A, Duff Jr MR, Howell EE, Reyes-De-Corcuera JI. 2017a. Effects of high hydrostatic pressure or hydrophobic modification on thermal stability of xanthine oxidase. Enzyme and Microbial Technology. 103:18-24.

Halalipour A, Duff Jr MR, Howell EE, Reyes-De-Corcuera JI. 2017b. Glucose oxidase stabilization against thermal inactivation using high hydrostatic pressure and hydrophobic modification. Biotechnology and Bioengineering. 114(3):516-525.

Halalipour A, Duff MR, Howell EE, Reyes-De-Corcuera JI. 2020. Catalytic activity and stabilization of phenyl-modified glucose oxidase at high hydrostatic pressure. Enzyme and Microbial Technology. 137:109538.

Hassan M, Tamer T, Omer A. 2016. Methods of enzyme immobilization. International Journal of Current Pharmaceutical Review and Research. 7(6):385-392.

He B, Liu H. 2020. Electrochemical biosensor based on pyruvate oxidase immobilized AuNRs@Cu2O-NDs as electroactive probes loaded poly (diallyldimethylammonium chloride) functionalized graphene for the detection of phosphate. Sensors and Actuators B: Chemical. 304:127303.

Herbst D, Peper S, Fernández JF, Ruck W, Niemeyer B. 2014. Pressure effects on activity and selectivity of *Candida rugosa* lipase in organic solvents. Journal of Molecular Catalysis B: Enzymatic. 100:104-110.

Hooda V, Kumar V, Gahlaut A, Hooda V. 2018. A novel amperometric bienzymatic biosensor based on alcohol oxidase coupled PVC reaction cell and nanomaterials modified working electrode for rapid quantification of alcohol. Preparative Biochemistry and Biotechnology. 48(10):877-886.

Hou Z, Zhao L, Wang Y, Liao X. 2019. Effects of high pressure on activities and properties of superoxide dismutase from chestnut rose. Food Chemistry. 294:557-564.

Huang W, Bi X, Zhang X, Liao X, Hu X, Wu J. 2013. Comparative study of enzymes, phenolics, carotenoids and color of apricot nectars treated by high hydrostatic pressure and high temperature short time. Innovative Food Science & Emerging Technologies. 18:74-82.

Huang W, Ji H, Liu S, Zhang C, Chen Y, Guo M, Hao J. 2014. Inactivation effects and kinetics of polyphenol oxidase from *Litopenaeus vannamei* by ultra-high pressure and heat. Innovative Food Science & Emerging Technologies. 26:108-115.

Huijuan Z, Jian P, Juan L, Xiaoxiao X. 2018. High-pressure effects on the mechanism of accumulated inosine 5′-monophosphate. Innovative Food Science & Emerging Technologies. 45:330-334.

Hummer G, Garde S, Garcia AE, Paulaitis ME, Pratt LR. 1998. The pressure dependence of hydrophobic interactions is consistent with the observed pressure denaturation of proteins. Proceedings of the National Academy of Sciences. 95(4):1552-1555.

Illanes A, Cauerhff A, Wilson L, Castro GR. 2012. Recent trends in biocatalysis engineering. Bioresource Technology. 115:48-57.

Jędrzak A, Rębiś T, Klapiszewski Ł, Zdarta J, Milczarek G, Jesionowski T. 2018. Carbon paste electrode based on functional GOx/silica-lignin system to prepare an amperometric glucose biosensor. Sensors and Actuators B: Chemical. 256:176-185.

Johnson QR, Lindsay RJ, Nellas RB, Shen T. 2016. Pressure-induced conformational switch of an interfacial protein. Proteins: Structure, Function, and Bioinformatics. 84(6):820-827.

Kakoti A, Kumar AK, Goswami P. 2012. Microsome-bound alcohol oxidase catalyzed production of carbonyl compounds from alcohol substrates. Journal of Molecular Catalysis B: Enzymatic. 78:98-104.

Kandimalla VB, Tripathi VS, Ju H. 2006. Immobilization of biomolecules in sol–gels: biological and analytical applications. Critical Reviews in Analytical Chemistry. 36(2):73-106.

Katchalski-Katzir E, Kraemer DM. 2000. Eupergit® C, a carrier for immobilization of enzymes of industrial potential. Journal of Molecular Catalysis B: Enzymatic. 10(1):157-176.

Katsaros G, Giannoglou M, Taoukis P. 2009. Kinetic study of the combined effect of high hydrostatic pressure and temperature on the activity of *Lactobacillus delbrueckii ssp.* bulgaricus aminopeptidases. Journal of Food Science. 74(5):E219-E225.

Kausaite-Minkstimiene A, Glumbokaite L, Ramanaviciene A, Dauksaite E, Ramanavicius A. 2018. An Amperometric Glucose Biosensor Based on Poly (Pyrrole-2-Carboxylic Acid)/Glucose Oxidase Biocomposite. Electroanalysis. 30(8):1642-1652.

Khun K, Ibupoto ZH, Nur O, Willander M. 2012. Development of galactose biosensor based on functionalized ZnO nanorods with galactose oxidase. Journal of Sensors. 2012.

Kim D-Y, Yeom S-J, Park C-S, Kim Y-S. 2016. Effect of high hydrostatic pressure treatment on isoquercetin production from rutin by commercial α-l-rhamnosidase. Biotechnology Letters. 38(10):1775-1780.

Kim N, Kim C-T. 2012. Reduced thermal inactivation of trypsin and Marugoto E by high-pressure treatment. Food Science and Technology Research. 18(6):911-917.

Kim N, Maeng J-S, Kim C-T. 2013. Effects of medium high pressure treatments on protease activity. Food Science and Biotechnology. 22(1):289-294.

Klos-Witkowska A, Martsenyuk V, Karpinskyi V. 2019. Analysis of Stability in Enzyme Biosensor Based on Michaelis-Menten Model with Time Delays. Acta Physica Polonica. 135:375-379.

Korkut S, Göl S, Kilic MS. 2019. Poly (pyrrole-co-pyrrole-2-carboxylic acid)/Pyruvate Oxidase Based Biosensor for Phosphate: Determination of the Potential, and Application in Streams. Electroanalysis.

Kucherenko IS, Soldatkin OO, Topolnikova YV, Dzyadevych SV, Soldatkin AP. 2019. Novel Multiplexed Biosensor System for the Determination of Lactate and Pyruvate in Blood Serum. Electroanalysis. 31(8):1608-1614.

Kucherenko IS, Topolnikova YV, Soldatkin OO. 2019. Advances in the biosensors for lactate and pyruvate detection for medical applications: A review. TrAC Trends in Analytical Chemistry. 110:160-172.

Kumar S, Haq I, Prakash J, Raj A. 2017. Improved enzyme properties upon glutaraldehyde cross-linking of alginate entrapped xylanase from *Bacillus licheniformis*. International Journal of Biological Macromolecules. 98:24-33.

Kwon CH, Ko Y, Shin D, Kwon M, Park J, Bae WK, Lee SW, Cho J. 2018. High-power hybrid biofuel cells using layer-by-layer assembled glucose oxidase-coated metallic cotton fibers. Nature Communications. 9(1):1-11.

Li H, Voutilainen S, Ojamo H, Turunen O. 2015. Stability and activity of Dictyoglomus thermophilum GH11 xylanase and its disulphide mutant at high pressure and temperature. Enzyme and Microbial Technology. 70:66-71.

Li S, Yang X, Yang S, Zhu M, Wang X. 2012. Technology prospection on enzymes: application, marketing and engineering. Computational and Structural Biotechnology Journal. 2(3):e201209017.

Li X, Zhang X, Xu S, Zhang H, Xu M, Yang T, Wang L, Qian H, Zhang H, Fang H. 2018. Simultaneous cell disruption and semi-quantitative activity assays for high-throughput screening of thermostable L-asparaginases. Scientific Reports. 8(1):1-12.

Li Y, Miao M, Chen X, Jiang B, Liu M, Feng B. 2015a. Improving the catalytic behavior of inulin fructotransferase under high hydrostatic pressure. Journal of the Science of Food and Agriculture. 95(13):2588-2594.

Li Y, Miao M, Liu M, Chen X, Jiang B, Feng B. 2015b. Enhancing the thermal stability of inulin fructotransferase with high hydrostatic pressure. International Journal of Biological Macromolecules. 74:171-178.

Liu S, Xu Q, Li X, Wang Y, Zhu J, Ning C, Chang X, Meng X. 2016. Effects of high hydrostatic pressure on physicochemical properties, enzymes activity, and antioxidant capacities of anthocyanins extracts of wild Lonicera caerulea berry. Innovative Food Science & Emerging Technologies. 36:48-58.

Low PS, Somero GN. 1975. Activation volumes in enzymic catalysis: their sources and modification by low-molecular-weight solutes. Proceedings of the National Academy of Sciences. 72(8):3014-3018.

Luong TQ, Winter R. 2015. Combined pressure and cosolvent effects on enzyme activity–a high-pressure stopped-flow kinetic study on α-chymotrypsin. Physical Chemistry Chemical Physics. 17(35):23273-23278.

Malik M, Chaudhary R, Pundir CS. 2019. An improved enzyme nanoparticles based amperometric pyruvate biosensor for detection of pyruvate in serum. Enzyme and Microbial Technology. 123:30-38.

Malinowska-Pańczyk E, Kołodziejska I. 2018. Changes in enzymatic activity of fish and slaughter animals meat after high pressure treatment at subzero temperatures. Polish Journal of Food and Nutrition Sciences. 68(2):125-131.

Malitesta C, Guascito MR. 2005. Heavy metal determination by biosensors based on enzyme immobilised by electropolymerisation. Biosensors and Bioelectronics. 20(8):1643-1647.

Marciniak A, Suwal S, Naderi N, Pouliot Y, Doyen A. 2018. Enhancing enzymatic hydrolysis of food proteins and production of bioactive peptides using high hydrostatic pressure technology. Trends in Food Science & Technology. 80:187-198.

Marketresearchfuture. 2019. Electrochemical Biosensors Market Research Report-Global Forecast till 2025. [accessed 2020 Mar 4]. https://www.marketresearchfuture.com/reports/electrochemical-biosensors-market-2792.

Marketsandmarkets. 2019. Biosensors Market worth $31.5 billion by 2024. [accessed 2020 Mar 4]. https://www.marketsandmarkets.com/PressReleases/biosensors.asp.

Mateo C, Palomo JM, Fernandez-Lorente G, Guisan JM, Fernandez-Lafuente R. 2007. Improvement of enzyme activity, stability and selectivity via immobilization techniques. Enzyme and Microbial Technology. 40(6):1451-1463.

Mazzei F, Botrè F, Botrè C. 1996. Acid phosphatase/glucose oxidase-based biosensors for the determination of pesticides. Analytica Chimica Acta. 336(1):67-75.

Medvedev KE, Kolchanov NA, Afonnikov DA. 2018. High temperature and pressure influence the interdomain orientation of Nip7 proteins from *P. abyssi* and *P. furiosus*: MD simulations. Journal of Biomolecular Structure and Dynamics. 36(1):68-82.

Mehrotra P. 2016. Biosensors and their applications-A review. Journal of Oral Biology and Craniofacial Research. 6(2):153-159.

Mentana A, Palermo C, Nardiello D, Quinto M, Centonze D. 2013. Simultaneous and accurate real-time monitoring of glucose and ethanol in alcoholic drinks, must, and biomass by a dual-amperometric biosensor. Journal of Agricultural and Food Chemistry. 61(1):61-68.

Miguel ÂSM, Martins-Meyer TS, Figueiredo E, Lobo BWP, Dellamora-Ortiz GM. 2013. Enzymes in bakery: current and future trends. Food Industry.278-321.

Mizutani F, Sawaguchi T, Sato Y, Yabuki S, Iijima S. 2001. Amperometric determination of acetic acid with a trienzyme/poly (dimethylsiloxane)-bilayer-based sensor. Analytical Chemistry. 73(23):5738-5742.

Monajati M, Borandeh S, Hesami A, Mansouri D, Tamaddon AM. 2018. Immobilization of l-asparaginase on aspartic acid functionalized graphene oxide nanosheet: Enzyme kinetics and stability studies. Chemical Engineering Journal. 354:1153-1163.

Monosik R, Stredansky M, Tkac J, Sturdik E. 2012. Application of enzyme biosensors in analysis of food and beverages. Food Analytical Methods. 5(1):40-53.

Monteiro T, Almeida MG. 2019. Electrochemical enzyme biosensors revisited: Old solutions for new problems. Critical Reviews in Analytical Chemistry. 49(1):44-66.

Mozhaev V, Melik-Nubarov N, Sergeeva M, Šikšnis V, Martinek K. 1990. Strategy for stabilizing enzymes part one: increasing stability of enzymes via their multi-point interaction with a support. Biocatalysis. 3(3):179-187.

Mozhaev VV, Lange R, Kudryashova EV, Balny C. 1996. Application of high hydrostatic pressure for increasing activity and stability of enzymes. Biotechnology and Bioengineering. 52(2):320-331.

Naderi Asrami P, Mozaffari SA, Saber Tehrani M, Aberoomand Azar P. 2018. A novel impedimetric glucose biosensor based on immobilized glucose oxidase on a CuO-Chitosan nanobiocomposite modified FTO electrode. International Journal of Biological Macromolecules. 118:649-660.

Nakatani HS, dos Santos LV, Pelegrine CP, Gomes S, Matsushita M, de Souza NE, Visentainer J. 2005. Biosensor based on xanthine oxidase for monitoring hypoxanthine in fish meat. American Journal of Biochemistry and Biotechnology. 1(2):85-89.

Narsaiah K, Jha SN, Bhardwaj R, Sharma R, Kumar R. 2012. Optical biosensors for food quality and safety assurance-a review. Journal of Food Science and Technology. 49(4):383-406.

Nguyen HH, Kim M. 2017. An overview of techniques in enzyme immobilization. Applied Science and Convergence Technology. 26(6):157-163.

Nguyen HH, Lee SH, Lee UJ, Fermin CD, Kim M. 2019. Immobilized enzymes in biosensor applications. Materials. 12(1):121.

Nguyen LM, Roche J. 2017. High-pressure NMR techniques for the study of protein dynamics, folding and aggregation. Journal of Magnetic Resonance. 277:179-185.

Nigam P, Singh D. 1995. Enzyme and microbial systems involved in starch processing. Enzyme and Microbial Technology. 17(9):770-778.

Novick SJ, Rozzell JD. 2005. Immobilization of enzymes by covalent attachment. Microbial enzymes and biotransformations. Springer; p. 247-271.

Odacı D, Timur S, Telefoncu A. 2004. Carboxyl esterase-alcohol oxidase based biosensor for the aspartame determination. Food Chemistry. 84(3):493-496.

Ohmae E, Murakami C, Gekko K, Kato C. 2007. Pressure effects on enzyme functions. International Journal of Biological Macromolecules. 7:23-29.

Ohmae E, Murakami C, Tate S-i, Gekko K, Hata K, Akasaka K, Kato C. 2012. Pressure dependence of activity and stability of dihydrofolate reductases of the deep-sea bacterium *Moritella profunda* and *Escherichia coli*. Biochimica et Biophysica Acta (BBA)-Proteins and Proteomics. 1824(3):511-519.

Okunade OA, Ghawi SK, Methven L, Niranjan K. 2015. Thermal and pressure stability of myrosinase enzymes from black mustard (*Brassica nigra* LWDJ Koch. var. *nigra*), brown mustard (*Brassica juncea* L. Czern. var. j*uncea*) and yellow mustard (*Sinapsis alba* L. subsp. *maire*) seeds. Food Chemistry. 187:485-490.

Ortuño C, Duong T, Balaban M, Benedito J. 2013. Combined high hydrostatic pressure and carbon dioxide inactivation of pectin methylesterase, polyphenol oxidase and peroxidase in feijoa puree. The Journal of Supercritical Fluids. 82:56-62.

Ozimek P, Veenhuis M, van der Klei IJ. 2005. Alcohol oxidase: A complex peroxisomal, oligomeric flavoprotein. FEMS Yeast Research. 5(11):975-983.

Pariza M, Foster E. 1983. Determining the safety of enzymes used in food processing. Journal of Food Protection. 46(5):453-468.

Patel AK, Singhania RR, Pandey A. 2016. Novel enzymatic processes applied to the food industry. Current Opinion in Food Science. 7:64-72.

Patel NG, Meier S, Cammann K, Chemnitius GC. 2001. Screen-printed biosensors using different alcohol oxidases. Sensors and Actuators B: Chemical. 75(1):101-110.

Pundir CS, Malik M, Chaudhary R. 2019. Quantification of pyruvate with special emphasis on biosensors: A review. Microchemical Journal. 146:1102-1112.

Pyeshkova V, Saiapina O, Soldatkin O, Dzyadevych S. 2009. Enzyme conductometric biosensor for maltose determination. Biopolymers and Cell. 25(4):272-278.

Radulescu M-C, Bucur M-P, Bucur B, Radu GL. 2019. Ester flavorants detection in foods with a bienzymatic biosensor based on a stable Prussian blue-copper electrodeposited on carbon paper electrode. Talanta. 199:541-546.

Rahman M, Ahammad A, Jin J-H, Ahn SJ, Lee J-J. 2010. A comprehensive review of glucose biosensors based on nanostructured metal-oxides. Sensors. 10(5):4855-4886.

Ramos-de-la-Peña AM, Aguilar O. 2019. High Pressure Processing of Lipase (*Thermomyces lanuginosus*): Kinetics and Structure Assessment. European Journal of Lipid Science and Technology.1900289.

Rashidi M, Soruraddin M, Taherzadeh F, Jouyban A. 2009. Catalytic activity and stability of xanthine oxidase in aqueous-organic mixtures. Biochemistry (Moscow). 74(1):97-101.

Rasor JP, Voss E. 2001. Enzyme-catalyzed processes in pharmaceutical industry. Applied Catalysis A: General. 221(1):145-158.

Rassas I, Braiek M, Bonhomme A, Bessueille F, Rafin G, Majdoub H, Jaffrezic-Renault N. 2019. Voltammetric glucose biosensor based on glucose oxidase encapsulation in a chitosan-kappa-carrageenan polyelectrolyte complex. Materials Science and Engineering: C. 95:152-159.

Raveendran S, Parameswaran B, Beevi Ummalyma S, Abraham A, Kuruvilla Mathew A, Madhavan A, Rebello S, Pandey A. 2018. Applications of microbial enzymes in food industry. Food Technology and Biotechnology. 56(1):16-30.

Researchandmarkets. 2020. Biosensors - Market Analysis, Trends, and Forecasts. [accessed 2020 Mar 4]. https://www.researchandmarkets.com/reports/338842/biosensors_market_analysis_trends_and.

Reyes-De-Corcuera J. 2015. Electrochemical biosensors. Encyclopedia of Agricultural Food and Biological Engineering.

Reyes-De-Corcuera JI, Cavalieri R. 2003. Biosensors. Encyclopedia of Agricultural. Food, and Biological Engineering.

Reyes-De-Corcuera JI, Olstad HE, García-Torres R. 2018. Stability and stabilization of enzyme biosensors: The key to successful application and commercialization. Annual Review of Food Science and Technology. 9:293-322.

Ribeiro DS, Henrique SM, Oliveira LS, Macedo GA, Fleuri LF. 2010. Enzymes in juice processing: a review. International Journal of Food Science & Technology. 45(4):635-641.

Roche J, Royer CA, Roumestand C. 2017. Monitoring protein folding through high pressure NMR spectroscopy. Progress in Nuclear Magnetic Resonance Spectroscopy. 102-103:15-31.

Rodríguez-Garayar M, Martín-Cabrejas MA, Esteban RM. 2017. High hydrostatic pressure in astringent and non-astringent persimmons to obtain fiber-enriched ingredients with improved functionality. Food and Bioprocess Technology. 10(5):854-865.

Ronkainen NJ, Halsall HB, Heineman WR. 2010. Electrochemical biosensors. Chemical Society Reviews. 39(5):1747-1763.

Rotariu L, Lagarde F, Jaffrezic-Renault N, Bala C. 2016. Electrochemical biosensors for fast detection of food contaminants-trends and perspective. TrAC Trends in Analytical Chemistry. 79:80-87.

Sahyar BY, Kaplan M, Ozsoz M, Celik E, Otles S. 2019. Electrochemical xanthine detection by enzymatic method based on Ag doped ZnO nanoparticles by using polypyrrole. Bioelectrochemistry. 130:107327.

Salvador ÂC, Santos MdC, Saraiva JA. 2010. Effect of the ionic liquid [bmim] Cl and high pressure on the activity of cellulase. Green Chemistry. 12(4):632-635.

Samphao A, Butmee P, Saejueng P, Pukahuta C, Švorc Ľ, Kalcher K. 2018. Monitoring of glucose and ethanol during wine fermentation by bienzymatic biosensor. Journal of Electroanalytical Chemistry. 816:179-188.

Santos LM, Oliveira FA, Ferreira EH, Rosenthal A. 2017. Application and possible benefits of high hydrostatic pressure or high-pressure homogenization on beer processing: A review. Food Science and Technology International. 23(7):561-581.

Schoemaker HE, Mink D, Wubbolts MG. 2003. Dispelling the myths--biocatalysis in industrial synthesis. Science. 299(5613):1694-1697.

Schuabb V, Winter R, Czeslik C. 2016. Improved activity of α-chymotrypsin on silica particles-A high-pressure stopped-flow study. Biophysical Chemistry. 218:1-6.

Şenel M, Bozgeyik İ, Çevik E, Fatih Abasıyanık M. 2011. A novel amperometric galactose biosensor based on galactose oxidase-poly(N-glycidylpyrrole-co-pyrrole). Synthetic Metals. 161(5):440-444.

Sharma M, Yadav P, Sharma M. 2019. Novel electrochemical sensing of galactose using GalOxNPs/CHIT modified pencil graphite electrode. Carbohydrate Research. 483:107749.

Sheldon RA, Brady D. 2018. The limits to biocatalysis: pushing the envelope. Chemical Communications. 54(48):6088-6104.

Sheldon RA, van Pelt S. 2013. Enzyme immobilisation in biocatalysis: why, what and how. Chemical Society Reviews. 42(15):6223-6235.

Si Y, Park JW, Jung S, Hwang G-S, Goh E, Lee HJ. 2018. Layer-by-layer electrochemical biosensors configuring xanthine oxidase and carbon nanotubes/graphene complexes for hypoxanthine and uric acid in human serum solutions. Biosensors and Bioelectronics. 121:265-271.

Silva NFD, Magalhães JMCS, Freire C, Delerue-Matos C. 2018. Electrochemical biosensors for *Salmonella*: State of the art and challenges in food safety assessment. Biosensors and Bioelectronics. 99:667-682.

Singh R, Kumar M, Mittal A, Mehta PK. 2016. Microbial enzymes: industrial progress in 21st century. 3 Biotech. 6(2):174.

Sirisha VL, Jain A, Jain A. 2016. Enzyme Immobilization: An Overview on Methods, Support Material, and Applications of Immobilized Enzymes. In: Kim S-K, Toldrá F, editors. Advances in Food and Nutrition Research. Academic Press; p. 179-211.

Soganci T, Soyleyici HC, Demirkol DO, Ak M, Timur S. 2018. Use of super-structural conducting polymer as functional immobilization matrix in biosensor design. Journal of The Electrochemical Society. 165(2):B22-B26.

Soldatkin OO, Peshkova VM, Dzyadevych SV, Soldatkin AP, Jaffrezic-Renault N, El'skaya AV. 2008. Novel sucrose three-enzyme conductometric biosensor. Materials Science and Engineering: C. 28(5):959-964.

Soylemez S, Goker S, Toppare L. 2019. A promising enzyme anchoring probe for selective ethanol sensing in beverages. International Journal of Biological Macromolecules. 133:1228-1235.

Srivastava G, Kayastha AM. 2014. β-Amylase from starchless seeds of *Trigonella foenum-graecum* and its localization in germinating seeds. Plos One. 9(2).

Stasyuk N, Gayda G, Zakalskiy A, Zakalska O, Serkiz R, Gonchar M. 2019. Amperometric biosensors based on oxidases and PtRu nanoparticles as artificial peroxidase. Food Chemistry. 285:213-220.

Su E, Xia T, Gao L, Dai Q, Zhang Z. 2010. Immobilization of β-glucosidase and its aroma-increasing effect on tea beverage. Food and Bioproducts Processing. 88(2):83-89.

Sutay Kocabaş D, Grumet R. 2019. Evolving regulatory policies regarding food enzymes produced by recombinant microorganisms. GM Crops & Food. 10(4):191-207.

Tang H, Cai D, Ren T, Xiong P, Liu Y, Gu H, Shi G. 2019. Fabrication of a low background signal glucose biosensor with 3D network materials as the electrocatalyst. Analytical Biochemistry. 567:63-71.

Tarasov S, Emets V, Kluyev A, Andreev V, Reshetilov A. 2018. Impedancemetric Detection of Glucose Using a Biosensor Based on Screen-Printed Electrodes. Protection of Metals and Physical Chemistry of Surfaces. 54(6):1217-1220.

Terefe NS, Delon A, Buckow R, Versteeg C. 2015. Blueberry polyphenol oxidase: Characterization and the kinetics of thermal and high pressure activation and inactivation. Food Chemistry. 188:193-200.

Terefe NS, Sheean P, Fernando S, Versteeg C. 2013. The stability of almond β-glucosidase during combined high pressure–thermal processing: a kinetic study. Applied Microbiology and Biotechnology. 97(7):2917-2928.

Terefe NS, Yang YH, Knoerzer K, Buckow R, Versteeg C. 2010. High pressure and thermal inactivation kinetics of polyphenol oxidase and peroxidase in strawberry puree. Innovative Food Science & Emerging Technologies. 11(1):52-60.

Terry LA, White SF, Tigwell LJ. 2005. The application of biosensors to fresh produce and the wider food industry. Journal of Agricultural and Food Chemistry. 53(5):1309-1316.

Toftgaard Pedersen A, Birmingham WR, Rehn G, Charnock SJ, Turner NJ, Woodley JM. 2015. Process requirements of galactose oxidase catalyzed oxidation of alcohols. Organic Process Research & Development. 19(11):1580-1589.

Tribst AAL, Ribeiro LR, Cristianini M. 2017. Comparison of the effects of high pressure homogenization and high pressure processing on the enzyme activity and antimicrobial profile of lysozyme. Innovative Food Science & Emerging Technologies. 43:60-67.

Uzak D, Atiroğlu A, Atiroğlu V, Çakıroğlu B, Özacar M. 2019. Reduced Graphene Oxide/Pt Nanoparticles/Zn-MOF-74 Nanomaterial for a Glucose Biosensor Construction. Electroanalysis.

Vanderroost M, Ragaert P, Devlieghere F, De Meulenaer B. 2014. Intelligent food packaging: The next generation. Trends in Food Science & Technology. 39(1):47-62.

Vashist SK. 2012. Non-invasive glucose monitoring technology in diabetes management: A review. Analytica Chimica Acta. 750:16-27.

Vila-Real H, Alfaia AJ, Calado AR, Phillips RS, Ribeiro MH. 2011. High pressure: a tool to improve the enzymatic production of glycosides. High Pressure Research. 31(3):475-487.

Vila-Real H, Alfaia AJ, Phillips RS, Calado AR, Ribeiro MH. 2010. Pressure-enhanced activity and stability of α-l-rhamnosidase and β-d-glucosidase activities expressed by naringinase. Journal of Molecular Catalysis B: Enzymatic. 65(1-4):102-109.

Wallace LS. 2017. The effect of high hydrostatic pressure on stability of pyruvate oxidase from *aeroccocus species*. University of Georgia Theses and Dissertations.19-50.

Wang G, Sun J, Yao Y, An X, Zhang H, Chu G, Jiang S, Guo Y, Sun X, Liu Y. 2020. Detection of Inosine Monophosphate (IMP) in Meat Using Double-Enzyme Sensor. Food Analytical Methods. 13(2):420-432.

Wang P, Dai S, Waezsada S, Tsao AY, Davison BH. 2001. Enzyme stabilization by covalent binding in nanoporous sol-gel glass for nonaqueous biocatalysis. Biotechnology and Bioengineering. 74(3):249-255.

Wang Z, Ma B, Shen C, Lai O-M, Tan C-P, Cheong L-Z. 2019. Electrochemical Biosensing of Chilled Seafood Freshness by Xanthine Oxidase Immobilized on Copper-Based Metal-Organic Framework Nanofiber Film. Food Analytical Methods. 12(8):1715-1724.

Wong CM, Wong KH, Chen XD. 2008. Glucose oxidase: natural occurrence, function, properties and industrial applications. Applied Microbiology and Biotechnology. 78(6):927-938.

Wu H, Lee C-J, Wang H, Hu Y, Young M, Han Y, Xu F-J, Cong H, Cheng G. 2018. Highly sensitive and stable zwitterionic poly (sulfobetaine-3, 4-ethylenedioxythiophene)(PSBEDOT) glucose biosensor. Chemical Science. 9(9):2540-2546.

Xavier JR, Ramana KV, Sharma RK. 2018. β-galactosidase: Biotechnological applications in food processing. Journal of Food Biochemistry. 42(5):e12564.

Xie J, Chen C, Zhou Y, Fei J, Ding Y, Zhao J. 2016. A galactose oxidase biosensor based on graphene composite film for the determination of galactose and dihydroxyacetone. Electroanalysis. 28(1):183-188.

Xu L-H, Li J-j, Zeng H-B, Zhang X-J, Cosnier S, Marks RS, Shan D. 2019. ATMP-induced three-dimensional conductive polymer hydrogel scaffold for a novel enhanced solid-state electrochemiluminescence biosensor. Biosensors and Bioelectronics. 143:111601.

Yadav GD, Sajgure AD, Dhoot SB. 2007. Enzyme catalysis in fine chemical and pharmacuetical industries. Enzyme Mixtures and Complex Biosynthesis.79-108.

Yang X, Chen G, Du H, Miao M, Feng B. 2016. Behavior of *Yarrowia lipolytica* Lipase Lip2 under high hydrostatic pressure: Conformational changes and isokineticity diagram. Journal of Molecular Catalysis B: Enzymatic. 127:34-39.

Yao P, Yu S, Shen H, Yang J, Min L, Yang Z, Zhu X. 2019. A TiO 2-SnS 2 nanocomposite as a novel matrix for the development of an enzymatic electrochemical glucose biosensor. New Journal of Chemistry. 43(42):16748-16752.

Yazdanparast S, Benvidi A, Abbasi S, Rezaeinasab M. 2019. Enzyme-based ultrasensitive electrochemical biosensor using poly(l-aspartic acid)/MWCNT bio-nanocomposite for xanthine detection: A meat freshness marker. Microchemical Journal. 149:104000.

Yi J, Feng H, Bi J, Zhou L, Zhou M, Cao J, Li J. 2016. High hydrostatic pressure induced physiological changes and physical damages in asparagus spears. Postharvest Biology and Technology. 118:1-10.

You S, Tu T, Zhang L, Wang Y, Huang H, Ma R, Shi P, Bai Y, Su X, Lin Z. 2016. Improvement of the thermostability and catalytic efficiency of a highly active β-glucanase from *Talaromyces leycettanus* JCM12802 by optimizing residual charge-charge interactions. Biotechnology for Biofuels. 9(1):124.

Yu H, Luo X, Shi W, Sha P, Volmer A, Xiao W, Cui Y. 2018. A Cork-Based Smart Biosensing System for Ethanol. IEEE Sensors Journal. 19(6):2313-2319.

Yu X-W, Yang M, Jiang C, Zhang X, Xu Y. 2017. N-Glycosylation engineering to improve the constitutive expression of *Rhizopus oryzae* lipase in Komagataella phaffii. Journal of Agricultural and Food Chemistry. 65(29):6009-6015.

Zhang Y, Geary T, Simpson BK. 2019. Genetically modified food enzymes: a review. Current Opinion in Food Science. 25:14-18.

Zhao Z, Herbst D, Niemeyer B, He L. 2015. High pressure enhances activity and selectivity of *Candida rugosa* lipase immobilized onto silica nanoparticles in organic solvent. Food and Bioproducts Processing. 96:240-244.

Zuo S, Zhang T, Jiang B, Mu W. 2015. Reduction of acrylamide level through blanching with treatment by an extremely thermostable L-asparaginase during French fries processing. Extremophiles. 19(4):841-851.

Table 1.1. Examples of the enzymes with low stability but having potential applications in the food industry and the strategies undertaken to improve the stability.

Enzymes	Role	Strategy	Stability increase	Reference
β-glucosidase (EC 3.2.1.21)	Aroma enhancement	Immobilization	Reusable for 10 cycles with 70% residual activity	(Agrawal R et al. 2016)
β-amylase (EC 3.2.1.2)	Maltose production	Immobilization	Retained 80% residual activity after 10 uses	(Das R et al. 2017)
		Immobilization	Retained 77% residual activity after 10 uses	(Agrawal DC et al. 2020)
Xylanase (EC 3.2.1.8)	Sensory property improvement in wheat bread, juice clarification, ethanol production optimization	Immobilization	Retained 80% residual activity after storing 30 days at 4 °C	(Kumar et al. 2017)
L-asparaginase (EC 3.5.1.1)	Acrylamide reduction	Screening	The stability increased with the half-life 105 min at 85 °C	(Li X et al. 2018)

		Immobilization	Retained 42% residual activity after 8 continuous reaction cycles	(Monajati et al. 2018)
		DNA recombinant	Retained 70% residual activity after incubating at 85 °C for 2 h	(Zuo et al. 2015)
1,3-1,4-β-glucanases (EC 3.2.1.73)	Degrading β-glucans during barley malting process	DNA recombinant	The half-life time increased at most to 31 min at 80 °C	(You et al. 2016)

Table 1.2. The unit price of oxidases retrieved from Sigma-Aldrich website in Feb. 2020

Enzyme	Unit price (USD per kilo unit)
Glucose oxidase from *Aspergillus niger*	1
Galactose oxidase from *Dactylium dendroides*	91
Alcohol oxidase from *Pichia pastoris*	187
Pyruvate oxidase from *Aerococcus sp.*	2560
Xanthine oxidase from bovine milk	3600

Table 1.3. Stability performance of selected glucose oxidase (GOx) biosensors (2018-)

Enzymes/source	Immobilization methods	Additional methods	Operational life	Storage life	Reference
GOx/*Aspergillus niger*	Entrapment into the chitosan gel onto the screen-printed electrodes	NA	NA	7 days without losing activity	(Tarasov et al. 2018)
GOx/*Aspergillus niger*	Absorption onto glassy carbon electrodes modified by chitosan	GOx was encapsulated in liposomes	NA	Retained 91% response after 48 h, 72% response after 7 days	(Guan et al. 2019)
GOx/*Aspergillus niger*	Adsorption onto glassy carbon electrodes	GOx was mixed with the TiO_2-SnS_2 composite and Nafion	NA	Retained 95% response after storing at 4 °C for 28 days	(Yao et al. 2019)
GOx/*Aspergillus niger*	Adsorption onto glassy carbon electrodes	The electrodes were modified with	10 successive tests with 7.1%	NA	(Uzak et al. 2019)

		platinum nanoparticles decorated reduced graphene oxide hybrid nanomaterial	relative standard deviation (RSD)		
GOx/*Aspergillus niger*	Adsorption onto glassy carbon and carbon paste electrodes	The enzyme was absorbed to the functional silica/lignin hybrid before immobilized to the electrodes	Retained 96% response after 150 scans	Retained 73% response after storing at 4 °C for 3 weeks	(Jędrzak et al. 2018)
GOx/*Aspergillus niger*	Adsorption by layer-by-layer deposition onto gold electrodes	The electrodes were modified with poly(3,4-ethylenedioxythiophene) for better conductivity	NA	Retained 65% response after a month	(David et al. 2018)

GOx/NA	Entrapment by electropolymerization with poly(sulfobetaine-3,4-ethylenedioxythiophene)	NA	NA	Retained 95% response after storing at room temperature in buffer or in air for 7 days	(Wu et al. 2018)
GOx/*Aspergillus niger*	Covalent binding onto the indium tin oxide electrodes	The electrode was modified by bio-derived nitrogen-doped carbon sheets wrapped titanium dioxide nanoparticles	NA	Retained 86% of responses after storing at 4 °C for 20 days	(Atchudan et al. 2019)
GOx/*Aspergillus niger*	Adsorption onto gold interdigital electrodes	The electrodes were modified with zinc oxide rods	Retained 90% responses after the use of 10	NA	(Fathollahzadeh et al. 2018)

			times a day for a week		
GOx/*Aspergillus niger*	Encapsulated in chitosan/κ-carrageenan polyelectrolyte complex	Glutaraldehyde was added after the GOx mixture was applied to the electrode surface	NA	No obvious change in response with 6% RSD after storing at 4 °C for 3 weeks	(Rassas et al. 2019)
GOx/*Aspergillus niger*	Cross-linking by glutaraldehyde	The microfabricated gold electrodes were modified with carbon quantum dots and gold nanoparticles	13 successive measurements with three biosensors with RSD 7.385%, 5.669%, and 4.427%, respectively	NA	(Buk et al. 2019)

GOx/*Aspergillus niger*	Absorption of the mixture of enzymes and core shell Fe_3O_4@Au nanoparticles onto carbon paste electrodes with the aid of an external magnetic field	The electrodes were modified with MnO_2	5 measurements with 2.5% RSD	Retained 50% response after 30 days	(Samphao et al. 2018)
GOx/*Aspergillus niger*	Layer-by-layer deposition through electrostatic interactions by tris-(2-aminoethyl)amine on highly porous metallic cotton fiber electrodes	NA	Retained 97.5% response after continuous operation for 1 h	NA	(Kwon et al. 2018)
GOx/*Aspergillus niger*	Entrapment by sol-gel process on gold nanoflowers modified glassy carbon electrodes	Glutaraldehyde steam was used for cross-linking	NA	Retained 79.53% response after storing at 4 °C for 40 days	(Tang et al. 2019)

GOx/*Aspergillus niger*	Covalent binding to poly (pyrrole-2-carboxylic acid) particles on the graphite rod electrode	Glutaraldehyde and bovine serum albumin were used for cross-linking	NA	Retained 95.3% response after storing at 4 °C for a month	(Kausaite-Minkstimiene et al. 2018)
GOx/*Aspergillus niger*	Covalent binding with glutaraldehyde to poly 5-amino-N^1,N^3- bis (2,5-di(thiophen-2-yl)-1H-pyrrol-1-yl) isophthalamide which was electropolymerized on a graphite electrode	NA	NA	Retained 87.46% response after storing 4 °C for 6 weeks	(Soganci et al. 2018)
GOx/*Aspergillus niger*	Covalent binding with glutaraldehyde to chitosan on the nanostructured copper oxide modified fluorinated-tin oxide electrode	NA	NA	Retained 87.5% response after 35 days	(Naderi Asrami et al. 2018)

NA: not available

Table 1.4. Stability performance of alcohol oxidase (AOx) biosensors (2018-)

Enzymes/source	Immobilization methods	Additional methods	Operational life	Storage life	Reference
AOx/*Hansenula polymorpha*	Adsorption onto the bimetallic PtRu nanoparticle covered graphite electrode and then covered by polymers	NA	NA	Retained 20% response after 14 days, half-life time was 10 days	(Stasyuk et al. 2019)
AOx/*Pichia pastoris*	Covalent binding with the (4,7-di(thiophen-2-yl)benzo[c][1,2,5]selenadiazole-*co*-1*H*-pyrrole-3-carboxylic acid) polymer which was electropolymerized on the graphite electrode	NA	7 consecutive measurements with 1.07% RSD	NA	(Soylemez et al. 2019)

AOx/Ogataea (Hansenula)	Adsorption onto green synthesized nanoparticle modified graphite electrodes and then covered by the mixture of chitosan and polyethyleneimine	NA	NA	Retained ~50% response after 3 days	(Gayda et al. 2019)
AOx/Hansenula sp.	Cross-linking with glutaraldehyde and bovine serum albumin onto carbon paper electrodes	The electrode was modified with Prussian blue-copper film	Retained over 80% response after over 40 measurements within 3.5 h	NA	(Radulescu et al. 2019)
AOx/*Pichia pastoris*	Covalently immobilized onto the inner surface of a polyvinylchloride beaker with glutaraldehyde	Horseradish peroxidase, silver nanoparticles, chitosan, carboxylated multi-wall carbon nanotubes and nafion	Retained 90% response after 20 successive measurements within 6 h	Retained 90% response after storing at 4 °C for 5 weeks	(Hooda et al. 2018)

		were immobilized onto the gold working electrode			
AOX/NA	Cross-linking with glutaraldehyde onto printed carbon nanotube electrodes	NA	NA	Total loss of response after storing at 4 °C for 5 days	(Yu H et al. 2018)

NA: not available

Table 1.5. Stability performance of xanthine oxidase (XOx) biosensors (2018-)

Enzymes/source	Immobilization methods	Additional methods	Operational life	Storage life	Reference
XOx/NA	Layer-by-layer assembly to positively charged poly(diallyldimethyl ammonium chloride) wrapped oxidized carbon nanotubes and graphene complexes on screen printed carbon electrodes	NA	NA	Retained 84% or 50% response after storing at 4 °C for 3 days or 1 week, respectively	(Si et al. 2018)
XOx/bovine milk	Entrapped to copper-based metal organic framework nanofibers and then absorbed onto glassy carbon electrodes	NA	Retained 80 or 70% activity after 100 usage for detecting hypoxanthine or xanthine, respectively	Retained more than 80% response after storing at 4 °C for 20 days	(Wang Z et al. 2019)

XOx/buttermilk	Cross-linking with glutaraldehyde and bovine serum albumin onto glassy carbon electrodes	NA	5 measurements with 2.4% RSD	Retained 75% response after storing at 4 °C for 15 days	(Ben Messaoud et al. 2018)
XOx/bovine milk	Photo-polymerization into an azide-unit pendant water-soluble photopolymer onto screen-printed graphite electrodes	The electrode was modified with Prussian blue	6 h continuous usage	Shelf life 2 days	(Becker et al. 2019)
XOx/bovine milk	Covalent binding with 1-ethyl-3-(3-dimethylaminopropyl) carbodiimide hydrochloride (EDC) and N-hydroxy succinimide (NHS) coupling mechanism onto glassy carbon electrodes modified with poly(L-aspartic acid) film	The electrode was coated with multi-wall carbon nanotubes	5 measurements intra-day RSD 3.9%, inter-day RSD 4.5%	Retained 80% response after storing at 4 °C for 30 days	(Yazdanparast et al. 2019)

XOx/NA	Electrochemical deposition onto polypyrrole film which was previously electropolymerized onto the pencil graphite electrode	The electrode was modified with silver-doped zinc oxide nanoparticles in the polypyrrole film	Retained 76.98% response after 25 measurements	Retained 77.82% response after 20 days	(Sahyar et al. 2019)
XOx/NA	Adsorption onto the glassy carbon electrode	The electrode was modified with polyaniline and silver nanoparticles functionalized by N-(aminobutyl)-N-(ethylisoluminol)	20 continuous scan cycles with RSD 0.992%	Retained 80% response after storing at 4 °C for 2 weeks	(Xu et al. 2019)
XOx/NA	Adsorption onto the glassy carbon electrode	The electrode was modified with MXene and Au@Pt nanoflowers	10 continuous tests with RSD 3.4%	Retained 95% response after storing at 4 °C for 2 weeks	(Wang G et al. 2020)

NA: not available

Table 1.6. Stability performance of pyruvate oxidase (POx) biosensors (2019-)

Enzymes/source	Immobilization methods	Additional methods	Operational life	Storage life	Reference
POx/*Aerococcus sp.*	Covalent binding to the gold electrode treated with piranha solution	Enzyme nanoparticles were used prepared by the desolvation method	NA	Retained 75% response after storing at 4 °C for 240 days	(Malik et al. 2019)
POx/*Aerococcus sp.*	Entrapment via polymerization with photopolymer containing styrylpyridine groups onto platinum electrodes	The electrode was modified with a permselective poly(phenylenediamine) membrane	NA	Retained 82% response after storing at 4 °C for 14 days	(Kucherenko Ivan S et al. 2019)
POx/NA	Adsorption to the gold nanoparticles on the gold electrode	The electrode was modified with (diallyldimethylammonium chloride) functionalized	NA	Retained 87.8% response after storing at 4 °C for 9 days	(He and Liu 2020)

		graphene and cuprous oxide nanodices			
POx/*Aerococcus sp.*	Covalent binding with EDC and NHS to the polymer coated gold electrode	The electrode was modified by the poly(pyrrole-*co*-pyrrole-2-carboxylic acid) film	7 successive measurements with RSD 0.07%	Retained 50% response after storing in the refrigerator for 10, 20, or 30 days	(Korkut et al. 2019)

NA: not available

Table 1.7. Stability performance of galactose oxidase (GaOx) biosensors (2010-)

Enzymes/source	Immobilization methods	Additional methods	Operational life	Storage life	Reference
GaOx/NA	Covalent binding to the poly (glycidyl methacrylate-co-vinylferrocene) coated platinum electrode	NA	Retained 50% response after 17 measurements	Retained 60% response after 30 days	(Çevik et al. 2010)
GaOx/NA	Adsorption onto zinc oxide nanorods	Glutaraldehyde was added to cross-link enzymes	NA	Life time ~4 weeks stored at 4 °C	(Khun et al. 2012)
GaOx/NA	Covalent binding to the poly(N-glycidylpyrrole-co-pyrrole) coated gold electrode	NA	Retained ~50% response after 15 measurements in the same day	Retained 45% response after 35 days	(Şenel et al. 2011)
GaOx/NA	Adsorption onto glassy carbon electrode	The enzyme was mixed with poly(L-	NA	Retained 95% response after	(Xie et al. 2016)

		lactide) modified gold nanoparticles and graphene nanocomposite		storing at 4 °C for 10 days	
GaOx/*Dactylium dendroides*	Adsorption onto the platinum electrode mixed with the laponite clay	Glutaraldehyde steam was used to cross-link the membrane	NA	Retained 75% response after storing at 4 °C for 1 month	(Charmantray et al. 2013)
GaOx/*Dactylium dendroides*	Cross-linking with glutaraldehyde to the glassy carbon electrodes modified with Co_3O_4 nanoparticles, chitosan, and either the multi-wall carbon nanotubes or graphene	Nafion was added to prevent enzyme leakage	5 tests for multi-wall carbon nanotubes or graphene modified with RSD 3.6% or	Retained 60% or 45% response after storing at 4 °C for 1 month for multi-wall carbon nanotubes or	(Dalkıran et al. 2016)

			1.7%, respectively	graphene modified, respectively	
GaOx/*Dactylium dendroides*	Adsorption to the chitosan decorated pencil graphite electrode	Enzyme nanoparticles were used prepared by the desolvation method	NA	Retained 60% response after storing at 4 °C for 90 days	(Sharma et al. 2019)
GaOx/*Dactylium dendroides*	Electropolymerization with polypyrrole and poly(3,4-ethylenedioxythiophene) onto platinum electrodes	NA	NA	Retained 40% response after storing at 4 °C for 1 day	(Gursoy et al. 2018)

NA: not available

Table 1.8. Enhancement effects of high pressure on the enzymes (2009-)

Enzyme/source	Pressures tested (MPa)	Temperature tested (°C)	Optimal conditions	Temperature-pressure test sequence	Effect	Reference
Adenosine monophosphate Deaminase/NA	0-400	20	300 MPa	Pressure alone	Activity increase to 220%	(Huijuan et al. 2018)
Alcohol dehydrogenase/asparagus spear	10-600	20	200-600 MPa	Pressure alone	Activity increase by 20%	(Yi et al. 2016)
Alcohol oxidase/*Pichia pastoris*	0.1-200	49.4-59.1	160 MPa, 49.4 °C	Heat while pressurized	Stability increase by 14-fold	(Buchholz-Afari et al. 2019)
Aminopeptidase (PepN, PepA, PepX, PepC)/*Lactobacillus*	100-700	20-40	200 MPa, 20 °C for 20 min	Heat while pressurized	Activity increase by 3-fold	(Katsaros et al. 2009)

delbrueckii ssp. *bulgaricus*						
α-amylase/*Bacillus subtilis*	0.1-750	10-50	>600 MPa, <20 °C or <200 MPa, >40 °C	Heat while pressured	Antagonistic effect of temperature and pressure	(Grauwet et al. 2009)
Cathepsin B and L/pork semitendinosus	600	NA	600 MPa	Pressure alone	Activity increase by 2-3 fold	(Grossi et al. 2012)
Cathepsin D/mackerel and horse mackerel	150, 300, 450	20	300 MPa	Pressure alone	Activity increase by 2-fold for mackerel and 60% for horse mackerel	(Fidalgo et al. 2014)
Cellulase/*Aspergillus niger*	0.1-600	30	100 MPa for 10 min	Pressure alone	Activity increase by 1.7-fold in 10% [bmin]Cl	(Salvador et al. 2010)

Chymotrypsin/bovine pancreas	0.1-600	37	250 MPa	Heat while pressured	Stability increase by retaining 106% activity instead of 88% without high pressure	(Bruins et al. 2009)
α-chymotrypsin/bovine pancreas	0.1-200	20	200 MPa	Pressure alone (*in-situ* activity determination)	Pressure increased the reaction rate (numeric number unavailable)	(Luong and Winter 2015)
Dextranase/*Chaetomium erraticum*	100-600	25-70	400 MPa, 55 °C	Heat while pressurized	Activity increase by 129%; half-life increase from 9 to 12 min	(Bashari et al. 2014)
Dihydrofolate reductase/*Moritella profunda*	0.1-250	25	50 MPa	Pressure alone	Activity increase to 120%	(Ohmae et al. 2012)
Fructotransferase/*Arthrobacter aurescens*	0.1-600	30-60	200 MPa, 60 °C	Heat while pressured (*in-*	Activity increase by 33.8%	(Li Y et al. 2015a)

				situ activity determination)		
Fructotransferase/NA	100, 200	70, 75, 80	200 MPa, 60 °C for activity; 200 MPa, 80 °C for stability	Heat while pressurized	Activity increase by 13.7%, stability increase by 55.9%	(Li Y et al. 2015b)
Glucose/*Aspergillus niger*	0.1-300	58.8-80.0	240 MPa, 74.5 °C	Heat while pressurized	Stability increase by 50 times	(Halalipour et al. 2017b)
β-glucosidase/almond	50-600	30-70	50 MPa, 60 °C	Heat while pressurized	Stability increase by 1.4-fold	(Terefe et al. 2013)
β-Glucosidase/*Pyrococcus furiosus*	0-900	25, 40, 60	100-400 MPa	Heat while pressured	Stability increase at low pressures (numeric number unavailable)	(Bruins et al. 2008)

β-Glucosidase/strawberry pulp	400, 500, 600	25	400 MPa for 25 min	Pressure alone	Activity increase by 16.6%	(Cao et al. 2011)
Hesperidinase/*Aspergillus niger*	0.1-200	35-75	100 MPa, 45 °C	Heat while pressured	Activity increase by 18-fold	(Furtado et al. 2012)
Lipase/*Thermomyces lanuginosus*	0.1, 100, 300	25	300 MPa	Pressure alone	Activity increase by 2-fold	(Ramos‐de‐la‐Peña and Aguilar 2019)
Lipase/*Rhizopus chinensis*	0.1-600	40	200 MPa, 40 °C	Heat while pressurized	Activity increase to 118%	(Chen et al. 2017)
Lipase (immobilized)/*Candida rugosa*	50, 100, 200	35	50 MPa	Pressure alone	Activity increase to 560%	(Zhao et al. 2015)

Lipase/*Candida rugosa*	50, 100, 200	20-55	200 MPa, 45 °C	Heat while pressurized	Activity increase by 4.8-fold	(Herbst et al. 2014)
Lipase/*Candida antarctica*	0.1-400	36-80	400 MPa, 80 °C for stability; 350 MPa, 80 °C for activity	Heat while pressurized	Stability increase by 152%, activity increase by 239%	(Eisenmenger and Reyes-De-Corcuera 2009a)
Lipase/*Yarrowia lipolytica*	100-600	25-60	450 MPa, 40 °C for 10 min for activity; 400 MPa, above 35 °C for stability	Heat while pressurized	Activity increase to 209%; stability increase (numeric number unavailable)	(Yang et al. 2016)
Lipase/*Candida antarctica*	0.1-250	40, 80	200 MPa, 40 or 80 °C	Heat while pressured	Activity increase by 10-fold	(Eisenmenger and Reyes-De-Corcuera 2010)

Lipoxygenase/green chili paste	100-600	30, 50	100 MPa, 30 °C for 20 min	Heat while pressurized	Activity increase to 126%	(Apichartsrangkoon et al. 2013)
Lysozyme/hen egg white	100-600	20, 50	400 MPa, 20 °C for 10 min	Heat while pressurized	Activity increase by 16.7%	(Tribst et al. 2017)
Myrosinase/black mustard seed	200-800	30-80	300 MPa, 80 °C	Heat while pressurized	Stability increase by retaining ~50% activity instead of fully inactivation without high pressure	(Okunade et al. 2015)
Naringinase/*Penicilliu m decumbens*	150	25-80	150 MPa, 80 °C	Heat while pressured	Stability increase by 4-fold, activity increase by having a negative activation volume	(Vila-Real et al. 2010)

Naringinase/*Penicilliu m decumbens*	0.1-250	75, 85	250 MPa, 85 °C	Heat while pressurized	Stability increase by 32-fold for α-L-rhamnosidase	(Vila-Real et al. 2011)
Peroxidase/*L. caerulea* berry	0.1-600	Room temperature	200 MPa for 10 min	Pressure alone	Activity increase by 181.89%	(Liu et al. 2016)
Peroxidase/green chili paste	100-600	30, 50	300 MPa, 30 °C for 20 min	Heat while pressurized	Activity increase to 107%	(Apichartsra ngkoon et al. 2013)
Peroxidase/strawberry puree	100-690	24-90	100-400 MPa	Heat while pressured	Antagonistic effect between pressure and temperature	(Terefe et al. 2010)
Peroxidase/feijoa puree	300, 450, 600	25	300 MPa for 5 min	Pressure alone	Activity increase to 140%	(Ortuño et al. 2013)
Peroxidase/apricot nectar	300, 400, 500	25	500 MPa for 5 min	Pressure alone	Activity increase by 46.8%	(Huang Wenshu et al. 2013)

Peroxidase/garlic	200, 400, 600	30	200 MPa	Pressure alone	Activity increase by 9%	(Eroman Unni et al. 2014)
Peroxidase/pineapple puree	0.1-600	30-70	200-300 MPa	Heat while pressurized	Stability increase (numeric number available)	(Chakraborty et al. 2015)
Pectinmethylesterase/non-astringent persimmon	200, 400	25	200 MPa or 400 MPa for 6 min	Pressure alone	Activity increase by 4-5 fold	(Rodríguez-Garayar et al. 2017)
Pectinmethylesterase/asparagus spear	10-600	20	200 MPa	Pressure alone	Activity increase by 20%	(Yi et al. 2016)
Pectinmethylesterase/peach pulp	0.1-800	30-70	100-600 MPa at 70 °C	Heat while pressured	Antagonistic effect between pressure and temperature	(Boulekou et al. 2010)

Polygalacturonase/astringent persimmon	200, 400	25	200 MPa for 3 min	Pressure alone	Activity increase by ~1.6 fold	(Rodríguez-Garayar et al. 2017)
Polyphenol oxidase/peach	100-600	25-45	200 MPa, 45 °C	Heat while pressurized	Activity increase by 66.5%	(Bleoanca et al. 2018)
Polyphenol oxidase/garlic	200, 400, 600	30	200 MPa	Pressure alone	Activity increase by 20%	(Eroman Unni et al. 2014)
Polyphenol oxidase/pineapple puree	0.1-600	30-70	200-300 MPa	Heat while pressurized	Stability increase (numeric number available)	(Chakraborty et al. 2015)
Polyphenol oxidase/*L. caerulea* berry	0.1-600	Room temperature	200 MPa for 10 min	Pressure alone	Activity increase by 156.55%	(Liu et al. 2016)
Polyphenol oxidase/green chili paste	100-600	30, 50	100 MPa, 30 °C for 20 min	Heat while pressurized	Activity increase to 125%	(Apichartsrangkoon et al. 2013)

Polyphenol oxidase/whiteleg shrimp	0.1-600	25	300 MPa, 25 °C, 1.5 min	Pressure alone	Activity increase by 57.61%	(Huang Wanyou et al. 2014)
Polyphenol oxidase/apricot nectar	300, 400, 500	25	300 MPa for 5 min	Pressure alone	Activity increase by 41.5%	(Huang Wenshu et al. 2013)
Polyphenol oxidase/blueberry	100-690	30-90	500 MPa, 30 °C for 20 min	Heat while pressurized	Activity increase by 6.1-fold	(Terefe et al. 2015)
Polyphenol oxidase/apple juice	0.1-700	20-80	400 MPa, 20 °C for 5 min for activity; 0.1-300 MPa for stability	Heat while pressured	Activity increase by 65%; antagonistic effects of pressure and temperature	(Buckow et al. 2009)
X-prolyl dipeptidyl aminopeptid	100-450	20, 30, 40	200 MPa, 20 °C	Heat while pressurized	Activity increase with the rate of activation 0.0017 min^{-1}	(Giannoglou et al. 2018)

ase/*Streptococcus thermophilus*						
Protease/bovine meat and porcine meat	60, 111, 194	-5, -10, -20	111 MPa for beef, 193 MPa for pork	Pressure alone	Activity increase by 25% for beef and 66% for pork.	(Malinowska-Pańczyk and Kołodziejska 2018)
Pyruvate decarboxylase/asparagus spear	10-600	20	Pressures higher than 100 MPa	Pressure alone	Activity increase by 30-40%	(Yi et al. 2016)
a-L-rhamnosidase/NA	0.1-400	30-70	150 MPa, 50 °C at pH 6.0	Heat while pressurized	Activity increase by 1.5-fold, thermostability increased by 2-4 fold	(Kim D-Y et al. 2016)
Superoxide dismutase/chestnut rose berry	100-500	30-50	30 °C at pressures above 100	Heat while pressurized	Activity increase by ~38%	(Hou et al. 2019)

			MPa for 20 min			
Trypsin/bovine pancreas	0.1, 300	40-60	300 MPa, 55 °C	Heat while pressurized	Stability increase by ~90-fold	(Kim N and Kim 2012)
Trypsin/bovine pancreas	100, 300	37	300 MPa	Heat while pressurized	Activity increase by 36.8%	(Kim N et al. 2013)
Xanthine oxidase/bovine milk	0.1-300	55-70	300 MPa, 70 °C	Heat while pressurized	Stability increase by 9.5-fold	(Halalipour et al. 2017a)
Xylanase/*Dictyoglomus thermophilum*	0.1-500	20-80	100 MPa, 80 °C	Heat while pressurized	Activity increase by 13%	(Li H et al. 2015)

NA: not available.

High pressure homogenization and high-pressure CO_2 are not included in this table.

CHAPTER 2

INCREASED THERMAL STABILITY OF A GLUCOSE OXIDASE BIOSENSOR UNDER HIGH HYDROSTATIC PRESSURE [1]

[1] Yang, D., Olstad, H.E., and Reyes-De-Corcuera J.I. 2020. *Enzyme and Microbial Technology.* 134:109486. Reprinted here with permission of the publisher.

Abstract

We report the effects of high hydrostatic pressure (HHP), immobilization in electrochemically generated poly-*o*-phenylenediamine nano-films, and reticulation with glutaraldehyde on the thermal stability of glucose oxidase (GOx). The pseudo-first-order rate constant of inactivation of immobilized GOx inactivated at 70 °C and atmospheric pressure was 20.6 times smaller than that of GOx in solution under the same conditions. Immobilized GOx inactivated at 70 °C and 180 MPa was 87.6 times more stable than GOx in solution inactivated at 70 °C and atmospheric pressure. However, applying high pressure during electropolymerization or cross-linking with glutaraldehyde only had minor influences on GOx thermal stability. The stabilizing effect of HHP was not retained upon depressurization.

Keywords: glucose oxidase; high hydrostatic pressure; biosensor; electropolymerization; cross-linking; enzyme stabilization

2.1. Introduction

Glucose oxidase (GOx) (EC 1.1.3.4) catalyzes the oxidation of β-D-glucose by oxygen to D-glucono-1,5-lactone and hydrogen peroxide. It is a flavin-dependent homodimer of approximately 160 kDa. Glucose oxidase has been widely used in industries including clinical, food, chemical, and biotechnology [1]. Glucose biosensors that use immobilized GOx have been extensively researched and used in the clinical industry for the last four decades [2]. Among all glucose biosensors, electrochemical glucose biosensors are the most frequently researched and are further classified as potentiometric, amperometric, or impedimetric/conductometric biosensors based on their transduction signal [2]. In first-generation amperometric glucose biosensors like the ones presented in this research, glucose oxidase is immobilized onto the surface of an electrode. The electrode potential is typically set to 700 mV *vs.* Ag|AgCl. As glucose diffuses into the immobilized GOx layer, it is oxidized into gluconic acid and hydrogen peroxide. Then, at the surface of the metal electrode, hydrogen peroxide is oxidized exchanging two electrons and producing an electrical current that is a function of the concentration of glucose in the sample. Glucose biosensors are calibrated by correlating the current response to solutions of known concentration of glucose.

Practical enzyme biosensors overcome the long sample analysis time and the complexity of conventional methods such as chromatographic or electrophoretic separations followed by spectrophotometric or electrochemical detection of individual analytes. Thus, biosensors provide a low-cost, fast, sensitive, and specific response to analytes in complex mixtures [3]. The global market of all types of biosensors was estimated at approximately 12 billion dollars in 2015 [4]. In the food industry, biosensors can be used to detect food components, pathogens, and food contaminants [5, 6]. Potentially, some biosensors can be integrated into food packaging [7].

However, the major market for enzyme biosensors is in medical care. The most successfully commercialized biosensors are GOx biosensors used to detect glucose for individuals with diabetes [4]. The main limitation that greatly hampers the development of practical enzyme biosensors, including GOx biosensors, is their short operational life which is due to the poor stability of enzymes [8].

High hydrostatic pressure (HHP) has been normally used to kill microbes and inactivate enzymes in food processing. However, at moderate levels, high pressure stabilizes and activates some enzymes [9]. The protective effect of HHP enables enzymes to remain active at temperatures above those that, at atmospheric pressure, would denature them. The increase in temperature also results in a faster reaction rate [10]. This stabilization effect has mainly been observed at temperatures above 50 ˚C and pressures below 400 MPa [11]. However, the stabilizing effect of HHP is lost upon depressurization, limiting the application of this approach to the availability of HHP reactors. We have recently reported the stabilization of glucose oxidase [12], alcohol oxidase [13], xanthine oxidase [14], and pyruvate oxidase [15] by HHP.

Stabilization of enzymes by immobilization has been well documented and reviewed [16-18]. A simple method of enzyme immobilization is the physical entrapment in electrochemically generated polymers. These polymers can be grown from aqueous solutions that contain both the enzyme and the monomer. When a sufficiently oxidizing potential is applied to the electrode, the monomer loses electrons and polymerizes. These polymers grow on the surface of the electrode and typically adhere well to the electrode surface [19]. Non-conducting polymers like poly(*o*-phenylenediamine) (PoPD), polyphenol, or poly(dichlorophenolindophenol) produce very thin, compact films that result in biosensors with fast response time, improved selectivity, and anti-fouling properties [20]. High storage stability of glucose biosensors with GOx immobilized in

PoPD films has been reported [21-26]. Among other immobilization methods, inter- and intra-molecular cross-linking have also been commonly used to stabilize proteins. Glutaraldehyde (GA) is one of the most commonly used cross-linkers [27]. Cross-linking with GA has increased the thermostability of enzymes [28]. Glutaraldehyde reacts mainly with the primary amino side groups of proteins and increases the stability of enzymes by restricting the conformation changes, i.e. protein unfolding. Three approaches to immobilize GOx by cross-linking with GA are commonly used: 1) Cross-linking GOx before the enzyme is immobilized onto supports with other techniques [29-31]; 2) Cross-linking as the method to bind GOx onto the support [32]; 3) Cross-linking after the enzyme has been immobilized [33]. In order to better cross-link with GA, glucose oxidase is often mixed with bovine serum albumin (BSA) before the addition of GA [34-37]. However, though the thermostability of the enzymes can be improved by the newly created microenvironment and the increased rigidity, the harsh conditions of immobilization sometimes inactivate the enzymes [38]. The effectiveness of the methods of immobilization to increase the stability of an enzyme depends also on the enzyme itself and has to be evaluated on a case-by-case basis [39].

To the best of our knowledge, high pressure has not been applied during enzyme immobilization or inactivation of immobilized enzymes to improve the stability of enzyme biosensors against thermal treatment. We hypothesized that combining HHP with electropolymerization of *o*-phenylenediamine (oPD) or cross-linking improves the stability of GOx-based biosensors.

Therefore, the objectives of this study were 1) to assess the effect of HHP during electropolymerization on the thermal stability of GOx biosensors, 2) to combine HHP and cross-

linking with GA to enhance the stability of GOx biosensors, and 3) to assess the effect of HHP during thermal inactivation on the stability of immobilized GOx.

2.2. Material and methods

2.2.1. Materials

Glucose oxidase from *Aspergillus Niger* (Product Number G7141), D-(+)-glucose, bovine serum albumin, and chloroplatinic acid hexahydrate were purchased from Sigma-Aldrich (St. Louis, MO, USA). Potassium phosphate monobasic, sodium acetate trihydrate, glutaraldehyde (25%), potassium chloride, and sulfuric acid were purchased from Fisher Scientific (Hampton, NH, USA). Lead (II) acetate trihydrate and *o*-phenylenediamine were purchased from Acros Organics (Geel, Belgium). All chemicals were reagent grade and solutions were made with ultrafiltered water, resistivity 18.2 MΩ cm^{-1}.

2.2.2. Equipment

Reference 600 potentiostats from Gamry Instruments (Warminster, PA, USA) were used for cyclic voltammetry, chronoamperometry, and chronocoulometry experiments. Framework or Echem computer programs from Gamry were used to operate the potentiostat or analyze data, respectively.

The high pressure system used in this research consisted of a piston pump (model MP5), a jacketed high pressure reactor (model U111), and a controller unit from Unipress Equipment (Warsaw, Poland). The system was previously described in the report by Halalipour, et al. [12], with the difference that the cap of the high pressure reactor had electrical feed-through connectors rated up to 700 MPa to carry out the electropolymerization under high pressure, shown in Fig. 2.1A.

2.2.3. Methods

2.2.3.1. Fabrication of electrochemical cell

An electrochemical cell was designed and fabricated specifically for the high pressure reactor in this research as shown in Fig. 2.1A. The cell was made of a silicone tubing (3 cm long, 0.95 cm outside diameter, 0.64 cm inside diameter) enclosed with one polytetrafluoroethylene cap (0.5 cm thick, 0.8 cm diameter) that holds the working and counter electrodes (platinum wire, 1.6 cm long, 0.8 mm diameter) (Fig. 2.1B) and one reference electrode. Pellets of Ag|AgCl mounted on silver wires were purchased from Warner Instruments (Hamden, CT, USA). The Ag|AgCl pellet was inserted in a heat shrinking tube filled with 3 M KCl with a porous glass frit heat-sealed at one end. Then, the silver wire was sealed at the other end with epoxy glue to form the bottom cap of the cell.

2.2.3.2. Fabrication of GOx biosensor

The method of fabricating a first generation glucose oxidase biosensor in this research was modified from Reyes-De-Corcuera, et al. [25].

2.2.3.2.1. Platinum electrodes preparation

The cap with platinum electrodes (Fig. 2.1B) was polished and cleaned before each use. The electrodes were sequentially polished with abrasive paper P320 grit, a nylon disk with 0.3 μm alumina slurry, and a microcloth disk with 0.05 μm alumina slurry. When reused, only the microcloth disk with 0.05 μm alumina slurry was needed. The electrodes were immersed in an ultrasound bath (output frequency 40 kHz) for 15 min in deionized water and immersed in concentrated sulfuric acid overnight. The electrodes were finally electrochemically cleaned in 0.1 M H_2SO_4 by cyclic voltammetry from -0.189 V to 1.461 V *vs.* Ag|AgCl in 3.5 M KCl at 500 mV s^{-1} for 80 cycles. The electrodes were rinsed with deionized water between each step.

To increase the surface area, platinum electrodes were platinized by chronocoulometry in 2 mM H_2PtCl_6, 1 mM $Pb(C_2H_3O_2)$, 0.1 M KCl deaerated solution at -0.089 V *vs.* Ag|AgCl in 3.5 M KCl to reach the total charge density 2.0 mC cm^{-2}. The electrodes were then ultrasonicated in 0.1 M phosphate buffer (pH 7) for 10 min to remove any loosely bound platinum deposit. Cyclic voltammetry in 0.5 M H_2SO_4 was carried out at 500 mV s^{-1} from -0.238 V to 1.211 V *vs.* Ag|AgCl in 3.5 M KCl for 10 cycles after the ultrasonic treatment to determine the electrochemical surface area of the electrodes as shown in Fig. 2.1C.

2.2.3.2.2. Enzyme immobilization and electrode characterization

Glucose oxidase was immobilized on the working electrode by entrapment in poly-*o*-phenylenediamine (PoPD) films electrochemically generated from the deaerated solution containing 10 mg mL^{-1} glucose oxidase, 5 mM oPD, and 0.2 M acetate acid buffer (pH 5.2). Cyclic voltammetry was carried out at 100 mV s^{-1} from 0 to 0.65 V *vs.* Ag|AgCl in 3.0 M KCl for 100 cycles. Platinized electrodes were immersed in the solution for 5 min before starting the electropolymerization to allow solution diffusion into the black platinum porous surface of the electrode.

The amperometric response of the electrodes was measured at 0.711 V *vs.* Ag|AgCl in 3.5 M KCl in stirred 0 to 20 mM glucose solutions. The sensitivity of the biosensors was determined as the slope of the calibration curves (current density *vs*. glucose concentration).

2.2.3.3. Effect of HHP during immobilization on the stability of GOx biosensors

The electropolymerization was carried out at 0.1 to 420 MPa. Immobilization treatments were carried out in triplicate. Then, each electrode was heated at 70 °C in 0.1 M phosphate buffer (pH 7) in a water bath for an accumulated time of 20, 40, 60, 120, and 180 min and were placed in 0.1 M phosphate buffer (pH 7) on ice for 5 min before measuring the amperometric response to 20

mM glucose solution at 25 °C. The stability of each biosensor was characterized in terms of the percent residual amperometric response *vs.* heat treatment time relative to the response at time 0 (fresh electrodes).

2.2.3.4. Effect of cross-linking on the stability of GOx biosensors

Before electropolymerization, GOx was either cross-linked with 0.5% (w/v) GA in 0.2 M acetate acid buffer (pH 5.2) at room temperature for 6 or 12 h at 0.1 or 180 MPa, or cross-linked with the mixture of 0.5% (w/v) GA and BSA (BSA: GOx = 1:1) at room temperature for 1 h at 0.1 or 180 MPa. Cross-linking agents were separated by pumping through a 5 mL HiTrap™ desalting column from GE Healthcare (Pittsburgh, PA, USA) to stop the reaction. The concentration of GOx was adjusted with 0.2 M acetate acid buffer (pH 5.2) to 10 mg mL^{-1} by measuring the absorbance at 280 nm relative to fresh enzyme. The cross-linked GOx was immobilized at 0.1 or 180 MPa and the resulting biosensors were characterized as described in sections 2.3.2 and 2.3.3.

Cross-linking was also carried out after electropolymerization. Glucose biosensors fabricated at 0.1 or 180 MPa were immersed in 2.5 or 5% (w/v) glutaraldehyde solutions at room temperature for 10 or 30 min at 0.1 MPa. The stability of the biosensors against thermal treatments was done as described in sections 2.3.2 and 2.3.3. All electrode fabrication conditions were done in triplicate.

Pressure 180 MPa was chosen because it was optimal for GOx stability [12].

2.2.3.5. Effect of HHP during thermal treatment on the stability of immobilized GOx

Enzyme immobilization by electropolymerization was carried out at 0.1 or 180 MPa. Electrodes fabricated at atmospheric pressure were heated at 70 °C in 0.1 M phosphate buffer (pH 7) in the high pressure reactor for an accumulated time of 0, 20, 40, 60, 120 and 180 min at 0.1, 180, or 360 MPa. Electrodes fabricated at 180 MPa were heated at 180 MPa. The electrodes were

cooled to 10 °C before measuring the amperometric response at room temperature. All treatments were done in triplicate.

2.2.4. Data analysis

Pseudo-first-order and pseudo-second-order models were used to fit the residual current density response of the electrodes as a function of time. For the pseudo-first-order model, the rate constant of inactivation (k_{inact}) was calculated from the linear regression of the natural logarithm of relative current density response to 20 mM glucose solution *vs.* treatment time. For the pseudo-second-order model, the rate constant of inactivation (k'_{inact}) was calculated from the linear regression of the reciprocal of the relative current density response *vs.* treatment time. Mean values ± 95% confidence intervals are reported. Statistical analysis was conducted by Minitab 16 software (State College, PA, USA) and JMP Pro 14 software (Cary, NC, USA). MATLAB software was used for non-linear model fitting. Tukey's method and Dunnett's method for multiple comparisons were used.

2.3. Results and discussion

2.3.1. Electrode inactivation model fitting

During thermal treatment, the current response of GOx biosensors decreased with treatment time. This can be attributed to the thermal inactivation of GOx, the leaching of GOx out of the oPD polymer matrix when heated, and/or the degradation of oPD polymer [40]. The decrease in the biosensor current response was most likely due to enzyme inactivation because there were only minor changes of current response to phosphate buffer in the absence of glucose throughout the entire duration of the thermal treatment. Therefore, it was unlikely that the degradation of polymer had a pronounced effect on the decrease in current response. Biosensor current response

was calculated as the difference of the current response to 20 mM glucose solution in 0.1 M phosphate buffer pH 7.0 and a glucose-free buffer solution.

The rate constant of inactivation was calculated using pseudo-first-order or pseudo-second-order models. The means of coefficient of determination (R^2) were used to partially assess model fit for all the experimental conditions of this study (Tables 2.1-2.4). The means and standard deviations of R^2 for all the experimental conditions of the pseudo-first-order and pseudo-second-order models were 0.84 ± 0.05 and 0.96 ± 0.03, respectively. Non-linear fitting of relative current density response *vs.* treatment time for the pseudo first and second order models confirm that the pseudo-second-order model fitted better the inactivation of the enzyme biosensor as shown in Fig. S2.1. As the level of inactivation decreased, the fit to the pseudo-first-order model improved but remained inferior to the pseudo-second-order model (Fig. S2.2). Although MATLAB and other statistical software calculate R^2 for non-linear regressions as a partial indicator of fit, it is not valid to compare it to that of a linear regression [41]. Figures S2.1 and S2.2 show that the fitting of the non-linear regression is not better than the linear fitting of the pseudo-second-order linearized data. Therefore, the pseudo-second-order model fitted better than the pseudo-first-order model and was used to compare results within this report. This is in agreement with Dumont and Fortier [40], stating the second-order model was adequate for the inactivation at 55 to 65 °C of immobilized GOx by electropolymerization into the films of polyaniline, polyindole, polypyrrole, PoPD, or poly(aniline/*p*-phenylediamine). Similarly, Ulbrich, et al. [42] found that the thermal inactivation of immobilized α-amylase, α-chymotrypsin, and trypsin followed biphasic kinetics rather than first-order kinetics of enzymes in solution. They suggested that the biphasic kinetics resulted from two different pathways of inactivation of the same enzyme caused by immobilization. However, many other studies have fitted a first-order model to the inactivation of GOx: in solution at 70 °C

[43], encapsulated in liposomes inactivated at 45 to 55 °C [44], and immobilized by absorption and cross-linking inactivated at room temperature [45]. Therefore, to compare results with other reports specifically concerning soluble GOx, pseudo-first-order model is also reported and discussed. Moreover, our data does not offer a mechanistic explanation for the pseudo-second order, though deviation from the most often reported pseudo-first-order indicates that the immobilization matrix contributes non-linearly to the kinetics of inactivation.

2.3.2. Effect of high pressure during immobilization on the stability of GOx biosensors

Table 2.1 shows the sensitivity, apparent Michaelis-Menten constant (K_m^{app}), k_{inact} and k'_{inact} for GOx biosensors fabricated at 0.1 to 420 MPa. For GOx biosensors fabricated at different pressures k'_{inact} ranged from $(1.9 \pm 2.0) \times 10^{-4}$ min^{-1} to $(3.3 \pm 1.0) \times 10^{-4}$ min^{-1}. Immobilization pressure didn't have a significant influence ($p > 0.05$) on the thermostability of biosensors based on k'_{inact} when treating the biosensors at 70 °C and 0.1 MPa. However, in our previous study, pressure had a stabilizing effect on the soluble GOx against thermal treatment and was at most ~20 times slower when inactivated at HHP and 69.1 °C [12]. This contradicted our hypothesis that the conformation changes of an enzyme under high pressure would be retained after depressurization when the enzyme was entrapped at HHP and would result in a more stable biosensor. Immobilization at HHP didn't have a significant influence ($p > 0.05$) on either the sensitivity or the K_m^{app}. Therefore, the enzyme was not inactivated at the pressures applied. For all the electrodes tested, the current response began to level off at glucose solution concentrations above 20 mM. This suggested that the entrapment of the enzyme was consistent for all electrodes, and pressure didn't affect the permeability of the polymer. The sensitivity of the biosensors, $(3.0 – 4.5) \times 10^{-3}$ $\mu A\ mm^{-2}\ mM^{-1}$, was in accordance with the other report using electropolymerization of oPD to immobilize GOx which was in the range of $(2.0 – 7.0) \times 10^{-3}$ $\mu A\ mm^{-2}\ mM^{-1}$ [23]. The K_m^{app}, (21.2

± 22.9 – 35.2 ± 13.2) mM, at any immobilization pressure at pH 7.0 was higher than 17.5 mM at pH 5.1 reported by Halalipour, et al. [12] and was not significantly different from 33 mM at pH 5.6 reported by Swoboda and Massey [46], both using soluble GOx from *A. niger*. The fact that the K_m^{app} of the immobilized enzyme is not different from the K_m^{app} of the enzyme in solution indicates that the biosensor response is under kinetic and not under diffusion control. This is explained by the small thickness of PoPD film (~20 nm) [25, 47]. Therefore, it is adequate to use the current density as the indirect measurement of enzyme activity and as an indicator to determine the enzyme inactivation.

2.3.3. Effect of cross-linking on the stability, sensitivity and K_m^{app} of GOx biosensors

2.3.3.1 Cross-linking before immobilization

Table 2.2 shows the sensitivity, K_m^{app}, k_{inact}, and k'_{inact} of GOx biosensors using GOx that was cross-linked with 0.5% (w/v) GA at 0.1 or 180 MPa before immobilization. The results when BSA was added or not were analyzed separately. In the absence of BSA, there was no statistically significant interaction between immobilization pressure, cross-linking pressure, and cross-linking reaction time ($p > 0.05$). In contrast, the simple main effect of pressure during immobilization on k'_{inact} was significant ($p < 0.01$) using the general linear model (GLM). The k'_{inact} of GOx biosensors immobilized at 180 MPa was up to two times greater than for GOx immobilized at 0.1 MPa, but it was not affected significantly by the reaction time (6 or 12 h) with GA (without BSA) or by the pressure applied during cross-linking. Adding BSA during cross-linking with GA did not affect the stability of the biosensors as indicated by the lack of significant difference ($p > 0.05$) on the k'_{inact}. Compared to the data in Table 2.1, biosensors cross-linked without BSA immobilized at 180 MPa and biosensors cross-linked with BSA immobilized at either 0.1 or 180 MPa had k'_{inact} significantly higher than biosensors fabricated at 0.1 MPa without any cross-linking based on

Dunnett's method. Therefore, cross-linking without BSA at 180 MPa or cross-linking with BSA at either pressure before immobilization decreased the thermostability. The lowest k'_{inact} when cross-linked with GA was $(5.1 \pm 1.8) \times 10^{-4}$ min^{-1} and the thermostability was 2.4 times less than the untreated GOx biosensors with k'_{inact} $(2.1 \pm 0.7) \times 10^{-4}$ min^{-1}. This was in agreement with the report by Busto, et al. [48], showing the humic-carboxymethyl cellulase cross-linked with GA became less stable. But the reason why thermostability decreased is unclear. Therefore, under the conditions of this study, cross-linking with GA or with GA and BSA did not add to the stability of GOx biosensors. Furthermore, immobilization at HHP by entrapment with cross-linked GOx resulted in less stable biosensors which contradicted our hypothesis. This suggests that either the cross-linking destabilized the enzyme or affected the growth of the film, resulting in a less compact polymer that restricts the enzyme less and prevents to a lesser extent the unfolding of the protein.

As for the sensitivity, though the immobilization pressure and the cross-linking pressure didn't have significant influence ($p > 0.05$) on the sensitivity when using BSA during cross-linking, two-way ANOVA and GLM indicated an interaction of immobilization pressure and cross-linking reaction time, an interaction between immobilization pressure and cross-linking pressure, and the main effect of cross-linking pressure had significant influence ($p < 0.05$) on the sensitivity of biosensors without using BSA during cross-linking. Without using BSA, the sensitivity was significantly higher when cross-linked at 0.1 MPa than when cross-linked at 180 MPa. Compared to the data in Table 2.1, the sensitivity of biosensors with cross-linking was higher than the biosensors without cross-linking. The lowest sensitivity when using cross-linked GOx was $(5.6 \pm 0.9) \times 10^{-3}$ $\mu A\ mm^{-2}\ mM^{-1}$ and the highest was $(9.6 \pm 0.9) \times 10^{-3}$ $\mu A\ mm^{-2}\ mM^{-1}$, which was 1.3 and 2.2 times greater than that of the control biosensor $(4.4 \pm 0.9) \times 10^{-3}$ $\mu A\ mm^{-2}\ mM^{-1}$. This was in contrast to the findings in literature where the activity of enzymes was decreased after

cross-linking or increasing the concentration of GA [48, 49]. One possible explanation is that greater concentrations of GOx were entrapped when immobilizing the cross-linked conjugate than the free enzyme. However, we do not have a quantitative measurement of the amount of GOx immobilized.

Similar to sensitivity, the immobilization pressure and cross-linking pressure didn't have significant influence ($p < 0.05$) on the K_m^{app} when using BSA, but the interaction between cross-linking pressure and cross-linking reaction time and the main effect of immobilization pressure had significant influence ($p < 0.05$) without using BSA. When the cross-linked GOx was immobilized at 180 MPa without using BSA, the K_m^{app} was higher than the biosensors immobilized at 0.1 MPa. Compared to the biosensors immobilized at 0.1 MPa without cross-linking in Table 2.1 with Dunnett's method, there was no significant difference in K_m^{app} between the control biosensors and the cross-linked GOx without using BSA and immobilized at 0.1 MPa, or between the control and the cross-linked GOx using BSA. But the cross-linked GOx without using BSA and immobilized at 180 MPa had a K_m^{app} that was significantly higher than the untreated biosensors. The highest K_m^{app} was 50.0 ± 10.4 mM which was 1.8 times higher than the untreated biosensors with K_m^{app} 28.4 ± 5.7 mM. This suggests that rearrangement of the conformation of the cross-linked enzyme conjugate entrapped in PoPD under high pressure hindered the access of the substrate to the active sites or produced a more compact polymer with reduced substrate permeability, which may also be the reason for the lower sensitivity mentioned above.

2.3.3.2. Cross-linking after immobilization

The sensitivity, k_{inact}, and k'_{inact} for the biosensors cross-linked with 2.5 or 5% (w/v) GA after the GOx immobilized at 0.1 or 180 MPa are shown in Table 2.3. There was no significant difference ($p > 0.05$) among the rate constant of inactivation by different immobilization pressure,

GA concentration, or cross-linking reaction time. However, all the k'_{inact} ($0.5 \pm 0.4 – 1.0 \pm 0.4$) × 10^{-4} min^{-1} were significantly lower ($p < 0.01$) than the biosensors without cross-linking immobilized at 0.1 MPa with the k'_{inact} (2.1 ± 0.7) × 10^{-4} min^{-1}. The cross-linking after immobilization made the biosensors approximately two times more stable than the untreated biosensors. Therefore, glutaraldehyde was able to diffuse into the polymer structure and probably resulted in intermolecular and/or intramolecular cross-linking with GOx which further restricted the unfolding of proteins under thermal treatment. The increase in stability can also be due to the prevention of enzyme leaching out from the polymer. Bhushan, et al. [50] and Kumar, et al. [51] used GA to cross-link with xylanase entrapped in alginate beads which reduced the impact of enzyme leaching by forming aggregates, thus improved the stability. Kowal and Parsons [52] also reported that GA cross-linking decreased the leakage of lactoperoxidase immobilized on Sepharose; and the higher concentration of GA resulted in less leakage and lower enzyme activity. However, Betancor, et al. [33] reported that the different concentration of GA didn't make any significant difference on the thermostability of enzymes which was in accordance with our results. This suggested that the different cross-linking conditions used in this research resulted in similar degree of cross-linking. However, the degree of cross-linking was not verified. In our preliminary experiments, excessive cross-linking from high concentration of GA (> 5% w/v) and long reacting time (overnight) with or without BSA resulted in non-functional electrodes.

The immobilization pressure significantly influenced ($p < 0.01$) biosensor sensitivity. Compared to Table 2.1, cross-linking GOx after entrapment in PoPD films electropolymerized at 0.1 MPa had minor effect on the sensitivity. In contrast, cross-linking GOx after entrapment in PoPD films electropolymerized at 180 MPa decreased the sensitivity up to approximately four times, suggesting cross-linking with the enzyme whose conformation was changed by HHP

hindered the access of the substrate to the enzyme. Unlike cross-linking before immobilization, the amount of GOx entrapped in PoPD could not have changed. The inter- or intra- cross-linking with GOx entrapped in PoPD didn't affect the activity of the enzymes if crosslinked at 0.1 MPa.

2.3.4. Effect of HHP during thermal inactivation on the stability of immobilized GOx

Calculated k_{inact} for the first 60 min and k_{inact} and k'_{inact} for the entire 180-min thermal treatment are shown in Table 2.4. The values of k_{inact} calculated based on the first 60 min and the entire 180 min are different. At longer treatment times, the pseudo-first-order model deviates from linearity as reflected by a lower R^2 and the better fit of the pseudo-second-order model. To compare with our previous report using soluble GOx, the pseudo-first-order model for the first 60 min of heating was used which corresponded approximately to the longest heating time by Halalipour, et al. [12]. Inactivation pressure had significant influence ($p < 0.01$) on the thermostability while immobilization pressure (0.1 or 180 MPa) had no significant ($p > 0.05$) effect. Tukey's method didn't find any significant difference between 180 MPa and 360 MPa treatments but both of them were significantly different from 0.1 MPa. The immobilized GOx inactivated at 180 MPa and 70 °C was 4.3 times more stable than when inactivated at 0.1 MPa and 70 °C (0 – 60 min).

Fig. 2.2 shows the pseudo-first-order plot of thermal inactivation with linear regression lines (0 – 180 min). There was an evident leveling-off in the trend when residual activity decreased below ~15%, suggesting the pseudo-second-order model was a better fit. Fig. 2.2 also includes the calculated inactivation of soluble GOx inactivated at 0.1 or 180 MPa based on the kinetic parameters reported by Halalipour, et al. [12]. The calculated k_{inact} of GOx in solution was 536×10^{-3} min^{-1} at 70 °C and 0.1 MPa, and 36×10^{-3} min^{-1} at 70 °C and 180 MPa. Therefore, immobilization alone with k_{inact} $(26.0 \pm 4.1) \times 10^{-3}$ min^{-1} at 70 °C and 0.1 MPa (0 – 60 min) increased the thermostability of GOx by 20.6 times, which was similar to the effect of applying

180 MPa during inactivation for soluble GOx at 70 °C with the increase by 14.9 times. At 180 MPa and 70 °C, k_{inact} $(6.1 \pm 3.6) \times 10^{-3}$ min^{-1} of immobilized GOx (0 – 60 min) was 87.6 times smaller than the soluble GOx inactivated at 0.1 MPa and 70 °C. This suggested that there was a synergistic effect between immobilization and high pressure on the thermostability, since the combined stabilizing effect was bigger than the sum of the individual effects.

The stabilizing effect of immobilization on enzymes have been widely reported. As a method of immobilization, electropolymerization has been widely used to develop biosensors due to the easily controlled one-step process [19, 20], and was reported to be able to increase the thermal stability of the immobilized GOx [40, 53]. *o*-phenylenediamine is one of the non-conducting monomers used during electropolymerization, and a number of reports had adopted it to produce GOx biosensors and showed high storage stability with the response retained from 41% to 88% after 30 days storage at 4 °C [21-26]. Electropolymerization only physically entraps the enzymes without any chemical bond formation between the enzyme and the polymer. The increase in thermal stability by electropolymerization can be attributed to the spatial restriction of the enzyme inside the polymer which reduces enzyme unfolding at high temperatures [53].

The stabilizing effect of HHP on enzymes has been reported, but the mechanism of stabilization is unclear [54-57]. Pressures higher than 400-500 MPa can denature proteins while low pressures result in reversible changes. Pressures above 200 MPa can change tertiary structures while pressures lower than 150-300 MPa affect quaternary structures [58]. High pressure decreases the volume of proteins following the Le Chatelier principle and compresses non-rigid internal voids through the displacement of helices [11, 59-61]. At moderate pressures, the protein is stabilized by increased Van der Waals forces resulting from compressed cavities [62]. At high pressures, the volume decrease is mainly from the penetration of water molecules into the cavities

which causes the inactivation of proteins by weakening electrostatic and hydrophobic interactions and disturbing the tertiary structures [63-65]. An antagonistic effect of pressure and temperature on the inactivation of enzymes is often observed, and the native state of enzymes is favored at high temperatures and moderately high pressures [9, 65]. Pressures typically below 300 MPa can counteract the unfolding of proteins caused by high temperature to increase the thermal stability of enzymes. High temperature can cause the disruption of highly ordered structure of electrostricted water, resulting in the essential water loss when the thermal inactivation starts, which will lead to structural rearrangement and protein denaturation. High pressure, on the other hand, can strengthen the hydration of charged and non-polar groups, compress the protein hydration shell, and counteract the process from high temperature [9, 11, 65, 66]. High temperature weakens the intermolecular oxygen-hydrogen interactions, resulting in a softened hydrogen bond network. On the contrary, HHP strengthens the intermolecular oxygen-hydrogen interactions by shortening the distance between hydrogen bonds and thereby stabilizing them [9, 10]. High pressure can also strengthen the ion pairs which further stabilizes the tertiary and quaternary structures of enzymes [10].

The mechanism of the synergistic stabilizing effect of high pressure and immobilization against thermal treatment observed in this study is unclear. It is reasonable to hypothesize that high pressure compresses surfaces, cavities, and hydrophobic regions while immobilization restricts protein unfolding and prevents enzyme aggregation. Also, compaction of the PoPD under HHP may contribute to the synergism. Nevertheless, this confirms that the stabilization mechanisms of the two treatments are different and complex. Structural analysis by fourier-transform infrared spectroscopy, fluorescence, or nuclear magnetic resonance spectroscopy are needed to elucidate the origin of the observed synergism. However, these studies are beyond the scope of this report.

2.4. Conclusions

Among the different methods tested, only applying HHP during thermal inactivation of immobilized GOx had a large increase in the thermostability. Cross-linking with GA at atmospheric pressure or at HHP had too small of an effect to be of practical significance. To the best of our knowledge, this was the first time reporting the synergistic effect of HHP and enzyme immobilization on improving the thermostability of enzymes. These combined stabilizing effects provided a new method to improve the biocatalysis of enzymes at high temperatures, which has the potential to be applied to other enzymes and result in economic saving in industry. However, the application of HHP to biosensor stability is not practical since its stabilization effect disappears after depressurization.

Acknowledgment

This work was supported by the USDA National Institute of Food and Agriculture [grant number 2014-67021-21604/ project accession no. 1001899].

2.5. References

[1] S.B. Bankar, M.V. Bule, R.S. Singhal, L. Ananthanarayan, Glucose oxidase-an overview, Biotechnol. Adv. 27(4) (2009) 489-501.

[2] M.M. Rahman, A.J.S. Ahammad, J.H. Jin, J.A. Sang, J.J. Lee, A comprehensive review of glucose biosensors based on nanostructured metal-oxides, Sens. 10(5) (2010) 4855-4886.

[3] L. Barthelmebs, C. Calas-Blanchard, G. Istamboulie, J.-L. Marty, T. Noguer, Biosensors as analytical tools in food fermentation industry, in: M.T. Giardi, G. Rea, B. Berra (Eds.), Bio-farms for nutraceuticals, Springer, Boston, 2010, pp. 293-307.

[4] E.B. Bahadır, M.K. Sezgintürk, Applications of commercial biosensors in clinical, food, environmental, and biothreat/biowarfare analyses, Anal. Biochem. 478 (2015) 107-120.

[5] J.I. Reyes-De-Corcuera, Electrochemical Biosensors, in: D.R. Heldman, C.I. Moraru (Eds.), Encyclopedia of Agricultural, Food, and Biological Engineering, CRC press, New York, 2015.

[6] K. Narsaiah, S.N. Jha, R. Bhardwaj, R. Sharma, R. Kumar, Optical biosensors for food quality and safety assurance-a review, J. Food Sci. Technol. 49(4) (2012) 383-406.

[7] M. Vanderroost, P. Ragaert, F. Devlieghere, B. De Meulenaer, Intelligent food packaging: The next generation, Trends Food Sci. Technol. 39(1) (2014) 47-62.

[8] J.I. Reyes-De-Corcuera, H.E. Olstad, R. García-Torres, Stability and stabilization of enzyme biosensors: The key to successful application and commercialization, Annu. Rev. Food Sci. Technol. 9 (2018) 293-322.

[9] M.J. Eisenmenger, J.I. Reyes-De-Corcuera, High pressure enhancement of enzymes: a review, Enzyme Microb. Technol. 45(5) (2009) 331-347.

[10] Y. Li, M. Miao, M. Liu, X. Chen, B. Jiang, B. Feng, Enhancing the thermal stability of inulin fructotransferase with high hydrostatic pressure, Int. J. Biol. Macromol. 74 (2015) 171-178.

[11] V.V. Mozhaev, R. Lange, E.V. Kudryashova, C. Balny, Application of high hydrostatic pressure for increasing activity and stability of enzymes, Biotechnol. Bioeng. 52(2) (1996) 320-331.

[12] A. Halalipour, M.R. Duff, E.E. Howell, J.I. Reyes-De-Corcuera, Glucose oxidase stabilization against thermal inactivation using high hydrostatic pressure and hydrophobic modification, Biotechnol. Bioeng. 114(3) (2016) 516-525.

[13] M.I. Buchholz-Afari, A. Halalipour, D. Yang, J.I. Reyes-De-Corcuera, Increased stability of alcohol oxidase under high hydrostatic pressure, J. Food Eng. 246 (2019) 95-101.

[14] A. Halalipour, M.R. Duff, E.E. Howell, J.I. Reyes-De-Corcuera, Effects of high hydrostatic pressure or hydrophobic modification on thermal stability of xanthine oxidase, Enzyme Microb. Technol. 103 (2017) 18-24.

[15] L.S. Wallace, The effect of high hydrostatic pressure on stability of pyruvate oxidase from *aeroccocus species*, University of Georgia Theses and Dissertations (2017) 19-50.

[16] C. Mateo, J.M. Palomo, G. Fernandez-Lorente, J.M. Guisan, R. Fernandez-Lafuente, Improvement of enzyme activity, stability and selectivity via immobilization techniques, Enzyme Microb. Technol. 40(6) (2007) 1451-1463.

[17] A. Dwevedi, Basics of enzyme immobilization, Enzyme Immobilization, Springer, Cham, 2016, pp. 21-44.

[18] T. Jesionowski, J. Zdarta, B. Krajewska, Enzyme immobilization by adsorption: a review, Adsorpt. 20(5-6) (2014) 801-821.

[19] H.H. Nguyen, M. Kim, An overview of techniques in enzyme immobilization, Appl. Sci. Converg. Technol. 26(6) (2017) 157-163.

[20] S. Cosnier, Biosensors based on electropolymerized films: new trends, Anal. Bioanal. Chem. 377(3) (2003) 507-520.

[21] S.Z. Bas, A gold nanoparticle functionalized multiwalled carbon nanotube-poly(*o*-phenylenediamine) composite film for glucose biosensing applications, Anal. Methods 6(19) (2014) 7752-7759.

[22] C. Deng, M. Li, Q. Xie, M. Liu, Y. Tan, X. Xu, S. Yao, New glucose biosensor based on a poly(*o*-phenylendiamine)/glucose oxidase-glutaraldehyde/Prussian blue/Au electrode with QCM monitoring of various electrode-surface modifications, Anal. Chim. Acta 557(1-2) (2006) 85-94.

[23] R. Garjonyte, A. Malinauskas, Amperometric glucose biosensor based on glucose oxidase immobilized in poly(*o*-phenylenediamine) layer, Sens. Actuators B: Chem. 56(1-2) (1999) 85-92.

[24] S. Luo, Y. Chen, M. Zhou, C. Yao, H. Xi, Y. Kong, L. Deng, Palygorskite-poly(*o*-phenylenediamine) nanocomposite: an enhanced electrochemical platform for glucose biosensing, Appl. Clay Sci. 86 (2013) 59-63.

[25] J.I. Reyes-De-Corcuera, R. Cavalieri, J.R. Powers, Improved platinization conditions produce a 60-fold increase in sensitivity of amperometric biosensors using glucose oxidase immobilized in poly-*o*-phenylenediamine, J. Electroanal. Chem. 575(2) (2005) 229-241.

[26] E. Turkmen, S.Z. Bas, H. Gulce, S. Yildiz, Glucose biosensor based on immobilization of glucose oxidase in electropolymerized poly(*o*-phenylenediamine) film on platinum nanoparticles-polyvinylferrocenium modified electrode, Electrochim. Acta 123 (2014) 93-102.

[27] O. Barbosa, C. Ortiz, Á. Berenguer-Murcia, R. Torres, R.C. Rodrigues, R. Fernandez-Lafuente, Glutaraldehyde in bio-catalysts design: a useful crosslinker and a versatile tool in enzyme immobilization, Rsc Adv. 4(4) (2014) 1583-1600.

[28] M.N. Gupta, S. Raghava, Enzyme stabilization via cross-linked enzyme aggregates, in: S.D. Minteer (Ed.) Enzyme Stabilization and Immobilization, Humana press, Totowa, 2011, pp. 133-145.

[29] T. Garcia-Perez, S.-G. Hong, J. Kim, S. Ha, Entrapping cross-linked glucose oxidase aggregates within a graphitized mesoporous carbon network for enzymatic biofuel cells, Enzyme Microb. Technol. 90 (2016) 26-34.

[30] X. Zhong, Y.-Q. Chai, R. Yuan, A novel strategy for synthesis of hollow gold nanosphere and its application in electrogenerated chemiluminescence glucose biosensor, Talanta 128 (2014) 9-14.

[31] Y. Chung, M. Christwardana, D.C. Tannia, K.J. Kim, Y. Kwon, Biocatalyst including porous enzyme cluster composite immobilized by two-step crosslinking and its utilization as enzymatic biofuel cell, J. Power Sources 360 (2017) 172-179.

[32] B. Wu, G. Zhang, S. Shuang, M.M. Choi, Biosensors for determination of glucose with glucose oxidase immobilized on an eggshell membrane, Talanta 64(2) (2004) 546-553.

[33] L. Betancor, F. López-Gallego, A. Hidalgo, N. Alonso-Morales, G. Dellamora-Ortiz, J.M. Guisán, R. Fernández-Lafuente, Preparation of a very stable immobilized biocatalyst of glucose oxidase from *Aspergillus niger*, J. Biotechnol. 121(2) (2006) 284-289.

[34] X. Wang, Y. Ma, M. Zhao, M. Zhou, Y. Xiao, Z. Sun, L. Tong, Determination of glucose in human stomach cancer cell extracts and single cells by capillary electrophoresis with a micro-biosensor, J. Chromatogr. 1469 (2016) 128-134.

[35] A. Mignani, E. Scavetta, D. Tonelli, Electrodeposited glucose oxidase/anionic clay for glucose biosensors design, Anal. Chim. Acta 577(1) (2006) 98-106.

[36] M. Florescu, C.M. Brett, Development and evaluation of electrochemical glucose enzyme biosensors based on carbon film electrodes, Talanta 65(2) (2005) 306-312.

[37] J. Li, P. Koinkar, Y. Fuchiwaki, M. Yasuzawa, A fine pointed glucose oxidase immobilized electrode for low-invasive amperometric glucose monitoring, Biosens. Bioelectron. 86 (2016) 90-94.

[38] P.V. Iyer, L. Ananthanarayan, Enzyme stability and stabilization-aqueous and non-aqueous environment, Process Biochem. 43(10) (2008) 1019-1032.

[39] A. Liese, L. Hilterhaus, Evaluation of immobilized enzymes for industrial applications, Chem. Soc. Rev. 42(15) (2013) 6236-6249.

[40] J. Dumont, G. Fortier, Behavior of glucose oxidase immobilized in various electropolymerized thin films, Biotechnol. Bioeng. 49(5) (1996) 544-552.

[41] T.O. Kvålseth, Cautionary note about R^2, The American Stat. 39(4) (1985) 279-285.

[42] R. Ulbrich, A. Schellenberger, W. Damerau, Studies on the thermal inactivation of immobilized enzymes, Biotechnol. Bioeng. 28(4) (1986) 511-522.

[43] H. Katano, Y. Sugimoto, K. Uematsu, T. Hibi, Kinetic study of the thermal inactivation of glucose oxidase in the presence of denaturant and stabilizer by means of bioelectrocatalysis method, Anal. Sci. 27(10) (2011) 979-979.

[44] J.M. Rodriguez-Nogales, Kinetic behaviour and stability of glucose oxidase entrapped in liposomes, J. Chem. Technol. Biotechnol. 79(1) (2004) 72-78.

[45] R.E. Kim, S.-G. Hong, S. Ha, J. Kim, Enzyme adsorption, precipitation and crosslinking of glucose oxidase and laccase on polyaniline nanofibers for highly stable enzymatic biofuel cells, Enzyme Microb. Technol. 66 (2014) 35-41.

[46] B.E. Swoboda, V. Massey, Purification and properties of the glucose oxidase from *Aspergillus niger*, J. Biol. Chem. 240 (1965) 2209-2215.

[47] C.-C. Wu, H.-C. Chang, Estimating the thickness of hydrated ultrathin poly(*o*-phenylenediamine) film by atomic force microscopy, Anal. Chim. Acta 505(2) (2004) 239-246.

[48] M.D. Busto, N. Ortega, M. Perez-Mateos, Stabilisation of cellulases by cross-linking with glutaraldehyde and soil humates, Bioresour. Technol. 60(1) (1997) 27-33.

[49] Ş.A. Çetinus, H.N. Öztop, Immobilization of catalase into chemically crosslinked chitosan beads, Enzyme Microb. Technol. 32(7) (2003) 889-894.

[50] B. Bhushan, A. Pal, V. Jain, Improved enzyme catalytic characteristics upon glutaraldehyde cross-linking of alginate entrapped xylanase isolated from *Aspergillus flavus* MTCC 9390, Enzyme Res. 2015 (2015) 9.

[51] S. Kumar, I. Haq, J. Prakash, A. Raj, Improved enzyme properties upon glutaraldehyde cross-linking of alginate entrapped xylanase from *Bacillus licheniformis*, Int. J. Biol. Macromol. 98 (2017) 24-33.

[52] R. Kowal, R.G. Parsons, Stabilization of proteins immobilized on Sepharose from leakage by glutaraldehyde crosslinking, Anal. Biochem. 102(1) (1980) 72-76.

[53] S.V. Sasso, R.J. Pierce, R. Walla, A.M. Yacynych, Electropolymerized 1, 2-diaminobenzene as a means to prevent interferences and fouling and to stabilize immobilized enzyme in electrochemical biosensors, Anal. Chem. 62(11) (1990) 1111-1117.

[54] M.E. Bruins, N. Creusot, H. Gruppen, A.E. Janssen, R.M. Boom, Pressure-aided proteolysis of β-casein, J. Agric. Food Chem. 57(12) (2009) 5529-5534.

[55] H. Vila-Real, A.J. Alfaia, A.R. Calado, R.S. Phillips, M.H. Ribeiro, High pressure: a tool to improve the enzymatic production of glycosides, High Press. Res. 31(3) (2011) 475-487.

[56] N. Kim, C.-T. Kim, Reduced thermal inactivation of trypsin and Marugoto E by high-pressure treatment, Food Sci. Technol. Res. 18(6) (2012) 911-917.

[57] S. Chakraborty, P.S. Rao, H.N. Mishra, Kinetic modeling of polyphenoloxidase and peroxidase inactivation in pineapple (*Ananas comosus* L.) puree during high-pressure and thermal treatments, Innov. Food Sci. Emerg. Technol. 27 (2015) 57-68.

[58] A. Furtado, P.M. Rosário, A.R. Calado, A.J. Alfaia, M.H. Ribeiro, High pressure studies on hesperitin production with hesperidinase free and immobilized in calcium alginate beads, High Press. Res. 32(1) (2012) 128-137.

[59] M.D. Collins, M.L. Quillin, G. Hummer, B.W. Matthews, S.M. Gruner, Structural rigidity of a large cavity-containing protein revealed by high-pressure crystallography, J. Mol. Biol. 367(3) (2007) 752-763.

[60] L.G. Fidalgo, J.A. Saraiva, S.P. Aubourg, M. Vázquez, J.A. Torres, High pressure effects on the activities of cathepsins B and D of mackerel and horse mackerel muscle, Czech J. Food Sci. 32 (2014) 188-193.

[61] C. Kirsch, J. Dahms, A.F. Kostko, M.A. McHugh, I. Smirnova, Pressure assisted stabilization of biocatalysts at elevated temperatures: Characterization by dynamic light scattering, Biotechnol. Bioeng. 110(6) (2013) 1674-1680.

[62] B.B. Boonyaratanakornkit, C.B. Park, D.S. Clark, Pressure effects on intra- and intermolecular interactions within proteins, Biochim. Biophys. Acta 1595(1-2) (2002) 235-249.

[63] J. Roche, C.A. Royer, C. Roumestand, Monitoring protein folding through high pressure NMR spectroscopy, Prog. Nucl. Magn. Reson. Spectrosc. 102-103 (2017) 15-31.

[64] G. Hummer, S. Garde, A.E. García, M.E. Paulaitis, L.R. Pratt, The pressure dependence of hydrophobic interactions is consistent with the observed pressure denaturation of proteins, Proc. Natl. Acad. Sci. 95(4) (1998) 1552-1555.

[65] P. Degraeve, P. Rubens, P. Lemay, K. Heremans, In situ observation of pressure-induced increased thermostability of two β-galactosidases with FT-IR spectroscopy in the diamond anvil cell, Enzyme Microb. Technol. 31(5) (2002) 673-684.

[66] N.S. Terefe, P. Sheean, S. Fernando, C. Versteeg, The stability of almond β-glucosidase during combined high pressure–thermal processing: a kinetic study, Appl. Microbiol. Biotechnol. 97(7) (2013) 2917-2928.

Table 2.1. Sensitivity, apparent Michaelis-Menten constant, and pseudo-first-order and pseudo-second-order rate constant of inactivation of GOx biosensors immobilized at pressures from 0.1 to 420 MPa. The biosensors were inactivated at 70 °C and 0.1 MPa. The values are reported as mean ± 95% confidence interval.

Pressure (MPa)	Sensitivity ($\mu A\ mm^{-2}\ mM^{-1}$) × 10^3	K_m^{app} (mM)	k_{inact} (min^{-1}) × 10^3	R^2	k'_{inact} (min^{-1}) × 10^4	R^2
0.1	4.4 ± 0.9	28.4 ± 5.7	6.6 ± 1.0	0.84	2.1 ± 0.7	0.95
180	3.0 ± 1.4	38.6 ± 8.7	7.7 ± 1.4	0.85	3.3 ± 1.0	0.97
240	3.8 ± 2.2	35.2 ± 13.2	5.7 ± 1.7	0.84	3.1 ± 1.2	0.94
300	4.5 ± 2.2	34.6 ± 13.2	5.6 ± 1.7	0.86	2.7 ± 1.2	0.98
420	4.4 ± 3.7	21.2 ± 22.9	7.6 ± 2.9	0.92	1.9 ± 2.0	0.98

No significant differences ($p < 0.05$) were found in means of sensitivity, K_m^{app}, k_{inact}, or k'_{inact}.

Table 2.2. Sensitivity, apparent Michaelis-Menten constant, and pseudo-first-order and pseudo-second order rate constant of inactivation of GOx biosensors. Glucose oxidase was cross-linked with 0.5% (w/v) glutaraldehyde at 0.1 or 180 MPa with or without the addition of BSA before electropolymerization at 0.1 or 180 MPa. The biosensors were inactivated at 70 °C and 0.1 MPa. The values are reported as mean ± 95% confidence interval.

Immobilization pressure (MPa)	Cross-linking pressure (MPa)	Cross-linking reaction time (h)	BSA added (Y/N)	Sensitivity (μA mm^{-2} mM^{-1}) × 10^3	K_m^{app} (mM)	k_{inact} (min^{-1}) × 10^3	R^2	k'_{inact} (min^{-1}) × 10^4	R^2
0.1	0.1	6	N	9.3^{abc} ± 0.9	21.2^{f} ± 10.4	9.0 ± 1.6	0.84	3.0 ± 1.4	0.97
0.1	180	6	N	7.5^{bcde} ± 0.9	31.7^{fgh} ± 10.4	8.1 ± 1.6	0.84	2.4 ± 1.4	0.98
0.1	0.1	12	N	8.6^{abcd} ± 0.9	24.2^{fg} ± 10.4	7.5 ± 1.6	0.84	2.1 ± 1.4	0.97
0.1	180	12	N	6.8^{de} ± 0.9	21.9^{f} ± 10.4	7.7 ± 1.6	0.80	2.3 ± 1.4	0.93
180	0.1	6	N	9.6^{ab} ± 0.9	37.8^{fgh} ± 10.4	9.9 ± 1.6	0.86	3.9 ± 1.4	0.99
180	180	6	N	5.6^{e} ± 0.9	46.6^{gh} ± 10.4	9.4 ± 1.6	0.81	3.6 ± 1.4	0.98
180	0.1	12	N	9.6^{a} ± 0.9	50.0^{h} ± 10.4	9.1 ± 1.6	0.84	3.2 ± 1.4	0.98
180	180	12	N	7.3^{cde} ± 0.9	35.4^{fgh} ± 10.4	10.2 ± 1.6	0.70	4.8 ± 1.4	0.91
0.1	0.1	1	Y	8.5^{i} ± 3.6	18.0^{j} ± 17.8	7.6 ± 1.8	0.81	2.3 ± 1.8	0.97
0.1	180	1	Y	7.5^{i} ± 3.6	27.7^{j} ± 17.8	9.6 ± 1.8	0.75	3.7 ± 1.8	0.95
180	0.1	1	Y	7.6^{i} ± 3.6	40.1^{j} ± 17.8	9.1 ± 1.8	0.82	3.5 ± 1.8	0.99
180	180	1	Y	7.2^{i} ± 3.6	28.2^{j} ± 17.8	10.7 ± 1.8	0.77	5.1 ± 1.8	0.96

No significant differences ($p < 0.05$) were found in means of k_{inact} or k'_{inact} in the absence of BSA or not.

[a-e]Differences in means of sensitivity with different letter without adding BSA were significant ($p < 0.05$).

[f-h]Differences in means of K_m^{app} with different letter without adding BSA were significant ($p < 0.05$).

[ij]No significant differences ($p < 0.05$) were found in means of sensitivity or K_m^{app} when the BSA was added.

Table 2.3. Sensitivity, pseudo-first-order and pseudo-second-order rate constant of inactivation of GOx biosensors inactivated at 70 °C and 0.1 MPa. Glucose oxidase was immobilized at 0.1 or 180 MPa and then cross-linked with 2.5 or 5% (w/v) glutaraldehyde at 0.1 MPa for 10 or 30 min. The values are reported as mean ± 95% confidence interval.

Immobilization pressure (MPa)	GA concentration (%)	Cross-linking reaction time (min)	Sensitivity (μA mm^{-2} mM^{-1}) × 10^3	k_{inact} (min^{-1}) × 10^3	R^2	k'_{inact} (min^{-1}) × 10^4	R^2
0.1	2.5	10	4.2^{a} ± 1.2	3.3 ± 1.5	0.95	0.5 ± 0.4	0.98
0.1	5	10	3.0^{ab} ± 1.2	4.6 ± 1.5	0.91	0.9 ± 0.4	0.97
180	2.5	10	1.4^{b} ± 1.2	5.0 ± 1.5	0.91	0.9 ± 0.4	0.95
180	5	10	1.1^{b} ± 1.2	3.7 ± 1.5	0.86	0.7 ± 0.4	0.91
0.1	2.5	30	4.1^{a} ± 1.2	4.8 ± 1.5	0.92	1.0 ± 0.4	0.98
180	2.5	30	1.6^{ab} ± 1.2	3.9 ± 1.5	0.82	0.7 ± 0.4	0.90
180	5	30	2.0^{ab} ± 1.2	4.9 ± 1.5	0.87	1.0 ± 0.4	0.96

No significant differences ($p < 0.05$) were found in means of k_{inact} or k'_{inact}.

[a-b]Differences in means of sensitivity with different letter were significant ($p < 0.05$).

Table 2.4. Pseudo-first-order and pseudo-second-order rate constant of inactivation of GOx biosensors immobilized at 0.1 or 180 MPa. The biosensors were inactivated at 70 °C and 0.1 to 360 MPa. The values are reported as mean ± 95% confidence interval.

Immobilization pressure (MPa)	Inactivation pressure (MPa)	k_{inact} (min^{-1}) × 10^3 (0 – 60 min)	R^2	k_{inact} (min^{-1}) × 10^3 (0 – 180 min)	R^2	k'_{inact} (min^{-1}) × 10^4 (0 – 180 min)	R^2
0.1	10	$26.0^a \pm 4.1$	0.84	$11.0^a \pm 1.4$	0.77	$5.2^a \pm 0.8$	0.98
0.1	180	$6.1^b \pm 3.6$	0.89	$2.6^b \pm 1.3$	0.83	$0.4^b \pm 0.7$	0.89
0.1	360	$8.8^b \pm 4.7$	0.91	$4.0^b \pm 1.6$	0.86	$0.8^b \pm 0.9$	0.93
180	180	$9.6^b \pm 4.7$	0.92	$4.3^b \pm 1.6$	0.84	$0.8^b \pm 0.9$	0.92

[a-b]Differences in means of k_{inact} or k'_{inact} with different letter within each column were significant ($p < 0.05$).

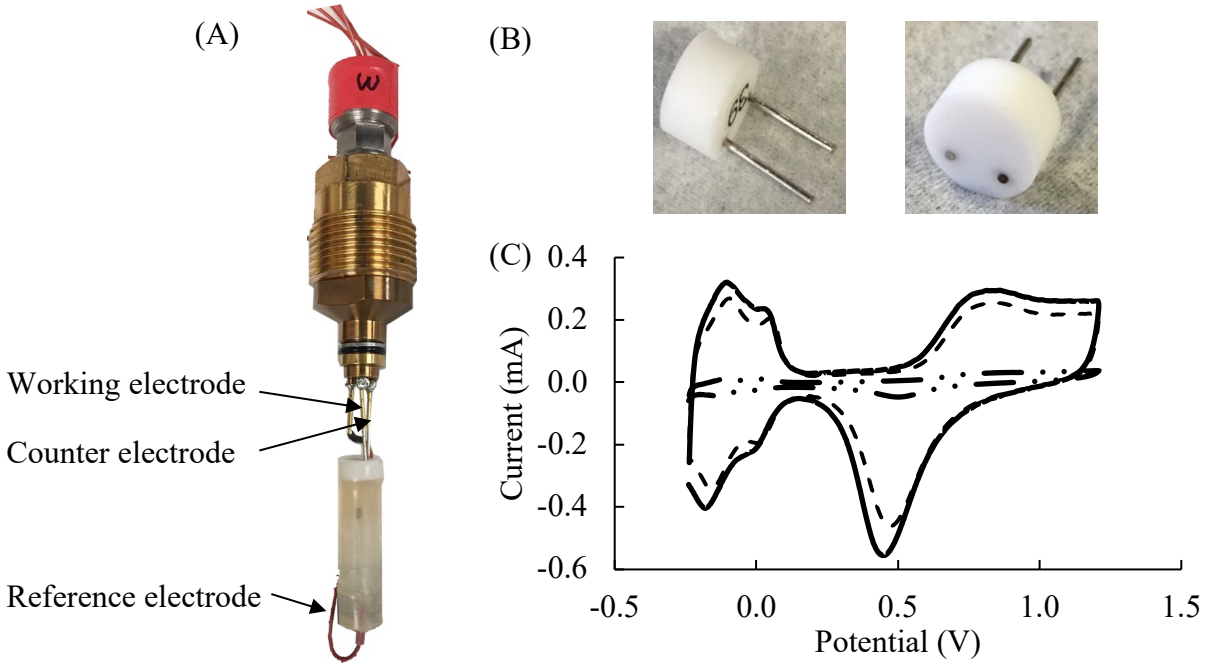

Fig. 2.1. (A) Electrochemical cell connected to the cap of the high pressure reactor; (B) polytetrafluoroethylene cap with platinized platinum electrodes; (C) cyclic voltammograms of (—• • —) polished, (—) platinized, and (- - -) platinized and ultrasonicated electrodes.

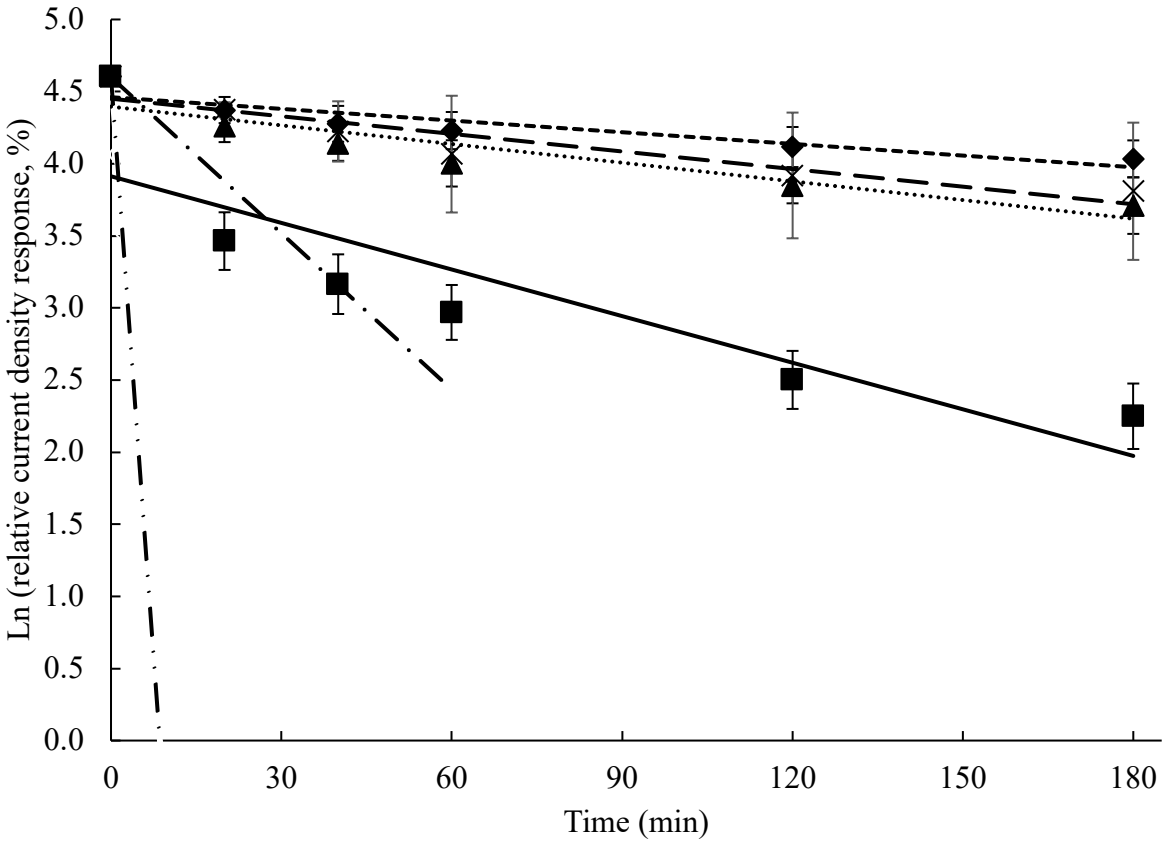

Fig. 2.2. Inactivation of GOx immobilized in PoPD at 0.1 MPa and inactivated at 70 °C and 0.1 MPa (■), 180 MPa (◆), or 360 MPa (×), or immobilized at 180 MPa and inactivated at 70 °C and 180 MPa (▲). Inactivation of GOx in solution at 70 °C and 0.1 MPa (— • • —) or 180 MPa (— • —) was calculated based on the data reported by Halalipour, et al. [12]. Error bars represent ± standard deviations. Each treatment was done at least in triplicate.

Supplemental materials

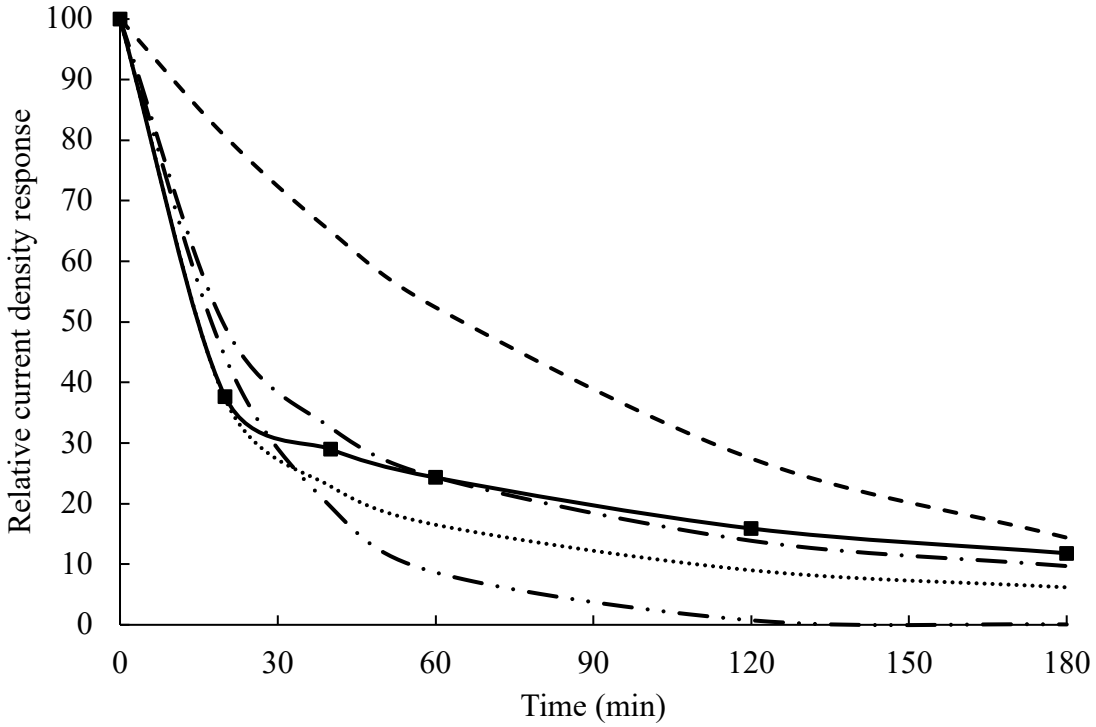

Fig. S2.1. The relative current density response change over treatment time of the original data (■), prediction from the linearized pseudo-first-order model (- - -), prediction from the linearized pseudo-second-order model (- • -), prediction from the non-linearized pseudo-first-order model (- • • -), and prediction from the non-linearized pseudo-second-order model (• • •). The GOx was immobilized in PoPD at 0.1 MPa and was inactivated at 70 °C and 0.1 MPa.

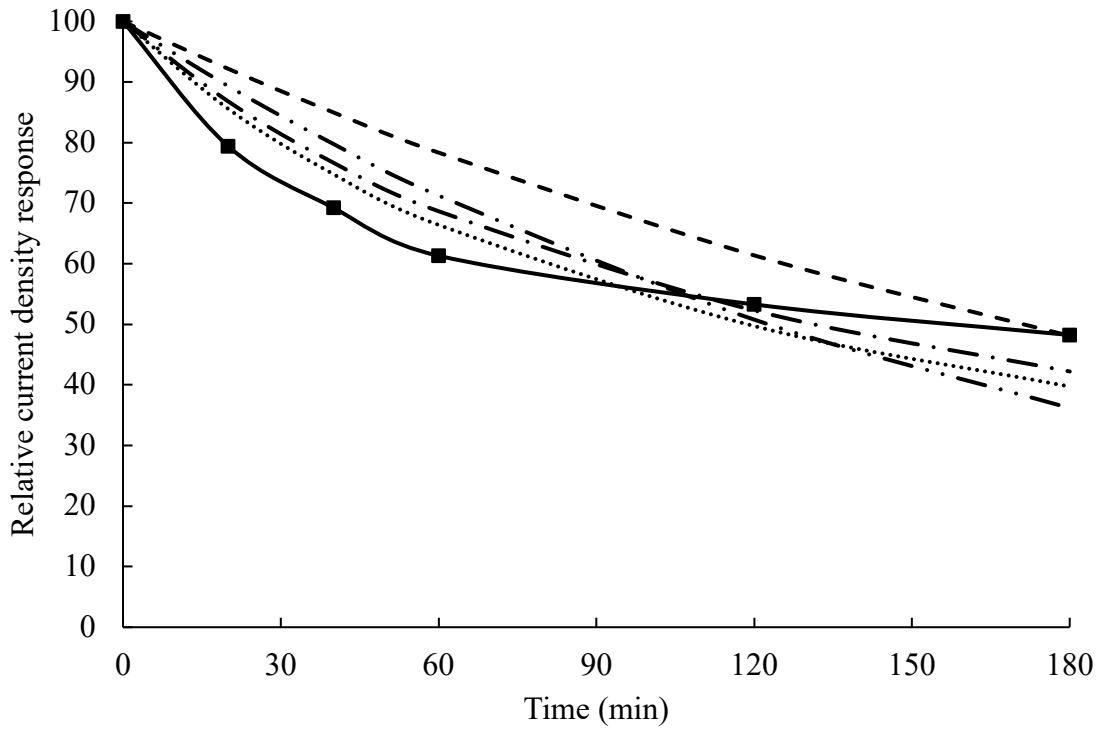

Fig. S2.2. The relative current density response change over treatment time of the original data (■), prediction from the linearized pseudo-first-order model (- - -), prediction from the linearized pseudo-second-order model (- • -), prediction from the non-linearized pseudo-first-order model (- • • -), and prediction from the non-linearized pseudo-second-order model (• • •). The GOx was immobilized in PoPD at 0.1 MPa and was inactivated at 70 °C and 360 MPa.

CHAPTER 3

INCREASED APPARENT ACTIVITY OF ALCOHOL OXIDASE AT HIGH HYDROSTATIC PRESSURE [1]

[1] Yang, D. and Reyes-De-Corcuera J.I. To be submitted to *Journal of Food Engineering*.

Abstract:

Alcohol oxidase (AOx) has applications in the production of carbonyl compounds and in the detection and quantification of alcohols. High hydrostatic pressure (HHP) increased the apparent activity of both the labile (L) + resistant (R) fractions and the R fraction AOx at some temperatures. The reaction rate of the R fraction at 50 °C was 17.9 ± 3.6 or 17.7 ± 0.8 μM min^{-1} at 80 or 160 MPa, respectively. It was approximately 6-times as much as the reaction rate, 3.2 ± 0.2 μM min^{-1}, at 25 °C and at atmospheric pressure. The increase in the catalytic activity of the R fraction AOx was attributed only to the stabilizing effect of HHP. There was no activating effect of HHP on the R fraction AOx at the selected pressures and temperatures. The higher activity of the R fraction AOx obtained using this method can be beneficial to the industrial applications in terms of higher efficiency and economic saving.

Keywords: high hydrostatic pressure, enzyme stabilization, enzyme activity, alcohol oxidase

3.1. Introduction

Alcohol oxidase (AOx; EC. 1.1.3.13) catalyzes the oxidation of alcohols into the corresponding carbonyl compound and hydrogen peroxide. It is an octamer of approximately 600 kDa and each subunit has a flavin adenine dinucleotide cofactor (Ozimek et al. 2005). It can be categorized into four groups based on the substrate specificity, including short chain alcohol oxidase, long chain alcohol oxidase, aromatic alcohol oxidase, and secondary alcohol oxidase (Goswami et al. 2013). Most of the AOxs are from yeasts such as *Pichia pastoris*, *Pichia angusta*, *Candida boidinii* and filamentous fungi including *Penicillium chrysogenum* and *Cladosporium fulvum*. The genes encoding the AOx protein were summarized by Ozimek et al. (2005). Particularly, the AOx from *Pichia pastoris* is encoded by two genes, AOx1 and AOx2 (Cregg et al. 1989). Two fractions in AOx from *Pichia pastoris* were observed named as the labile (L) fraction and the resistant (R) fraction according to their thermal stability. The R fraction only accounted for approximately one third of the total activity of the L+R mixture (Buchholz-Afari et al. 2019).

Alcohol oxidase is used to detect and quantify alcohols. It is important in the clinical and forensic tests to analyze the human fluids, including blood, urine, serum, etc. It can be used for quality control in the food, beverage, and pulp industries, and to monitor the progress of alcoholic fermentations (Patel et al. 2001). To overcome some of the shortcomings of the chemical methods, e.g., titration, colorimetric, chromatographic, or spectroscopic methods, alcohol oxidase biosensors have been researched (Azevedo et al. 2005). Alcohol oxidase can also be used to synthesize carbonyl compounds that are important to produce solvents, pharmaceuticals, or as the ingredients in fragrances and flavors, e.g. n-heptanal, which is the starting material of many aroma and flavor compounds (Kakoti et al. 2012). The conversion of alcohols to the corresponding

carbonyl products has been summarized by Kakoti et al. (2012). This AOx-catalyzed reaction is important because it does not produce undesirable or harmful by-products. However, the development of practical AOx-based biosensors and AOx-based industrial bioconversions is hampered by the low activity, the poor stability, and the high cost of the enzyme (Goswami et al. 2013; Choi et al. 2015; Reyes-De-Corcuera et al. 2018).

High hydrostatic pressure (HHP) has been used in the food industry to extend the shelf life of products by killing microbes and inactivating enzymes. However, pressures below 300 MPa activate and stabilize some enzymes. The enhancing effects of HHP on various enzymes and enzymatic hydrolysis of food proteins were well summarized by Eisenmenger and Reyes-De-Corcuera (2009) and Marciniak et al. (2018). We have reported the stabilizing effect of HHP on glucose oxidase (GOx) (Halalipour et al. 2017a), AOx (Buchholz-Afari et al. 2019), xanthine oxidase (XOx) (Halalipour et al. 2017b), pyruvate oxidase (POx) (Wallace 2017), and a GOx biosensor (Yang et al. 2020). For AOx, HHP increased the stability of the L fraction up to 14 times at 49.4 °C and at 160 MPa compared to the same condition at 0.1 MPa (Buchholz-Afari et al. 2019). The stabilizing effect of HHP resulted in a faster reaction rate by enabling enzymes to work at high temperatures under which they would normally be inactivated (Li et al. 2015b). Furthermore, the catalytic activity of the enzyme can also increase by an activating effect of HHP. Therefore, the increase in the activity of some enzymes at high pressures and relatively high temperatures are attributed to both the stabilizing effect and activating effect of HHP. The effect of HHP on the catalytic activities of various enzymes at different pressures and temperatures has been studied. For example, we reported that the native, aniline-modified, or benzoate-modified GOx increased its catalytic activity with HHP at temperatures from 25 to 69.1 °C, and reached the maximum activity at around 180 MPa; the aniline-modified GOx had the reaction rate 11.3 times

at 69.1 °C and 180 MPa relative to the rate at 25 °C and 0.1 MPa (Halalipour et al. 2020). The optimal pressure 180 MPa for GOx activity was also the optimal pressure for its stability (Halalipour et al. 2017a). This verified that the increasing in the enzyme activity was contributed by the increased enzyme stability at HHP. Other examples of higher enzyme activities at HHP include the activity of lipase from *Candida rugosa* was increased by 4.8-fold at 200 MPa and 45 °C (Herbst et al. 2014). The activity of polyphenol oxidase from peach or blueberry was increased by 66.5 % at 200 MPa and 45 °C (Bleoanca et al. 2018) or 6.1-fold at 500 MPa and 30 °C (Terefe et al. 2015), respectively. The activity of fructotransferase from *Arthrobacter aurescens* was increased by 33.8 % at 200 MPa and 60 °C (Li et al. 2015a). Possible mechanisms of how the HHP affects the rate of enzyme-catalyzed reactions as summarized by Eisenmenger and Reyes-De-Corcuera (2009) include changing the protein conformation, changing the rate-limiting step, or changing the property of the substrate or solvent such as the density. To the best of our knowledge, the effects of high pressure on the activity of AOx have not been studied. A higher reaction rate of AOx would be beneficial to the industries to produce the carbonyl products. Both GOx and AOx are flavin-dependent oxidases that catalyze the oxidation of small substrates, following a ping-pang mechanism and produce H_2O_2. However, these enzymes have different properties such as the protein size, number of subunits, and cavities. It was hypothesized that similar to GOx, the activity of AOx would be higher at HHP than at ambient pressure. We also reported that the thermostability of the L fraction AOx was lower than that of the R fraction AOx at HHP (Buchholz-Afari et al. 2019). Therefore, the R fraction AOx with higher thermostability is more likely to have applications in the practical industrial processing than the L fraction, even though it accounts for only about one third of the activity in the L+R fractions. Therefore, the main objective of this study was to determine the activity of the R fraction AOx at selected pressures near the optimal pressure

for maximal stability and at temperatures that do not cause enzyme inactivation. A preliminary study on the effect of HHP in the activity of the L+R fractions is also presented, and the results can be found in the supplemental materials.

3.2. Material and methods

3.2.1. Materials and equipment

Alcohol oxidase from *Pichia pastoris* was purchased from MP Biochemicals (Solon, OH, USA). Peroxidase (POD) from horseradish was purchased from the MilliporeSigma (St. Louis, MO, USA). Methanol (99.9 %), hydrogen peroxide (30 %), and potassium phosphate monobasic were purchased from Fisher Scientific (Hampton, NH, USA). 2,2'-azino-bis (3-ethylbenzothiazoline-6-sulfonic acid) diammonium salt (ABTS, 98 %) was purchased from Alfa Aesar (Ward Hill, MA, USA). All chemicals were reagent grade.

The high pressure system used in this report was previously described by Halalipour et al. (2020). The high pressure cell was connected to a spectrometer (model SD2000) and a light source (model DH-2000-BAL) with optic fibers (core diameter 400 μm) from Ocean Optics (Dunedin, FL, USA). A type K thermocouple was inserted into the high pressure reactor to measure the temperature. The schematic of the high pressure system is shown in Fig. 3.1. Cylindrical quartz cuvettes were selected to snugly fit in the high pressure optical cell. The cuvettes were made of a quartz tubing (inside diameter 7.4 mm, outside diameter 9.6 mm, length 20.8 mm) enclosed with two polytetrafluoroethylene caps with O-rings. The volume of the cuvettes with caps on and with two small magnetic beads in (Fisher Scientific, Hampton, NH, USA) was approximately 340 μL. Silicone oil (Sil 180 Thermo-Fisher, Rockford, IL) was used as the pressurization fluid. OceanView 1.5.0 software from Ocean Optics was used to collect data. A microplate reader (model SynergyTM HTX, BioTek, Winooski, VT) was used to determine the activity of AOx at

atmospheric pressure to prepare the enzyme stock solutions and ensure similar initial activity for all the samples.

3.2.2. Methods

3.2.2.1. Enzyme activity assay at atmospheric pressure

The enzyme activity assay was modified from the method used by Buchholz-Afari et al. (2019). The change in absorbance at 405 nm at 25 °C was recorded for 5 min after mixing 10 μL AOx sample (approximate concentration 0.074 U mL^{-1}) with other reagents with the final concentration of 3.0 mU mL^{-1} AOx, 10.0 U mL^{-1} POD, 1.6 % (v/v) methanol, and 2.0 mM ABTS. All solutions were prepared in 0.1 M phosphate buffer (pH 7.5). The absorbance was measured with a microplate reader with ABTS and methanol added with automatic injectors. The AOx sample and POD were put on ice when not in use. One unit of AOx was defined as oxidizing 1 μmol methanol to formaldehyde per minute at 25 °C at pH 7.5. The AOx enzyme activity was calculated as Eq. 1, modified from the enzyme activity methods by Keesey (1987) and Janssen and Ruelius (1968), referenced by MilliporeSigma.

$$E_{Acty}(U\ mL^{-1}) = \frac{dA_{405}}{dt} \times \frac{V_T}{V_E \times \varepsilon_{p,T}} \quad (1)$$

Where A_{405} is the absorbance at 405 nm, t is the time in minutes, V_T is the total volume of the reaction solution, V_E is the volume of enzyme stock solution, and $\varepsilon_{p,T}$ is the extinction coefficient of oxidized ABTS at the selected temperature and pressure.

3.2.2.2. Determination of two enzyme fractions and the difference in their thermal stability

The commercial AOx formulation used in our previous research was purchased from Sigma-Aldrich Chemical Company. We reported the enzyme contained a labile (L) fraction and a resistant (R) fraction (Buchholz-Afari et al. 2019). To verify the enzyme formulation purchased from MP Biochemicals used in this research contained the same fractions, the AOx samples diluted

in 0.1 M phosphate buffer (pH 7.5) were heated in a water bath at 50 °C for up to 240 min. The enzyme activity assay after each heating treatment was done as described in section 3.2.2.1 and the residual activity was calculated as the enzyme activity at each heat treatment time relative to the enzyme activity at heating time 0. The two linear regions on the plots of logarithm of residual activity *vs.* heating time were used to determine the two enzyme fractions (Buchholz-Afari et al. 2019). The R fraction was obtained by heating the AOx sample in 0.1 M phosphate buffer (pH 7.5) at 50 °C for 15 min and then immediately cooled in ice. The L fraction after the 15 min thermal treatment was fully inactivated, while over 95 % of the R fraction was retained after the 15 min heating. The residual activity of the L fraction in the L+R fraction was calculated by subtracting the residual activity of the R fraction. The difference in the thermal stability of the L+R fractions (no heat treatment) and the R fraction was determined by heating each of the two fractions in a water bath at 50 °C for up to 3 min and calculating the pseudo-first-order rate constant of inactivation.

3.2.2.3. Determination of the extinction coefficient (ε) of oxidized ABTS

To account for the effect of temperature and pressure on the extinction coefficient (ε) of oxidized ABTS, the ε at all the temperature-pressure combinations used for enzyme activity measurements were determined. A volume of 12 mL of 3.125 mM ABTS was oxidized by 100 μL of approximately 30 mM H_2O_2 and 3 mL of 62.5 U mL^{-1} POD. The final concentration of the solution was 2.5 mM ABTS, 0.2 mM H_2O_2, and 12.4 U mL^{-1} POD. As the blank, a solution without H_2O_2 but with the same concentrations of POD and ABTS was used. The H_2O_2 was not in excess and was assumed to be fully consumed when the absorbance of diluted oxidized ABTS at 405 nm at 25 °C remained constant for 30 min. The effective pathlength of cylindrical quartz cuvettes was determined by comparing the absorbance of the oxidized ABTS with the standard 1 cm quartz

cuvettes. The ABTS and the blank solutions were diluted with 0.1 M phosphate buffer (pH 7.5) to ensure the absorbance signal was within the detecting limit. Because the exact concentration of H_2O_2 was not known due to the instability of H_2O_2 solutions, the concentration of the diluted oxidized ABTS was calculated according to Beer's Law using the extinction coefficient of oxidized ABTS (ε = 36.8 $mM^{-1}cm^{-1}$) at 25 °C. The diluted oxidized ABTS was used as the stock solution with the concentration 0.024 mM. The concentration changes induced by pressure were corrected by using the volume ratio $V_{0.1\ MPa,\ 25\ °C}$ / $V_{p,\ T}$ of water. A volume of 340 µL of the diluted oxidized ABTS was pipetted into the cylindrical quartz cuvette to put into the high pressure system each time. The absorbance at 405 nm was recorded at temperature-pressure combinations of 30 °C, 35 °C, 40 °C, 45 °C, or 50 °C and 0.1 MPa, 40 MPa, 80 MPa, 120 MPa, 160 MPa, or 200 MPa. The $\varepsilon_{p,\ T}$ was calculated using the Beer's Law.

3.2.2.4. *In-situ* enzyme activity determination

The *in-situ* enzyme activity was determined by measuring the rate of change of absorbance at 405 nm in the cylindrical quartz cuvette at selected temperatures and pressures. Two magnetic bars and the solution of 340 µL with the final concentration of 3.0 U mL^{-1} AOx, 10.0 U mL^{-1} POD, 1.6 % (v/v) methanol, and 2.0 mM ABTS were added into the cuvette in sequence. Then the quartz cuvette was closed with the Teflon cap avoiding the inclusion of air bubbles. All solutions were prepared in the 0.1 M phosphate buffer (pH 7.5). As the blank, a solution without AOx but with the same concentrations of all the reagents was used. The solutions were mixed by flipping the cuvette 5 times before putting into the high pressure reactor. The absorbance was then measured by the spectrometer connected to the high pressure optical cell. The enzyme activity was calculated as Eq. 2 in terms of the reaction rate.

$$\text{Reaction rate}\left(\mu M\ min^{-1}\right) = \frac{dA_{405}}{dt} \times \frac{1000}{L \times \varepsilon_{p,T}} \quad (2)$$

Where A_{405} is the absorbance at 405 nm, t is the time in minutes, 1000 is the conversion factor from mM to μM, L is the pathlength of the cuvette, and $\varepsilon_{p,T}$ is the extinction coefficient of oxidized ABTS at the selected temperature and pressure.

3.2.2.5. Effect of HHP on the activity of AOx

The enzyme sample was prepared fresh by diluting both the L+R fractions and the R fraction AOx with 0.1 M phosphate buffer (pH 7.5) to a concentration of 0.074 ± 0.005 U mL^{-1}, verified as described in section 3.2.2.1. The *in-situ* activity of the L+R fractions or the R fraction AOx was measured as described in section 3.2.2.4 at the temperature-pressure combinations of 30 °C, 40 °C, or 50 °C and at 0.1 MPa, 80 MPa, or 160 MPa. The high pressure reactor filled with silicone oil was kept at 10 °C when the cuvette was placed in. The selected pressure was applied before the temperature was raised. The recording of the absorbance started when the temperature of the HHP system reached 95 % of the set temperature and lasted for at least 3 min and at a rate of at least one measurement per second. To compensate for the heating transient inside the cuvette, a temperature correction was done to ensure the correct temperature was reached inside the cuvette. A thermocouple was placed inside the quartz cuvette filled with water. At atmospheric pressure, the changes of temperatures inside and outside the cuvette were recorded simultaneously by both the thermocouples inside and outside the cuvette when the system was set to 30 °C, 40 °C, or 50 °C, respectively. The temperature difference tests were done in triplicate at each temperature. An example of the difference of the temperatures inside and outside the cuvette at 30 °C can be found in the supplemental material Fig. S3.1. Because the temperature inside the cuvette increased slowly during the entire experiment, the changes of absorbance were recorded at temperatures inside the cuvette within -2 °C to + 2 °C of the set point of temperatures.

3.2.3. Data analysis

To test the effect of HHP on the activity of the L+R fractions and of the R fraction AOx, a randomized complete block design with temperatures as blocks was used. Temperature was used as the block because it was time-consuming for the HHP system to switch to different temperatures due to the slow heating or cooling speed of the waterbaths. To assure the same conditions of the reagents and to increase the effectiveness of the experiments, each temperature block was performed at a time. All treatments were done in triplicate. Statistical analyses (ANOVA and general linear model) were conducted using Minitab 16 software (State College, PA, USA) and JMP Pro 14 software (Cary, NC, USA). Tukey's method was used for multiple comparisons.

To quantify the effect of temperature on the kinetics of AOx catalyzed at different pressures, the activation energy was calculated using the Arrhenius equation (Eq. 3).

$$k = Ae^{\frac{-E_a}{RT}} \tag{3}$$

Eq. 4 can be transformed into a linear form used for graphical analysis (Eq. 4).

$$\ln k = -\frac{E_a}{R} \times \frac{1}{T} + \ln k_0 \tag{4}$$

Where k is the rate constant of activation, A is the constant relating to the frequency of collisions, E_a is the activation energy, R is the gas constant (8.314 J mol^{-1} K^{-1}), and T is the absolute temperature.

To determine the effect of HHP on the reaction rate, the activation volume was calculated using the Eyring's equation based on the transition-state theory (Eq. 5).

$$\left(\frac{\partial \ln k}{\partial p}\right)_T = -\frac{\Delta V^{\neq}}{RT} \tag{5}$$

Eq. 6 can be transformed into a linear form which is often used for graphical analysis (Eq. 6).

$$\text{Ln } k_p = -\frac{\Delta V^{\neq}}{RT} + \text{Ln } k_0 \qquad \text{Eq. 6}$$

Where $\Delta V^{\neq}$ is the activation volume, which is the difference of the molar volume between the reactants (enzyme-substrate complex) and the transition state, k is the rate constant of activation, p is the pressure, T is the absolute temperature, R is the gas constant (8.314 cm^3 MPa K^{-1} mol^{-1}).

3.3. Results and discussion

3.3.1. Enzyme fractions and their difference in stability

To confirm the existence of the two fractions of AOx purchased from MP Biochemicals used in this research, the diluted enzyme solution was heated at 50 °C for up to 240 min. The changes of the logarithm of residual activity of the AOx *vs.* heating time when heated at 50 °C for up to 60 min is shown in Fig. 3.2A. The thermal inactivation of AOx did not follow the first-order kinetics and the curve started to level off after heating for 2 min. There are two linear regions on Fig. 3.2A. The first linear region (heating time 0.75 – 2 min) is enlarged as Fig. 3.2B. The second linear region is shown in Fig. 3.2C. These two regions are consistent with Buchholz-Afari et al. (2019) who reported that the AOx from *P. pastoris* purchased from the Sigma-Aldrich Chemical Company (St. Louis, MO, USA) had two enzyme fractions which had similar residual enzyme activity behavior when heated at 50 °C. In *P. pastoris*, there are two genes to code for two proteins of AOx1 and AOx2, in which AOx1 accounts for the majority of the activity while AOx2 accounts for approximately one-third of the total activity (Cregg et al. 1989). It was assumed that the two linear regions on the curve (Fig. 3.2B and Fig. 3.2C) represent the two isoenzymes of AOx. As in our previous report, we designated the first linear region as the labile (L) fraction and the second region as the resistant (R) fraction. It is worth studying the kinetics of the L+R fractions and the R fraction separately because of their different thermal stability. We were unable to separate the L

fraction from the mixture because of the minor differences in the molecular weight of the two isozymes (Buchholz-Afari et al. 2019). The L+R fractions instead of the L fraction were thereby used, also because the L fraction accounted for the majority of the enzyme activity of the L+R fractions. The R fraction was separated based on the difference in thermal stability by inactivating the L fraction through heating the sample (L+R fractions) at 50 °C for 15 min, as described in section 2.2.2, and the residual activity of the R fraction was ~35 % after 15 min heating. It is worth mentioning that the L fraction denatured during storage while frozen. The residual activity of the R fraction AOx from the same batch was approximately 10 % less than 35 % about one year before, indicating the less proportion of the L fraction due to its denaturation over storage time. Therefore, it is difficult to obtain the exact same ratio of the two fractions in the L+R fractions AOx. If a new batch enzyme is used or the enzyme has been stored for a while, the residual activity of each fraction needs to be determined again. To further confirm the difference of the thermal stability of the L+R fractions and the R fraction obtained by heating the L+R fractions, the changes of the residual activity of the L+R fractions or the R fraction AOx when heated at 50 °C for 3 min were shown in Fig. 3.3. The differences in the changes of the residual activity in Fig. 3.3 verified that the R fraction was more stable than the L+R fractions. The pseudo-first-order rate constant of inactivation (k_{inact}) of the linear region in Fig. 3.2B representing the L+R fractions was 0.53 ± 0.05 min^{-1} and the k_{inact} of the linear region in Fig.3.2C representing the R fraction was $(3.4 \pm 0.1) \times 10^{-3}$ min^{-1}. The k_{inact} of the R fraction was 156 times smaller than the L+R fractions, suggesting the R fraction was much more stable against thermal treatment than the L+R fractions. Therefore, the L fraction having low thermostability is not likely to have applications in the practical industrial processing even though it accounts for the majority of the activity. However, the activity of the L+R fractions was determined as a reference and the preliminary results were shown in the

supplemental material Table S3.1. The k_{inact} of the L+R fractions was comparable to 0.66 min^{-1} reported by Buchholz-Afari et al. (2019) using the AOx purchased from a different supplier, suggesting the similarity of the AOx from the two suppliers. The k_{inact} of the R fraction was much lower than 0.19 min^{-1} previously reported by Buchholz-Afari et al. (2019) who used the R fraction where the L fraction might not have been totally inactivated by only heating 4 min at 50 °C. As for the activity of the combined fractions, it needs to be studied differently from the thermostability where the inactivation during the first ~7 min at 50 °C accounts mostly for the loss of activity of the L fraction because the inactivation of the R fraction is negligible (Buchholz-Afari et al. 2019). The activity of the L+R fractions is the sum of the activity of the L fraction and the R fraction.

3.3.2. Effect of HHP and temperature on the ε of oxidized ABTS

To adjust the effects of pressure and temperature on the extinction coefficient of oxidized ABTS, the $\varepsilon_{p,T}$ of the oxidized ABTS at each pressure-temperature treatment was tested and reported in Table 3.1. The values in the parentheses are the ratio of $V_{p,\,T}$ / $V_{0.1\ MPa,\ 25\ °C}$ of water (from NIST Chemistry WebBook, SRD 69). The concentration of the oxidized ABTS was multiplied by the ratio to correct the effect of pressure and temperature on the volume of the solution. The values of ε increased as the pressure or the temperature increased. The effect of temperature on ε was significant ($p < 0.05$) using the general linear model (GLM). This was in accordance with Mukerji et al. (2002) who reported the increase of the extinction coefficient of chromic acid, iodine, and potassium oxalate with the increase of temperature. However, it was the opposite to the finding of the ε of o-dianisidine reported by Halalipour et al. (2020), where the ε decreased when temperatures increased. The importance of correcting the effect of temperature on the ε to get accurate results was emphasized by Kim and Liu (2007) through estimating the errors when calculating the concentrations of hemoglobin without considering the variation of the ε. The

effect of pressure on ε was not significant ($p < 0.05$) using the GLM. Only at 30 °C, pressure had significant influence ($p < 0.05$) on the ε using one-way ANOVA. It was not significant ($p < 0.05$) at other temperatures. Differently, the ε of o-dianisidine reported by Halalipour et al. (2020) was higher at high pressures above 0.1 MPa. These differences may be from the different interactions of the sulfonate groups on ABTS and the methoxy or amine groups on o-dianisidine at different temperatures and pressures, and thereby affecting the way the chemicals interact with light. For the ε of oxidized ABTS in all the temperature-pressure conditions, the lowest ε was 32.9 ± 0.5 $mM^{-1}cm^{-1}$ at 0.1 MPa and at 30 °C and the highest ε was 38.5 ± 5.4 $mM^{-1}cm^{-1}$ at 200 MPa and at 50 °C. The determined ε of oxidized ABTS at each temperature-pressure treatment was used to calculate the enzyme activity determined in the corresponding conditions.

3.3.3. Effect of HHP on the activity of AOx

To assess the effect of HHP on the activity of AOx at different temperatures, the reaction rate of the L+R fractions or the R fraction AOx was determined at 30 °C, 40 °C, and 50 °C, and at 0.1 MPa, 80 MPa, and 160 MPa. The reaction rates of the R fraction can be found in Table 3.2. The enzyme activity of the R fraction AOx at 80 or 160 MPa and 50 °C was 17.9 ± 3.6 or 17.7 ± 0.8 μM min^{-1}, respectively. The activity was about 3 times as high as the activity at 0.1 MPa and 30 °C. To avoid the error from preparing the enzyme stock solution, the enzyme activity tests of the R fraction AOx at three different temperature blocks were performed on the same day in the random order where the enzyme stock solution was prepared fresh and the enzyme activity was diluted to 0.078 ± 0.005 U mL^{-1} or 3.2 ± 0.2 μM min^{-1} at 25 °C and 0.1 MPa. At 160 MPa and 50 °C, the enzyme activity of the L+R fractions was 18.4 ± 2.7 μM min^{-1}, similar to the activity of the R fraction in the same conditions, 17.7 ± 0.8 μM min^{-1}. Therefore, the activity of the L+R fractions or the R fraction AOx increased up to approximately 6 times at 50 °C and 160 MPa

compared to the activity at 25 °C and 0.1 MPa. However, the comparison of the activity of the R fraction at 50 °C and 160 MPa to the activity at 50 °C and 0.1 MPa was not valid because the enzyme started to inactivate during the experiment at 0.1 MPa. If there was no enzyme inactivation, the activity of the R fraction at 50 °C and 0.1 MPa would be higher than the rate of 7.4 ± 0.4 μM min^{-1}, determined from the non-linear region. The inactivation was indicated by the deviations from linearity in the absorbance *vs.* time curves. Similar enzyme inactivation was observed for the L+R fractions at higher temperatures and lower pressures. An example is shown in Fig. 3.4, by comparing one replicate from the L+R fractions at 30 °C (Fig. 3.4A) and one replicate at 50 °C (Fig. 3.4B), both at atmospheric pressure. Unlike the more stable R fraction, the less stable L+R fractions started to inactivate at 40 °C, making the results at many temperature-pressure combinations no longer represent the activity at constant concentration of active AOx. Therefore, only the results of the R fraction AOx is discussed.

From Table 3.2 at 50 °C, the R fraction was inactivated at 0.1 MPa but not at 80 MPa or 160 MPa, indicating the stabilizing effect of HHP against thermal inactivation. This was in accordance with the thermal stability increase of the AOx by HHP, previously reported by Buchholz-Afari et al. (2019). Therefore, the stabilizing effect of HHP enabled the R fraction AOx to work at higher temperatures without detectable denaturation within the time frame of our experiments and resulted in a higher reaction rate. The dependence of the enzyme activity on the temperature was estimated by calculating the apparent activation energy (E_a) shown in Table 3.2. Since the enzyme started to be inactivated at 50 °C and 0.1 MPa, the E_a at 0.1 MPa was not determined because the estimate was crude only using the results at 30 °C and 40 °C at 0.1 MPa. The Arrhenius plots to obtain the E_a can be found in the supplemental materials Fig. S3.2. The E_a at 80 MPa, 41.4 ± 10.5 kJ mol^{-1}, had no difference with the E_a at 160 MPa, 43.8 ± 7.8kJ mol^{-1}.

This suggested that there was no difference in the dependence of the activity of the R fraction AOx on the temperature between 80 MPa and 160 MPa. Different from AOx, the E_a of the native GOx increased with higher pressures, suggesting a less effective enzyme catalyst at higher pressures (Halalipour et al. 2020). Therefore, for the R fraction AOx the enzyme activity had the same increase with temperatures at 80 MPa or 160 MPa. The stabilizing effect of HHP contributed to the increase in the enzyme activity of AOx at high temperatures by protecting the enzymes with high activities from thermal inactivation. However, the mechanism of the stabilizing effect of HHP on enzymes still remained unclear. According to Le Chatelier principle, the high pressure reduces the volume of protein solutions (Kirsch et al. 2013). High pressure also decreases the volume of non-rigid internal cavities of proteins through the displacement of helices (Collins et al. 2007). At moderate pressures, the compressed cavities result in an increase in the Van de Waals forces which stabilizes the proteins (Boonyaratanakornkit et al. 2002). The increase in the thermal stability of enzymes by HHP can also be attributed to the antagonistic effect of pressure and high temperature (Yang et al. 2020). Pressure and temperature are reported to have antagonistic effect on the enzymes which can be described with elliptical shaped contour plots where the native state of enzymes is retained at high temperatures and moderately high pressures (Degraeve et al. 2002; Terefe et al. 2013; Reyes-De-Corcuera et al. 2018). High pressures, typically below 300 MPa, counteract the unfolding of proteins caused by high temperatures through 1) strengthening the hydration of charge and non-polar groups to prevent the water loss (Mozhaev et al. 1996), 2) strengthening the hydrogen bonds to maintain the intermolecular oxygen-hydrogen interactions (Hédoux et al. 2011), and 3) strengthening the ion pairs (Eisenmenger and Reyes-De-Corcuera 2009).

High pressure was not only reported to have the ability to stabilize enzymes, but the ability to activate enzymes as well (Eisenmenger and Reyes-De-Corcuera 2009). The increase in the activity of GOx was attributed to both the stabilizing effect and activating effect of HHP (Halalipour et al. 2020). However, from Table 3.2, high pressure did not have significant influence on the activity of the R fraction AOx at each of the three temperatures. At 30 °C and 40 °C, there was no inactivation of the R fraction AOx at all the three pressures, indicated not only by the linearity of the absorbance *vs.* time curves but also verified by the prediction using the results from Buchholz-Afari et al. (2019). Therefore, the no difference in the reaction rate at different pressures and at the same temperature was not the result of the combined effect of enzyme inactivation by temperature and enzyme activation by HHP. It suggested that HHP had no activating effect on the R fraction AOx. According to Le Chatelier principle, a system at equilibrium will counteract itself to restore the equilibrium state when the high pressure is applied, which results in the decrease in the overall volume of the system. In transition-state theory, the effect of HHP on the reaction rate can be described using the Eyring's equation (Eq. 6). When the reaction rate is increased by HHP, the energy barrier for the reaction is lowered and the activation volume is negative (Li et al. 2015a). Examples of the negative activation volumes with increased enzyme activities by HHP include the enzyme α-chymotrypsin (Mozhaev et al. 1996; Luong and Winter 2015; Schuabb et al. 2016), and α-L-rhamnosidase and naringinase (Vila-Real et al. 2010). The negative activation volume may result from the destruction of the electrostatic interactions when forming the transition state, which strengthens the hydration caused by the interaction of water with charged and polar amino acids exposed by HHP (Mozhaev et al. 1996; Luong and Winter 2015). In contrast, when the enzymatic reaction is suppressed by HHP, the activation volume is positive (Ohmae et al. 2007). The volume changes induced by HHP can be attributed to the reactants themselves or the result of the

interactions between the reactants and the solvents (Boonyaratanakornkit et al. 2002). To assess the dependence of the enzyme activity on pressure, the activation volumes were calculated in Table 3.2. However, the activation volumes were statistically zero as expected since the HHP did not activate or suppress the catalytic reactions of the R fraction AOx. The different behavior of the R fraction AOx that cannot be activated at HHP from GOx that can be activated at HHP could be attributed to the different conformation changes at HHP. The AOx and GOx are both flavin dependent oxidases but with different properties such as size, number of subunits, and cavities. The active site of AOx from *P. pastoris* is solvent inaccessible and it is surrounded by the side chains of Asn616, His567, and an isoalloxazine ring (Koch et al. 2016). The active site of GOx from *A. niger* is in a deep pocket close to Glu412, His516, and His519 (Leskovac et al. 2005). Moderate high pressures can alter the tertiary or quaternary structures of proteins without denaturation. The changes in enzyme activity is reported to be related to the conformation changes of proteins at high pressures (Nguyen and Roche 2017). The increase in the rate of reactions can be attributed to the changes in the active site of enzymes and the enzyme flexibility. For example, the molecular dynamics simulation of lipase activated at high pressure (> 100 MPa) revealed that the channel access to the active site was opened through a conformation change induced by HHP (Johnson et al. 2016). Therefore, it was possible that HHP increased the accessibility of the active sites of GOx but not AOx. In order to better understand the possibly different protein conformation changes of the two enzymes at HHP, the protein structure is needed to be analyzed by fluorescence, nuclear magnetic resonance (NMR) spectroscopy, or Fourier-transform infrared spectroscopy. The development of NMR spectroscopy or X-ray crystallography at high pressure makes the investigation possible (Cioni and Gabellieri 2011). However, these studies are beyond the scope of this study.

3.4. Summary

The activity of both the L+R fractions and the R fraction AOx was increased at HHP. The increase in the apparent activity of the R fraction AOx was attributed only to the stabilizing effect of HHP. The increase in the activity was not related to the activating effect of HHP, verified by the calculated activation volume statistically zero. The activation energy of the R fraction AOx was not different between 80 MPa and 160 MPa, suggesting there was no difference in the dependence of the activity on the temperature. The activity of the R fraction was increased up to approximately 6 times at high pressures (80 or 160 MPa) at 50 °C compared to the activity at ambient pressure and at 25 °C. Because the R fraction AOx only accounted for ~35 % of the activity of the L+R fractions, it can save about 50 % of the enzyme if working at 80 or 160 MPa and 50 °C using only the R fraction AOx compared to working at 0.1 MPa and 25 °C using the L+R fractions AOx. The increase in the activity of the R fraction AOx under HHP provided a new method to improve the catalyst AOx as a biocatalyst. The higher activity of the R fraction AOx obtained using this method can be beneficial to the industrial applications in terms of higher efficiency and economic savings.

Acknowledgment

This work was supported by the USDA National Institute of Food and Agriculture [grant number 2014-67021-21604/ project accession no. 1001899].

3.5. References

Azevedo AM, Prazeres DMF, Cabral JMS, Fonseca LP. 2005. Ethanol biosensors based on alcohol oxidase. Biosensors and Bioelectronics. 21(2):235-247.

Bleoanca I, Neagu C, Turtoi M, Borda D. 2018. Mild-thermal and high pressure processing inactivation kinetics of polyphenol oxidase from peach puree. Journal of Food Process Engineering. 41(7):e12871.

Boonyaratanakornkit BB, Park CB, Clark DS. 2002. Pressure effects on intra- and intermolecular interactions within proteins. Biochimica et Biophysica Acta - Protein Structure and Molecular Enzymology. 1595(1):235-249.

Buchholz-Afari MI, Halalipour A, Yang D, Reyes-De-Corcuera JI. 2019. Increased stability of alcohol oxidase under high hydrostatic pressure. Journal of Food Engineering. 246:95-101.

Choi J-M, Han S-S, Kim H-S. 2015. Industrial applications of enzyme biocatalysis: Current status and future aspects. Biotechnology Advances. 33(7):1443-1454.

Cioni P, Gabellieri E. 2011. Protein dynamics and pressure: What can high pressure tell us about protein structural flexibility? Biochimica et Biophysica Acta - Proteins and Proteomics. 1814(8):934-941.

Collins MD, Quillin ML, Hummer G, Matthews BW, Gruner SM. 2007. Structural rigidity of a large cavity-containing protein revealed by high-pressure crystallography. Journal of Molecular Biology. 367(3):752-763.

Cregg JM, Madden KR, Barringer KJ, Thill GP, Stillman CA. 1989. Functional characterization of the two alcohol oxidase genes from the yeast *Pichia pastoris*. Molecular and Cellular Biology. 9(3):1316.

Degraeve P, Rubens P, Lemay P, Heremans K. 2002. In situ observation of pressure-induced increased thermostability of two β-galactosidases with FT-IR spectroscopy in the diamond anvil cell. Enzyme and Microbial Technology. 31(5):673-684.

Eisenmenger MJ, Reyes-De-Corcuera JI. 2009. High pressure enhancement of enzymes: a review. Enzyme and Microbial Technology. 45(5):331-347.

Goswami P, Chinnadayyala SSR, Chakraborty M, Kumar AK, Kakoti A. 2013. An overview on alcohol oxidases and their potential applications. Applied Microbiology and Biotechnology. 97(10):4259-4275.

Halalipour A, Duff Jr MR, Howell EE, Reyes-De-Corcuera JI. 2017a. Glucose oxidase stabilization against thermal inactivation using high hydrostatic pressure and hydrophobic modification. Biotechnology and Bioengineering. 114(3):516-525.

Halalipour A, Duff MR, Howell EE, Reyes-De-Corcuera JI. 2017b. Effects of high hydrostatic pressure or hydrophobic modification on thermal stability of xanthine oxidase. Enzyme and Microbial Technology. 103:18-24.

Halalipour A, Duff MR, Howell EE, Reyes-De-Corcuera JI. 2020. Catalytic activity and stabilization of phenyl-modified glucose oxidase at high hydrostatic pressure. Enzyme and Microbial Technology. 137:109538.

Hédoux A, Guinet Y, Paccou L. 2011. Analysis of the mechanism of lysozyme pressure denaturation from Raman spectroscopy investigations, and comparison with thermal denaturation. The Journal of Physical Chemistry B. 115(20):6740-6748.

Herbst D, Peper S, Fernández JF, Ruck W, Niemeyer B. 2014. Pressure effects on activity and selectivity of *Candida rugosa* lipase in organic solvents. Journal of Molecular Catalysis B: Enzymatic. 100:104-110.

Janssen FW, Ruelius HW. 1968. Alcohol oxidase, a flavoprotein from several basidiomycetes species: Crystallization by fractional precipitation with polyethylene glycol. Biochimica et Biophysica Acta - Enzymology. 151(2):330-342.

Johnson QR, Lindsay RJ, Nellas RB, Shen T. 2016. Pressure-induced conformational switch of an interfacial protein. Proteins: Structure, Function, and Bioinformatics. 84(6):820-827.

Kakoti A, Kumar AK, Goswami P. 2012. Microsome-bound alcohol oxidase catalyzed production of carbonyl compounds from alcohol substrates. Journal of Molecular Catalysis B: Enzymatic. 78:98-104.

Keesey J. 1987. Boehringer Mannheim Biochemicals. Biochemica Information. p. 58.

Kim JG, Liu H. 2007. Variation of haemoglobin extinction coefficients can cause errors in the determination of haemoglobin concentration measured by near-infrared spectroscopy. Physics in Medicine & Biology. 52(20):6295.

Kirsch C, Dahms J, Kostko AF, McHugh MA, Smirnova I. 2013. Pressure assisted stabilization of biocatalysts at elevated temperatures: characterization by dynamic light scattering. Biotechnology and Bioengineering. 110(6):1674-1680.

Koch C, Neumann P, Valerius O, Feussner I, Ficner R. 2016. Crystal structure of alcohol oxidase from *Pichia pastoris*. PLoS One. 11(2).

Leskovac V, Trivić S, Wohlfahrt G, Kandrač J, Peričin D. 2005. Glucose oxidase from *Aspergillus niger*: the mechanism of action with molecular oxygen, quinones, and one-electron acceptors. The International Journal of Biochemistry & Cell Biology. 37(4):731-750.

Li Y, Miao M, Chen X, Jiang B, Liu M, Feng B. 2015a. Improving the catalytic behavior of inulin fructotransferase under high hydrostatic pressure. Journal of the Science of Food and Agriculture. 95(13):2588-2594.

Li Y, Miao M, Liu M, Chen X, Jiang B, Feng B. 2015b. Enhancing the thermal stability of inulin fructotransferase with high hydrostatic pressure. International Journal of Biological Macromolecules. 74:171-178.

Luong TQ, Winter R. 2015. Combined pressure and cosolvent effects on enzyme activity–a high-pressure stopped-flow kinetic study on α-chymotrypsin. Physical Chemistry Chemical Physics. 17(35):23273-23278.

Marciniak A, Suwal S, Naderi N, Pouliot Y, Doyen A. 2018. Enhancing enzymatic hydrolysis of food proteins and production of bioactive peptides using high hydrostatic pressure technology. Trends in Food Science & Technology. 80:187-198.

Mozhaev VV, Lange R, Kudryashova EV, Balny C. 1996. Application of high hydrostatic pressure for increasing activity and stability of enzymes. Biotechnology and Bioengineering. 52(2):320-331.

Mukerji B, Bhattacharji A, Dhar N. 2002. The variation of the extinction-coefficient with temperature. The Journal of Physical Chemistry. 32(12):1834-1840.

Nguyen LM, Roche J. 2017. High-pressure NMR techniques for the study of protein dynamics, folding and aggregation. Journal of Magnetic Resonance. 277:179-185.

Ohmae E, Murakami C, Gekko K, Kato C. 2007. Pressure effects on enzyme functions. International Journal of Biological Macromolecules. 7:23-29.

Ozimek P, Veenhuis M, van der Klei IJ. 2005. Alcohol oxidase: a complex peroxisomal, oligomeric flavoprotein. FEMS Yeast Research. 5(11):975-983.

Patel NG, Meier S, Cammann K, Chemnitius GC. 2001. Screen-printed biosensors using different alcohol oxidases. Sensors and Actuators B: Chemical. 75(1):101-110.

Reyes-De-Corcuera JI, Olstad HE, García-Torres R. 2018. Stability and stabilization of enzyme biosensors: the key to successful application and commercialization. Annual Review of Food Science and Technology. 9:293-322.

Schuabb V, Winter R, Czeslik C. 2016. Improved activity of α-chymotrypsin on silica particles–A high-pressure stopped-flow study. Biophysical Chemistry. 218:1-6.

Terefe NS, Delon A, Buckow R, Versteeg C. 2015. Blueberry polyphenol oxidase: Characterization and the kinetics of thermal and high pressure activation and inactivation. Food Chemistry. 188:193-200.

Terefe NS, Sheean P, Fernando S, Versteeg C. 2013. The stability of almond β-glucosidase during combined high pressure–thermal processing: a kinetic study. Applied Microbiology and Biotechnology. 97(7):2917-2928.

Vila-Real H, Alfaia AJ, Phillips RS, Calado AR, Ribeiro MH. 2010. Pressure-enhanced activity and stability of α-l-rhamnosidase and β-d-glucosidase activities expressed by naringinase. Journal of Molecular Catalysis B: Enzymatic. 65(1-4):102-109.

Wallace LS. 2017. The effect of high hydrostatic pressure on stability of pyruvate oxidase from *aeroccocus species*. University of Georgia Theses and Dissertations.19-50.

Yang D, Olstad HE, Reyes-De-Corcuera JI. 2020. Increased thermal stability of a glucose oxidase biosensor under high hydrostatic pressure. Enzyme and Microbial Technology. 134:109486.

Table 3.1. The extinction coefficients of the oxidized ABTS at each pressure-temperature treatment ± one standard deviation (n = 3). The values of $V_{p, T} / V_{0.1\ MPa, 25\ °C}$ of water shown in the parentheses were used to correct the effect of pressure and temperature on the concentration of oxidized ABTS.

Pressure (MPa)	Temperature (°C)				
	30	35	40	45	50
	ε ($mM^{-1}cm^{-1}$)				
0.1	32.9[a] ± 0.5	31.9 ± 0.4	36.0 ± 2.6	35.6 ± 1.5	34.3 ± 5.5
	(1.000)	(0.983)	(0.968)	(0.954)	(0.941)
40	33.7[ab] ± 0.2	33.7 ± 1.4	36.3 ± 2.7	36.5 ± 1.6	35.2 ± 5.4
	(1.001)	(0.984)	(0.969)	(0.956)	(0.943)
80	34.3[abc] ± 0.5	33.4 ± 0.9	36.2 ± 1.9	36.6 ± 1.7	37.4 ± 5.3
	(1.003)	(0.986)	(0.971)	(0.958)	(0.945)
120	34.3[abc] ± 0.4	33.7 ± 0.7	36.6 ± 1.6	37.5 ± 0.9	37.2 ± 4.5
	(1.005)	(0.988)	(0.973)	(0.960)	(0.947)
160	35.1[bc] ± 1.0	34.3 ± 1.1	37.2 ± 1.8	37.6 ± 1.8	37.5 ± 4.9
	(1.007)	(0.990)	(0.975)	(0.962)	(0.949)
200	35.2[c] ± 0.8	34.8 ± 1.8	37.5 ± 2.8	37.9 ± 1.3	38.5 ± 5.4
	(1.009)	(0.992)	(0.977)	(0.964)	(0.951)

[a - c] Differences in the ε between different pressures at 30 °C with different letter were significant ($p < 0.05$), no significant difference was found between different pressures at other temperatures. No significant difference ($p > 0.05$) was found in the ε between different temperatures at each pressure.

Table 3.2. The mean rate of reaction ± one standard deviation (n = 3) of the R fraction AOx at each temperature-pressure treatment, the activation energy (E_a) ± standard error calculated at each pressure, and the activation volume ($\Delta V^{\neq}$) ± standard error calculated at each temperature.

	Temperature (°C)			
	30	40	50	E_a (kJ mol^{-1})
Pressure (MPa)	Reaction rate (μM min^{-1})			
0.1	6.1^{a} ± 0.2	9.2^{abc} ± 0.7	7.4^{ab} ± 0.4*	ND
80	6.4^{a} ± 0.0	16.1^{bc} ± 6.6	17.9^{c} ± 3.6	41.4 ± 10.5
160	6.2^{a} ± 0.1	12.2^{abc} ± 4.3	17.7^{c} ± 0.8	43.8 ± 7.8
$\Delta V^{\neq}$ (cm^3 mol^{-1})	-0.03 ± 0.40	-3.41 ± 4.37	ND	

[a - c] Differences in the mean of reaction rate across the table with different letter were significant ($p < 0.05$).

* The data collected for AOx activity were not in the linear range indicating enzyme inactivation. ND = Not determined because the enzyme started to be inactivated during the experiment at 50 °C and 0.1 MPa.

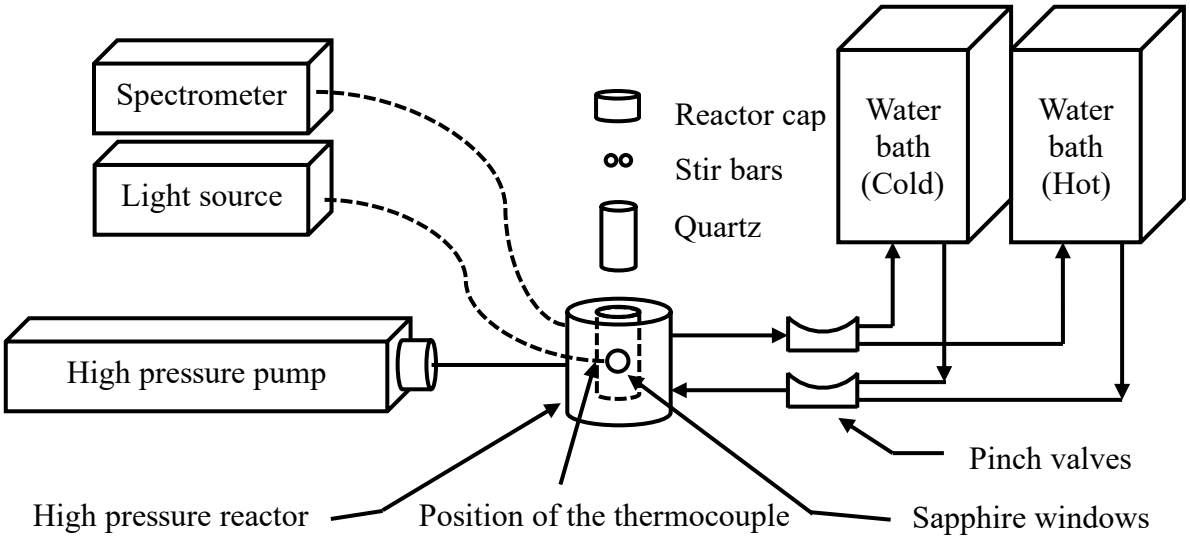

Fig. 3.1. Schematic diagram of the high pressure system used to determine the *in-situ* activity of enzymes.

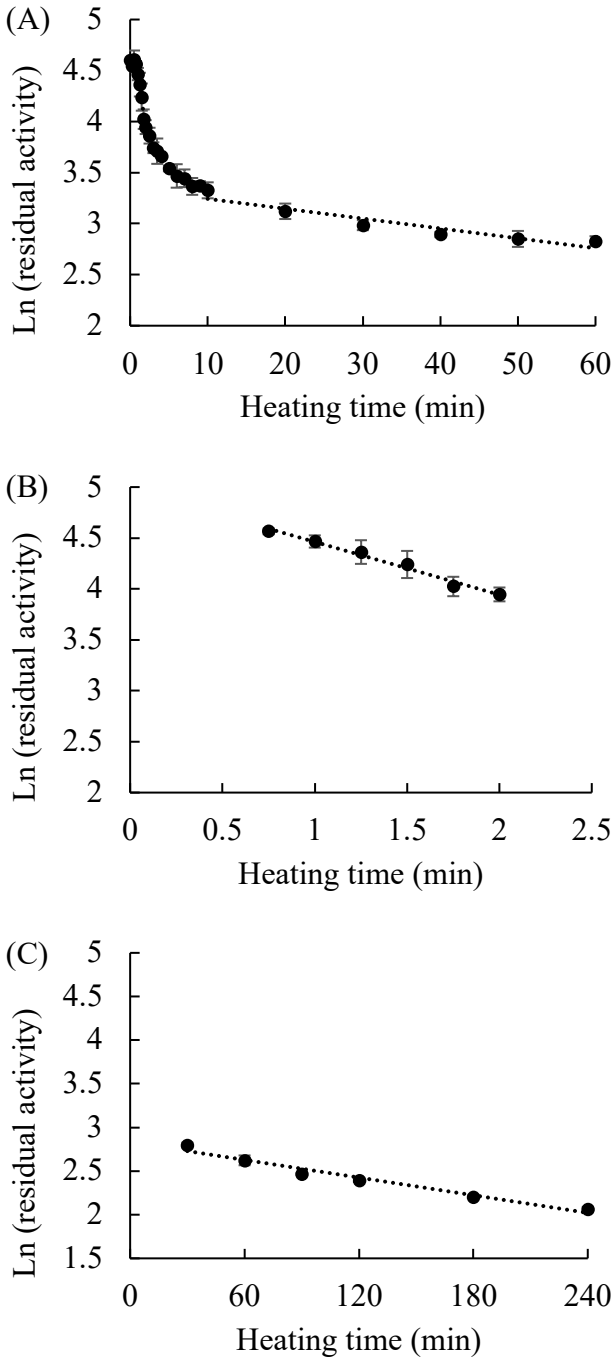

Fig. 3.2. (A) The changes of ln (residual activity) of soluble AOx when heated at 50 °C in 0.1 M phosphate buffer pH 7.5 (0 – 60 min); (B) Linear regression fitted to the labile fraction of AOx (0.75 – 2 min); (C) Linear regression fitted to the resistant fraction of AOx (30 – 240 min). Error bars represent ± one standard deviation (n = 3).

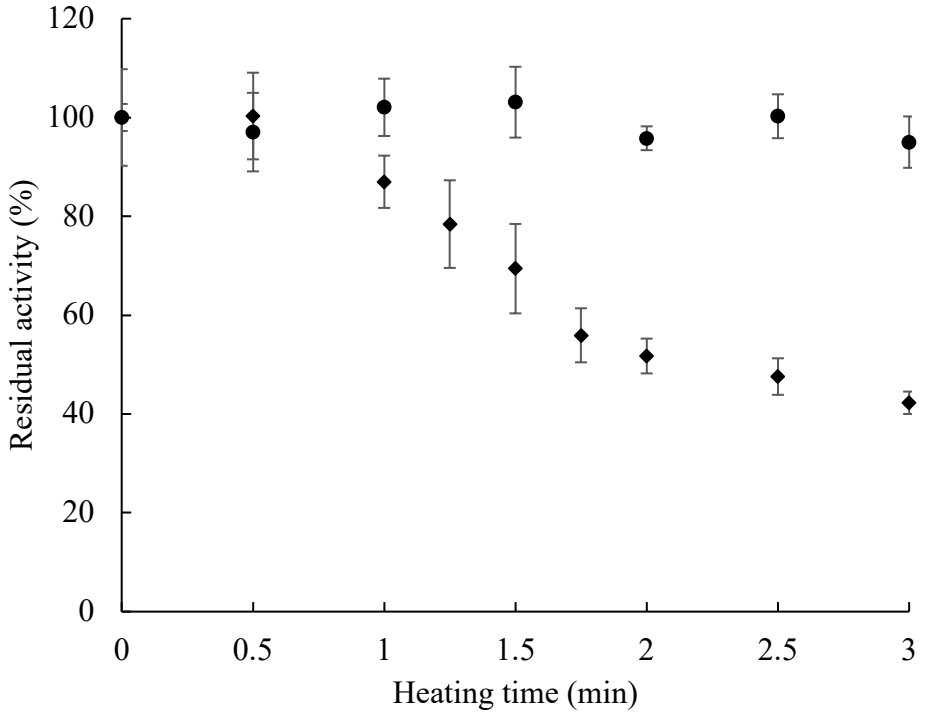

Fig. 3.3. The changes of the residual activity of the L+R fractions (◆) or the R fraction (●) AOx when heated at 50 °C in 0.1 M phosphate buffer pH 7.5 for 3 min. Error bars represent ± one standard deviation (n = 3).

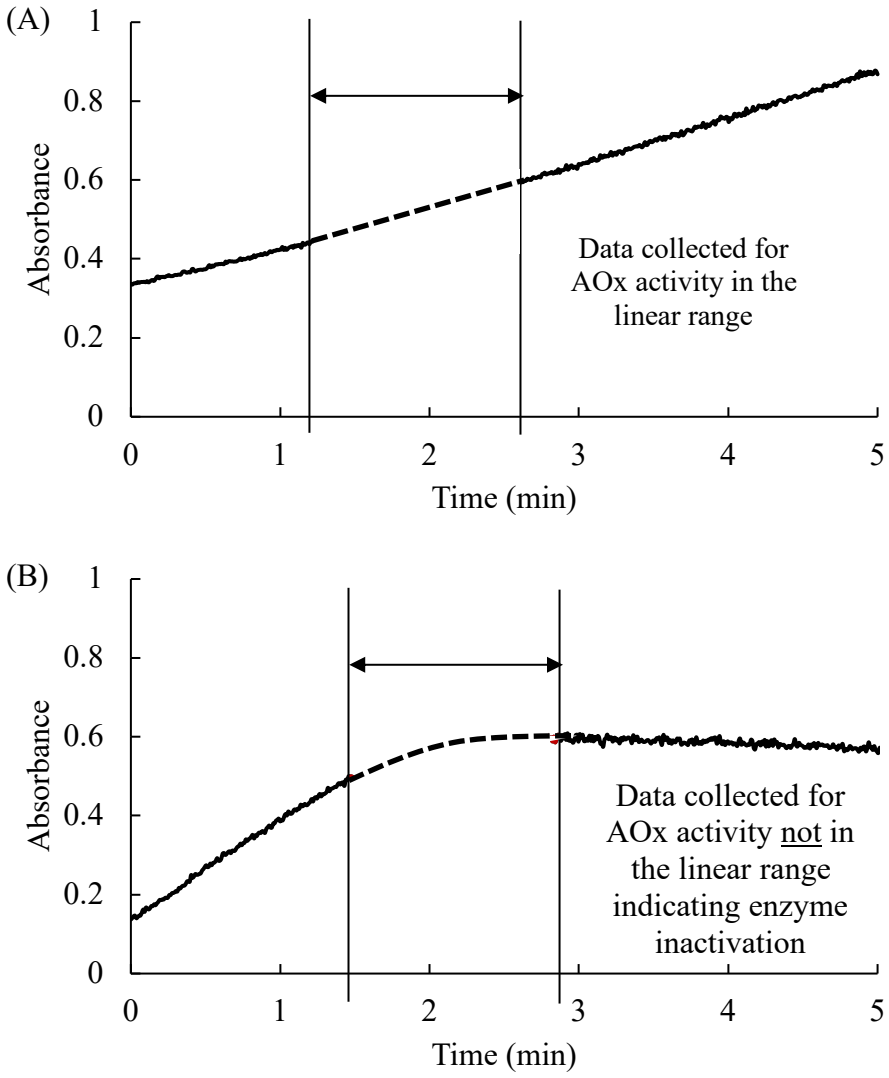

Fig. 3.4. Examples of the absorbance change at 405 nm *vs.* time. Data used to calculate AOx activity was recorded for ~1.3 min starting when the temperature inside the high pressure reactor reached 95 % of the set temperature (time 0 in Fig. 3.4A and Fig. 3.4.B). (A) One replicate of the L+R fraction treated at 30 °C and atmospheric pressure; (B) one replicate of the L+R fraction treated at 50 °C and atmospheric pressure when the enzyme started to be inactivated. The portion marked as (---) corresponds to the temperature range of 28 – 32 °C (A) or 48 – 52 °C (B) inside the quartz cuvette.

Supplemental materials

Table S3.1. The mean rate of reaction ± one standard deviation (n = 3) at each temperature-pressure treatment.

		Temperature (°C)				
		30	35	40	45	50
Pressure (MPa)	Enzyme fraction	Reaction rate (μM min^{-1})				
0.1	L+R	$7.0^{a} \pm 2.5$	$2.8^{a} \pm 0.2$	$1.3^{a} \pm 0.3$*	$3.5^{a} \pm 0.6$	$2.7^{a} \pm 0.7$*
	R	$6.6^{a} \pm 0.9$	$6.1^{abcd} \pm 0.7$	$3.8^{ab} \pm 0.2$*	$5.6^{abc} \pm 0.4$	$5.9^{ab} \pm 0.1$*
40	L+R	$11.8^{ab} \pm 7.4$	$5.2^{abc} \pm 0.5$	$4.5^{ab} \pm 1.8$*	$5.3^{ab} \pm 1.3$	$7.0^{abc} \pm 0.6$*
	R	$11.1^{ab} \pm 4.5$	$7.8^{bcd} \pm 0.9$	$7.9^{abc} \pm 0.9$	$7.3^{abc} \pm 0.3$	$25.5^{cde} \pm 14.5$
80	L+R	$14.7^{ab} \pm 1.8$	$4.8^{abc} \pm 1.3$	$7.4^{abc} \pm 2.9$	$6.3^{abc} \pm 1.9$	$8.8^{abcd} \pm 1.5$*
	R	$20.0^{b} \pm 8.7$	$8.8^{d} \pm 2.1$	$12.2^{bc} \pm 1.6$	$9.4^{bc} \pm 1.4$	$18.9^{abcde} \pm 5.9$
120	L+R	$14.6^{ab} \pm 2.5$	$5.7^{abcd} \pm 1.6$	$10.1^{abc} \pm 5.1$	$4.8^{ab} \pm 1.8$	$10.7^{abcde} \pm 2.2$
	R	$10.6^{ab} \pm 4.0$	$8.4^{cd} \pm 0.7$	$15.3^{c} \pm 4.7$	$10.9^{c} \pm 4.6$	$26.8^{de} \pm 6.2$
160	L+R	$16.6^{ab} \pm 6.0$	$4.8^{ab} \pm 0.8$	$10.6^{bc} \pm 1.8$	$7.5^{abc} \pm 1.7$	$18.4^{abcde} \pm 2.7$
	R	$11.4^{ab} \pm 3.1$	$7.7^{bcd} \pm 2.2$	$14.5^{c} \pm 2.5$	$7.6^{abc} \pm 0.9$	$22.4^{bcde} \pm 5.3$
200	L+R	$6.1^{a} \pm 1.7$	$4.0^{a} \pm 0.6$	$7.6^{abc} \pm 2.0$	$5.9^{abc} \pm 1.1$	$14.1^{abcde} \pm 4.3$
	R	$13.5^{ab} \pm 2.7$	$8.0^{bcd} \pm 1.9$	$14.0^{c} \pm 6.1$	$8.4^{abc} \pm 1.2$	$28.2^{e} \pm 11.5$

[a - e] Differences in the reaction rate at each temperature with different letter were significant ($p < 0.05$).

* The enzyme started to be inactivated during the experiment.

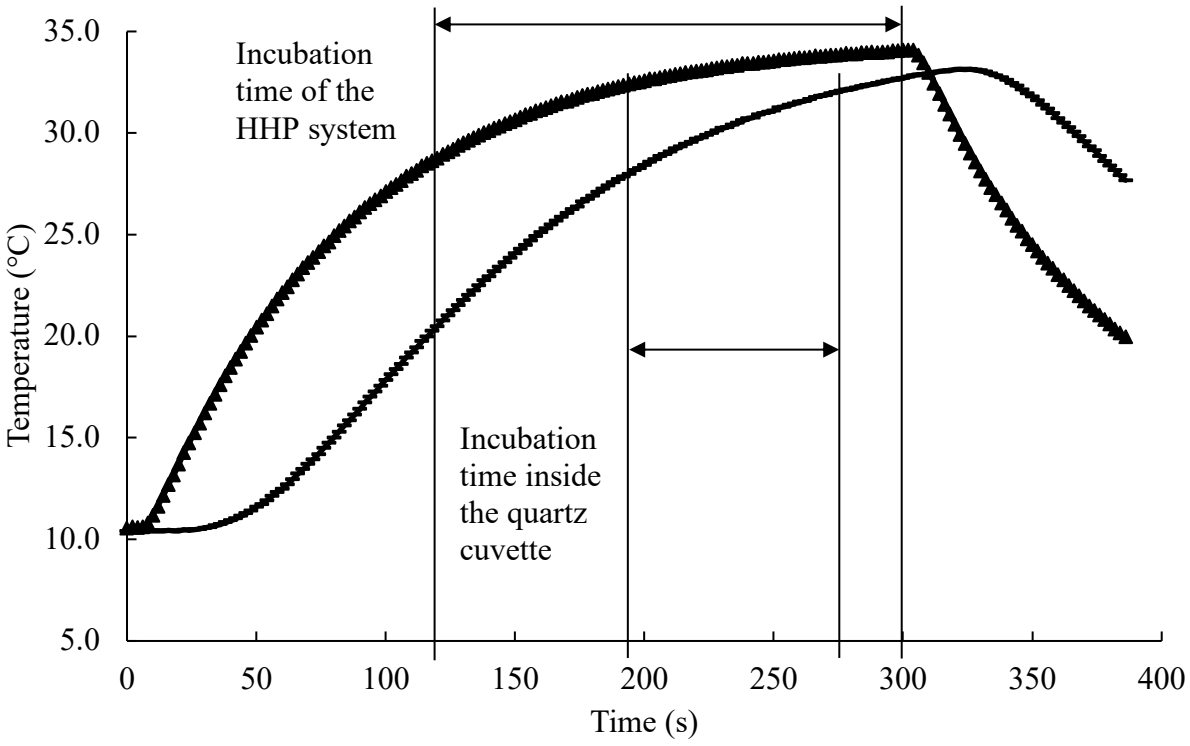

Fig. S3.1. Heating transients inside (-) and outside (▲) the quartz cuvette when using the high pressure system with the setpoint temperature of 30 °C, at atmospheric pressure, and HHP system incubation time 3 min.

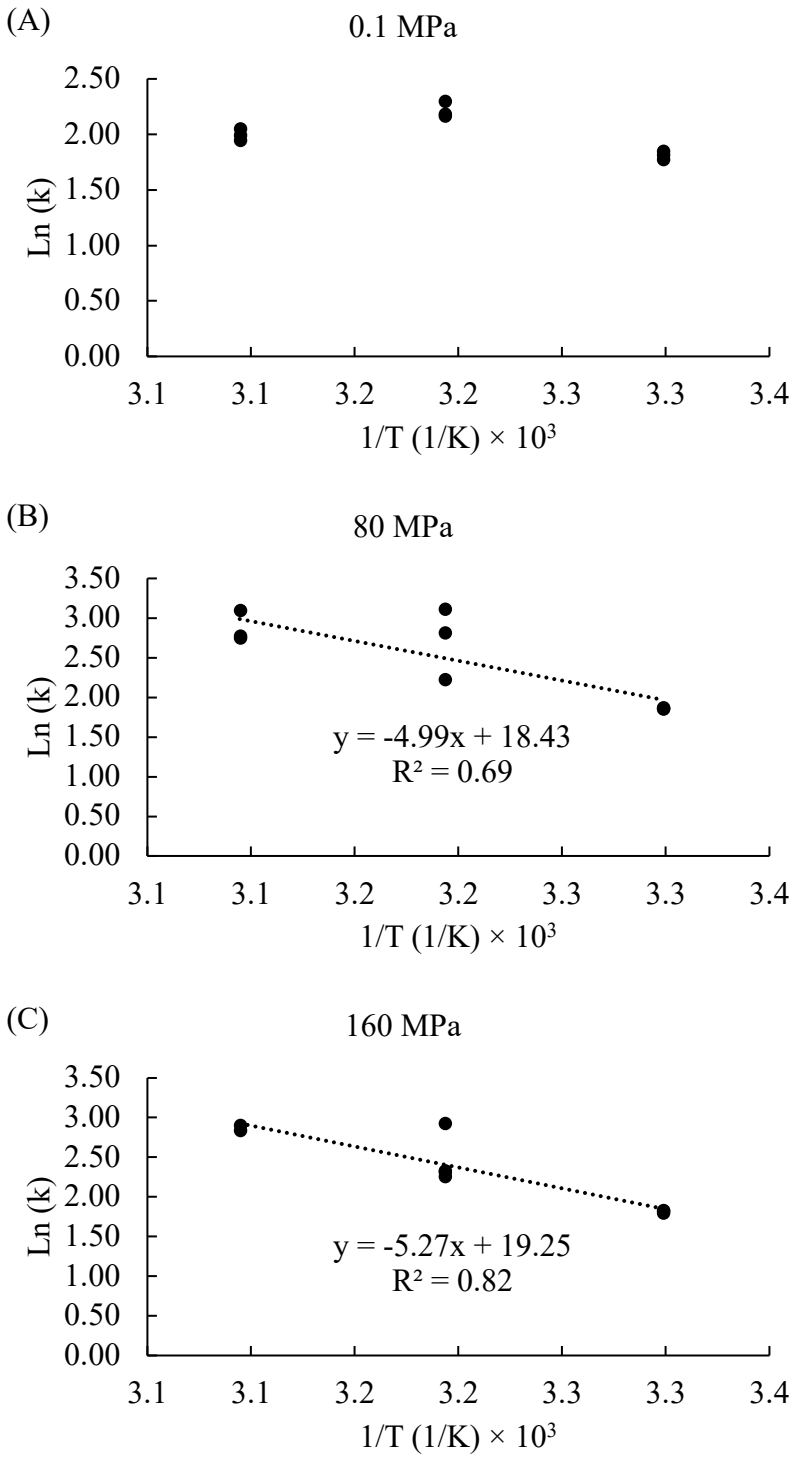

Fig. S3.2. Arrhenius plots to obtain the apparent activation energy from linear regression of ln (k) *vs.* inverse of absolute temperature at 0.1 MPa (A), 80 MPa (B), or 160 MPa (C).

CHAPTER 4

ENTRAPMENT OF ALCOHOL OXIDASE IN POLY(*O*-PHENYLENEDIAMINE) FOR BIOSENSOR FABRICATION [1]

[1] Yang, D. and Reyes-De-Corcuera J.I. To be submitted to the *Journal of Enzyme and Microbial Technology*

Abstract:

The effect of immobilization by electropolymerization in electrochemically generated poly(*o*-phenylenediamine) (PoPD) films on the storage and thermal stability of alcohol oxidase (AOx) is reported. The labile + resistant (L+R) fractions AOx and the resistant (R) fraction AOx were studied. The pseudo-first-order rate constants of response loss of the immobilized L+R fractions and of the immobilized R fraction alone were not significantly different and were approximately 44 times greater than the pseudo-first-order rate constant of inactivation of the R fraction AOx in solution, suggesting the decrease in the effective amperometric response was caused by enzyme leaching out of the immobilization matrix rather than enzyme inactivation. Indeed, the thickness of the PoPD film is similar to the diameter of the AOx from *P. pastoris*. Therefore, electrochemically generated PoPD is not an adequate immobilization material for AOx. The effect of high hydrostatic pressure (HHP) on the stability of the AOx biosensors in terms of the stability of AOx could not be determined.

Keywords: alcohol oxidase; high hydrostatic pressure; biosensor; electropolymerization; enzyme leaching

4.1. Introduction

Alcohol oxidase (AOx; EC. 1.1.3.13) catalyzes the oxidation of alcohols into the corresponding carbonyl compounds and hydrogen peroxide. The enzyme can be used as a biocatalyst to synthesize carbonyl compounds that are important as solvents, pharmaceuticals, or ingredients in fragrances and flavors without producing undesirable harmful by-products [1]. Alcohol oxidase is also one of the main enzymes used to detect alcohols, which is important in the clinical and forensic analysis of human fluids such as blood, urine, and serum. It is also important in the quality control in the food, beverage, and pulp industries and in monitoring the progress of alcoholic fermentation [2].

Biosensors have been extensively researched, driven by the needs of many industries and government agencies to develop efficient analytical methods to assess the composition of environmental, food, or industrial samples [3]. For example, biosensors have been developed as an early detection method for plant diseases [4]. They have also been used to detect food compositions and food contaminants [5, 6]. Typical analytical methods such as chromatographic or electrophoretic separations followed by spectrophotometric or electrochemical detections have shortcomings, including long analysis time, complexity, and high cost [7, 8]. Biosensors have the potential to overcome these shortcomings and provide a method with low cost, high selectivity, high specificity, and the ability to be made into simple, portable, and automated equipment suitable for laboratory or field applications [7]. Biosensors can be classified by the biological elements, including enzymes, microorganisms, and bio-affinity groups such as antibodies and nucleic acids, or the methods of transduction such as the electrochemical, optical, and mass-based [9]. Among all types of biosensors, enzyme biosensors are extensively studied because of their high specificity and high reaction rate [10]. Electrochemical biosensors have advantages of making simple, rapid,

low cost, and highly sensitive devices [10]. Based on the output signals, electrochemical biosensors can be classified as amperometric, potentiometric, conductometric, or impedimetric biosensors [11]. The most commonly AOx biosensors are the amperometric biosensors where a constant potential is applied and the current generated from the redox reaction is collected [12]. Alcohol oxidase biosensors have been applied to determine ethanol or methanol in food products during fermentation or in alcoholic products [7, 13]. A dual-enzyme biosensor consisting of carboxyl esterase and alcohol oxidase was also developed for the determination of aspartame in soft drinks and sweeteners [14].

Only a few instruments using AOx biosensors to detect ethanol in food products or during fermentation processes have been developed and commercialized. The commercial biosensing instruments including four commercial AOx biosensors have been summarized by Bahadır and Sezgintürk [15]. The main limitation that hampers the development of practical AOx biosensors is the low storage and operational life which is due to the low stability of AOx [16-18]. To the best of our knowledge, the most stable AOx biosensor was the one developed by Wen, et al. [19] who immobilized the AOx with chitosan on a membrane of eggshell; the biosensor retained 87 % of its original response after storing at 4 °C for three months and there was no loss of response after 36 measurements at 20 – 25 °C within 10 h. Another stable AOx biosensor was the one developed by Chinnadayyala, et al. [20] through immobilizing polyaniline encapsulated AOx-gold nanoparticles with chitosan onto glassy carbon electrodes; it retained 93 % of its initial response after storing at 4 °C for 5 weeks and it retained 93.7 % of its initial response after 25 successive measurements within 5 hours. However, most AOx biosensors had low stability. For example, the AOx biosensor developed by Stasyuk, et al. [21] or Gayda, et al. [22] retained 50 % of its initial response after 10

days or 3 days, respectively. However, the storage conditions of these biosensors were not reported.

Immobilization is the most commonly used method to stabilize enzymes and is also the critical step in fabricating enzyme biosensors by making enzymes get contact with the transducers [23, 24]. Electropolymerization is an entrapment method that immobilizes enzymes by forming a polymeric network by applying a potential to a mixture of enzymes and monomers to trigger the polymerization. It is an easy, one-step method to physically entrap enzymes without any chemical interaction [25]. Poly(*o*-phenylenediamine) (PoPD), formed through electropolymerization of *o*-phenylenediamine (oPD), is a non-conducting polymer commonly used in enzyme biosensors. The thickness of PoPD film is in the scale of nanometers, as reported to be ~20 nm [26] or <10 nm [27], which results in faster response time. The non-conducting compact PoPD film also shows permselectivity and anti-fouling properties against electroactive interferents and proteins [28, 29]. The formation of PoPD film through electropolymerization is affected by the pH in the oPD solution. Lower pH tends to trigger the phenazine-forming oxidation resulting in a more compact film than the process of elongation to trimers or tetramers that is dominated at higher pH [30]. Electropolymerization of oPD has been used to form biosensors such as glucose oxidase biosensor [29], L-lysine biosensor [31], and alcohol dehydrogenase biosensor [32].

High hydrostatic pressure (HHP) has been reported to be able to activate and stabilize enzymes at moderate levels [33]. The stabilizing effect of HHP enables enzymes to work at temperatures that would normally be inactivated and thereby resulting in a faster reaction rate [34]. At high temperatures and moderately high pressures, an antagonistic effect of pressure and temperature is often observed [33]. High pressure protects the thermal inactivation by strengthening the hydration to prevent water loss [35], strengthening hydrogen bonds [36],

strengthening ions pairs [33], and introducing disulfide bonds [37]. The enzymes can also be stabilized by the increased Van der Waals forces resulting from compressed non-rigid cavities through the displacement of α-helices by HHP [38, 39]. We reported the stabilization effect of HHP on glucose oxidase (GOx) [40], AOx [41], xanthine oxidase [42], pyruvate oxidase [43], and GOx biosensor [44]. The soluble GOx was stabilized up to 50 times at 240 MPa and 74.5 °C compared the GOx at 0.1 MPa and 74.5 °C [40]. The soluble labile (L) fraction AOx was stabilized up to 14 times at 160 MPa and 49.4 °C relative to the AOx at 0.1 MPa and 49.4 °C [41]. We recently also reported that the thermostability of GOx immobilized in PoPD increased by up to 87.6 times when inactivated at 70 °C and 180 MPa relative to the GOx in solution inactivated at 70 °C and atmospheric pressure [44]. However, the high pressure applied during electropolymerization did not increase the thermostability of the GOx biosensors, that was, the stabilizing effect of HHP on GOx was not retained upon depressurization [44]. Alcohol oxidase and GOx both belong to the class of oxidoreductase and are both flavin-dependent proteins. But AOx is an octamer of ~600 kDa, bigger than the GOx which is a dimer of ~160 kDa. To the best of our knowledge, high pressure has not been used to improve the stability of AOx biosensors when applied during the immobilization of AOx or during the thermal inactivation of immobilized AOx. Therefore, it was hypothesized that applying HHP during thermal inactivation of AOx immobilized in PoPD would increase the thermostability of AOx biosensors. Alcohol oxidase was reported to consist of two fractions, the labile fraction (L) and the resistant (R) fraction. Both the L fraction and the R fraction in solution were stabilized at high pressures and the L fraction was stabilized more at HHP than the R fraction [41]. As described in Chapter 3, HHP increased the apparent activity of AOx. The increase in the activity of AOx was attributed to the stabilizing effects of HHP. The R fraction in solution was ~150 times more stable than the L fraction. A lower

pressure was needed to protect the R fraction from losing its activity. The stabilizing effect of HHP on the R fraction was not as pronounced as for the L fraction [41]. Therefore, it was hypothesized that the effect of immobilization and the effect of HHP applied during immobilization or inactivation would be different for the two fractions of AOx.

To test the hypotheses, the objectives of this study were 1) to assess the effects of immobilization through electropolymerization and the effect of applying HHP during electropolymerization on the storage and thermal stability of the L+R fractions and the R fraction AOx biosensors, 2) to assess the effect of HHP during thermal inactivation of immobilized AOx.

4.2. Material and methods

4.2.1. Materials

Alcohol oxidase from *Pichia pastoris* was purchased from MP Biochemicals (Solon, OH, USA). Chloroplatinic acid hexahydrate was purchased from Sigma-Aldrich (St. Louis, MO, USA). Potassium phosphate monobasic, potassium chloride, and sulfuric acid were purchased from Fisher Scientific (Hampton, NH, USA). Lead (II) acetate trihydrate and *o*-phenylenediamine were purchased from Acros Organics (Geel, Belgium). Ethanol (200 proof) was purchased from VWR International (Suwanee, GA, USA). All chemicals were reagent grade, and solutions were made with deionized water.

4.2.2. Equipment

The high pressure system used in this report was previously described elsewhere [40, 44]. Briefly, a piston pump connected to a jacketed high pressure reactor was controlled by a controller unit, purchased from Unipress Equipment (Warsaw, Poland). Two water baths from Fisher Scientific (Hampton, NH, USA) with hot and cold water were used to control the temperature in the system. Reference 600 potentiostats from Gamry Instruments (Warminster, PA, USA) were

used for all electrochemical experiments, such as cyclic voltammetry, chronoamperometry, and chronocoulometry. The potentiostat was connected to the high pressure reactor through an electrical feed-through connector in the cap of the reactor to perform the electropolymerization under high pressure.

The electrochemical cell used to perform electropolymerization in the high pressure reactor was described previously [44]. Briefly, platinum wires were used as working and counter electrodes. Ag|AgCl pellets mounted on silver wires purchased from Warner Instruments (Hamden, CT, USA) were used as the reference electrode. The cell was made of a silicone tubing with one polytetrafluoroethylene cap that holds the working and counter electrodes as one end and an epoxy glue cap that holds the silver wire connected to the Ag|AgCl pellet as the other end. A picture and a schematic diagram of the cell are shown in Fig. 4.1.

4.2.3. Methods

4.2.3.1. Electrode preparation

The methods to clean and platinize platinum electrodes were previously described [44]. The electrodes were polished and cleaned every time before using, by polishing with nylon disks with 0.3 μm alumina slurry and microcloth disks with 0.05 μm alumina slurry before ultrasonication in deionized water for 15 min and immersing in concentrated sulfuric acid overnight followed by electrochemical cleaning. The electrochemical cleaning was carried out in 0.1 M H_2SO_4 by cyclic voltammetry from -0.189 V to 1.461 V *vs.* Ag|AgCl in 3.5 M KCl at 500 mV s^{-1} for 80 cycles. The platinization was performed by chronocoulometry at -0.089 V *vs.* Ag|AgCl in 3.5 M KCl to reach the total charge density of 2.0 mC cm^{-2} in a deaerated solution consisting of 2 mM H_2PtCl_6, 1 mM $Pb(C_2H_3O_2)$, and 0.1 M KCl. Loosely bound platinum deposits were removed by ultrasonication in 0.1 M phosphate buffer pH 7 for 10 min using an ultrasonic

bath (output frequency 40 kHz) from Fisher Scientific (Hampton, NH, USA). Electrochemical surface areas were determined by cyclic voltammetry from -0.238 V to 1.211 V *vs.* Ag|AgCl in 3.5 M KCl for 10 cycles at the rate of 500 mV s^{-1} in 0.5 M H_2SO_4.

4.2.3.2. Enzyme preparation

A commercial AOx formulation purchased from MP Biochemicals used in this research contains the labile (L) and the resistant (R) fractions, which was confirmed in Chapter 3. The L+R fractions AOx was the fresh enzyme without further treatments. The R fraction AOx was obtained by heating the L+R fractions at 50 °C in 0.1 M phosphate buffer (pH 7.5) in a water bath for 15 min and cooling down on ice. The enzyme activity of the two fractions of AOx was determined using a microplate reader (model SynergyTM HTX, BioTek, Winooski, VT). The enzyme concentration of the L+R fractions AOx was diluted with phosphate or acetate acid buffer to 4 mg mL^{-1} (80 U mL^{-1}), while the concentration of the R fraction AOx was diluted to the same concentration by referring to the fact that the residual activity of enzyme after 15 min heating was ~35 % relative to the fresh enzyme. As reported previously and confirmed in Chapter 3, the L fraction accounted for the majority of the activity while the R fraction was more stable than the L fraction. Therefore, the stability of the L+R fraction was mostly the stability of the L fraction [41].

4.2.3.3. Immobilization and sensitivity of AOx biosensors

Alcohol oxidase was entrapped via electropolymerization in PoPD films through cyclic voltammetry at 100 mV s^{-1} from 0 to 0.65 V *vs.* Ag|AgCl in 3.0 M KCl for 100 cycles. The cyclic voltammetry was carried out in a mixed deaerated solution of 4 mg mL^{-1} (80 U mL^{-1}) AOx, 5 mM oPD, and 0.1 M phosphate buffer (pH 7.0) or 0.2 M acetate acid buffer (pH 5.2). The concentration of AOx was chosen by comparing the amperometric response to biosensors fabricated with 0.5, 1, 2, 3, 4, and 5 mg mL^{-1} AOx. Concentrations below than 3 mg mL^{-1} were not able to generate the

amperometric response high enough to produce linear calibration curves with coefficients of determination (R^2) greater than 0.9. Concentrations higher than 4 mg mL^{-1} were not used to save enzyme.

The AOx biosensors were conditioned by applying 0.711 V *vs.* Ag|AgCl in 3.5 M KCl in the 0.1 M phosphate buffer (pH 7.5) for 30 min after immobilization to remove any loosely bound enzyme or oPD. The amperometric response of the biosensors was determined by chronoamperometry at 0.711 V *vs.* Ag|AgCl in 3.5 M KCl in stirred 0 mM (0.1 M phosphate buffer pH 7.5) to 80 or 100 mM ethanol solutions. The calibration was performed using the ethanol solutions of 0, 20, 40, 60, and 80 mM or 0, 20, 40, 60, 80, and 100 mM. The biosensor sensitivity was determined as the slope of the current density *vs.* ethanol concentration (0 to 80 mM or 0 to 100 mM). The ethanol solution was prepared by diluting the ethanol (200-proof) with 0.1 M phosphate buffer (pH 7.5).

4.2.3.4. Effect of HHP during immobilization on the stability of AOx biosensors

High pressures (0.1, 60, 180, or 240 MPa) were applied during immobilization of the L+R fraction AOx at pH 7.0 and at room temperature (23 ± 1 °C). Each treatment was performed in duplicate. The immobilized AOx was then inactivated at 50 °C in 0.1 M phosphate buffer (pH 7.5) in a water bath for an accumulated time of 1, 2, 4, 6, 8, and 10 min. The amperometric response to 100 mM ethanol solution at room temperature was measured after placing each electrode in 0.1 M phosphate buffer (pH 7.5) on ice for 5 min. The biosensor thermostability was determined as the percent residual current density at 100 mM ethanol solution *vs.* heat treatment time to the current density at heating time 0.

To assess the effect of HHP during immobilization on the thermostability of the two fractions of AOx, the L+R fractions or the R fraction AOx were immobilized at pH 7.0 and at

either 0.1 or 160 MPa. Then the electrodes were heated at 50 °C in 0.1 M phosphate buffer (pH 7.5) in a water bath for an accumulated time of 1, 2, 4, 6, 8, and 10 min. The thermostability was determined as the percent residual current density at 100 mM ethanol solution *vs.* heat treatment time to the current density at heating time 0. All treatments were done at least in duplicate.

The effect of HHP during immobilization on the storage stability of the two fractions of AOx was also determined. The L+R fractions or the R fraction AOx were immobilized at pH 7.0 and at either 0.1 or 240 MPa. Then the electrodes were stored in 0.1 M phosphate buffer (pH 7.5) at room temperature (23 ± 1 °C) for 15 days. Amperometric response was measured each day and the calibration curves were determined on day 1 and day 15. The storage stability was determined as the percent residual current density response to 80 mM ethanol solution *vs.* storage time to the current density at day 1. All treatments were done in triplicate.

4.2.3.5. Effect of HHP during thermal treatment and the effect of pH during electropolymerization on the stability of immobilized AOx

Alcohol oxidase (L+R fractions) was immobilized at pH 7.0 and at room temperature and atmospheric pressure. The L+R fractions or the R fraction AOx were also immobilized at pH 5.2 and at room temperature and atmospheric pressure. The immobilized AOx was heated at 0.1 or 160 MPa in 0.1 M phosphate buffer (pH 7.5) in the high pressure reactor at 50 °C for an accumulated time of 1, 2, 4, 6, 8, and 10 min. The system was cooled to 10 °C after the treatment. The amperometric response was measured at room temperature. The thermostability was determined as described in section 4.2.3.4. The treatments were carried out in quadruplicate.

4.2.4. Data analysis

The pseudo-first-order model was used to fit the residual current density responses as a function of heating or storage time. The rate constant of response loss (k) was determined from

the linear regression of the natural logarithm of relative current density to the treatment time. All results of k and sensitivity are reported as mean values ± 95% confidence intervals if not noted differently. Statistics analysis was performed using the software Minitab 16 (State College, PA, USA). Tukey's method was used for multiple comparisons. MATLAB software (Natick, MA, USA) was used for non-linear model fitting.

4.3. Results and discussion

4.3.1. Calculation of effective amperometric responses

To determine the effective amperometric response of the AOx biosensors, the amperometric response to the phosphate buffer was subtracted from the amperometric response to the ethanol solutions. The current density of the AOx biosensors to the phosphate buffer was 2.6 ± 0.8 nA mm^{-2} (n = 24). The current density of the AOx biosensors in 0.1 M phosphate buffer (pH 7.5) decreased at 50 °C or storing at room temperature. Examples of the changes of the residual current density to the buffer over heating time can be found in the supplemental material Table S4.1. To determine whether the decrease in amperometric response was attributed to the PoPD film instead of enzymes, the responses to the H_2O_2 solutions of two electrodes covered with PoPD in the absence of AOx were recorded (Fig. S4.1). The H_2O_2 solution was prepared by diluting with 0.1 M phosphate buffer (pH 7.5) to a concentration (~100 mM) corresponding to the amperometric response of ~15 nA mm^{-2}, which was in the range of the typical current density response of a AOx biosensor fabricated as described in section 4.2.3.3 to 100 mM ethanol. These two electrodes were tested by heating at 50 °C in 0.1 M phosphate buffer (pH 7.5) in a water bath for an accumulated time of 1, 2, 4, 6, 8, and 10 min. The average percent current density to the H_2O_2 solution or the phosphate buffer at 10 min relative to 0 min was 82.9 % or 75.7 %, respectively. This suggested that the decrease in the amperometric response to the phosphate buffer can be attributed to the

possible changes of the PoPD film. Lai, et al. [45] reported that there were no redox reactions when applying potentials from 0.5 to 1.2 V *vs.* reversible hydrogen electrode to platinum electrode in phosphate buffer from pH 6 to 9. Therefore, the amperometric response to the buffer was a non-faradaic process, possibly charging and discharging the electrical double layer. Because of the thicknesses of both the electrical double layer and the PoPD film are in the scale of nanometers, the changes in the PoPD film may change the electrical double layer and thereby changing the current response. If the PoPD film becomes more compact, the surface area of the electrical double layer would be smaller, resulting in the decrease in the amperometric response to the buffer. The PoPD microsphere was reported to transform from the ladder aromatic structure to the polycyclic structure under thermal treatment (350 to 950 °C) where the nitrogen was incorporated in the structure, resulting in a more compact carbon sphere with the same particle size and hollow structure but a smaller shell thickness (from ~35 nm to ~25 nm) [46]. However, to the best of our knowledge, whether the same transformation of PoPD could occur at lower temperatures (50 °C or room temperature) has not been reported. Therefore, the exact mechanism of the decrease in the response to buffer remained unclear. Different from the GOx biosensors using the same immobilization method where the changes of the response to the buffer was negligible [44], the ratio of the response of the AOx biosensors to 100 mM ethanol relative to phosphate buffer was 3.5 ± 0.8 (n = 8) before thermal treatment. This was most likely the result of a lower concentration of AOx than GOx used for immobilization. Therefore, the effective amperometric response was used.

4.3.2. Factors affecting the changes of the effective amperometric responses

The effective amperometric response of AOx biosensors decreased with the heat treatment at 50 °C and with the storage at room temperature. The decrease in current density could be

attributed to 1) the inactivation of enzymes, 2) enzyme leaching from the PoPD polymeric network, 3) the degradation of PoPD matrix, 4) a combination of two or more factors [47]. To determine the effect of HHP on the stability of AOx biosensors, the changes in the amperometric responses need to be attributed only to the inactivation of enzymes. Pseudo-zero, first, or second order model was used to characterize the changes between the relative current density and treatment time. The coefficient of determination (R^2) was used to partially assess the fitting of the three models. The means of R^2 of each fitting for different AOx biosensors can be found in the supplemental material Table S4.2. Examples of the non-linear fittings of relative current density *vs.* treatment time using MATLAB software can also be found in the supplemental material Fig. S4.2 and Fig. S4.3. Different from GOx biosensors in Chapter 2 where the pseudo-second-order model fitted better than the pseudo-first-order model, the pseudo-second-order model did not always fit better than the pseudo-first-order model for AOx biosensors (Fig S4.2). To compare the k of the AOx biosensors with the pseudo-first-order rate constant of inactivation of AOx in solution from Chapter 3, the pseudo-first-order model was used.

To test whether the decrease in the effective amperometric response was due to the enzyme inactivation, one method was to compare the pseudo-first-order k of the AOx biosensors with the pseudo-first-order rate constant of inactivation (k_{inact}) of the AOx in solution. If the decrease was only from the enzyme inactivation, the k of the AOx biosensor should be equal or lower than the k_{inact} of the AOx in solution. That is because immobilization typically stabilizes enzymes. If not stabilizing enzymes, decreasing the enzyme stability is very unlikely by entrapping the AOx in PoPD because immobilization through electrochemically generating PoPD film does not have chemical interactions with the proteins [25]. To determine the effect of HHP during immobilization on the thermostability of the AOx biosensors, the AOx biosensors immobilized at

different pressures were heated at 50 °C for up to 10 min. The results of the pseudo-first-order k of the L+R fractions AOx biosensors immobilized at 0.1 to 240 MPa and the pseudo-first-order k of the L+R fractions or the R fraction AOx biosensors immobilized at 0.1 or 160 MPa are shown in Table 4.1 and Table 4.2, respectively. There was no significant difference ($p > 0.05$) between the k using different enzyme fractions regardless of the immobilization pressure. The average pseudo-first-order k ± one standard deviation of the AOx biosensors from Table 4.2 was 0.15 ± 0.05 min^{-1}. This was different from the AOx in solution. It was reported and also verified in Chapter 3 that the R fraction was ~150 times more stable than the L fraction in solution [41]. The AOx from *Pichia pastoris* is encoded by two genes accounting for two isozymes which have homologous primary sequences but nonhomologous flanking sequences [48]. The differences in thermostability of the two isozymes might be attributed from the conformation difference expressed by the two different genes. From Chapter 3, the pseudo-first-order k_{inact} of the soluble L+R fractions or the R fraction AOx during thermal treatment at 50 °C was 0.53 ± 0.05 min^{-1} and (3.4 ± 0.1) × 10^{-3} min^{-1}, respectively. The pseudo-first-order k of the AOx biosensors heated at 50 °C (0.15 ± 0.05 min^{-1}) was approximately 3.4 time less compared to 0.52 min^{-1} while 45.3 times as high as the 3.4 × 10^{-3} min^{-1} so that the immobilized AOx regardless of the enzyme fractions was 2.4 times more stable than the L+R fractions in solution while 44.3 times less stable than the R fraction in solution. Therefore, the decrease in the current density over time was attributed to the other factors besides enzyme inactivation. Also, the decrease in the current density induced by enzyme inactivation was negligible because the k of the AOx biosensors was much lower than the k_{inact} of the R fraction in solution. Though it was not certain whether the R fraction AOx was stabilized after immobilization, it was reasonable to assume that immobilization stabilized the L fraction to the similar stability of the immobilized R fraction because the k of the biosensors using

the two enzyme fractions were not significantly different. If the inactivation of the L fraction AOx was fast enough to make a difference, the k of the L+R fractions AOx biosensor would be significantly higher than the k of the R fraction AOx biosensor. The stabilization of the L fraction AOx was possibly through restricting the protein unfolding by entrapping the enzyme in the PoPD. However, the exact stabilizing effect of immobilization on the L or R fraction AOx could not be calculated using the pseudo-first-order k.

Other possible factors affecting amperometric response besides enzyme inactivation include PoPD polymer degradation and/or enzyme leaching. The degradation of the PoPD film over heating was not likely, otherwise the response to the buffer described in section 4.3.1 would increase due to the increased surface area of the electrical double layer. The GOx biosensors we previously reported had a pseudo-first-order k_{inact} ~6.6×10^{-3} min^{-1} at 70 °C and 0.1 MPa using the same immobilization protocol at pH 5.2, much lower than the k of the AOx biosensors at 50 °C and 0.1 MPa immobilized at the same pH in this study (Table 4.3) [44]. This also suggested that the degradation of the PoPD film at high temperatures was unlikely or the effect was negligible, otherwise the k_{inact} of the GOx biosensors and the k of the AOx biosensors would be similar, or the k_{inact} of the GOx biosensors at 70 °C would be bigger. The degradation of the polymer by H_2O_2 was also unlikely. Hydrogen peroxide was reported to be able to decompose oPD through photocatalytic degradation with catalyst under UV condition; but the effect of decomposition (H_2O_2 concentration up to 100 mM) was negligible without UV and photocatalyst [49]. Therefore, the degradation of PoPD was not responsible for the decrease of the effective amperometric responses. Enzyme leaching is another factor that may decrease the response. It was possible that the protein of AOx having the protein size of ~600 kDa was too big to be entirely entrapped in the PoPD film, resulting in the enzyme leaching. The approximate dimensions of the AOx octamer

from *P. pastoris* is 12.2 nm × 13.4 nm × 13.5 nm [50]. But the thickness of the PoPD film could be thinner than 10 nm [27]. Therefore, it was possible that the overall diameter of the AOx was bigger than the thickness of the PoPD film, resulting in a situation where only a portion of the protein was in the polymer. These partially entrapped AOx may leach out from the polymer over time. On the other hand, the approximate dimensions of the GOx dimer from *A. niger* is 6.0 nm × 5.2 nm × 7.7 nm [51]. Different from AOx, the smaller GOx is able to be fully entrapped in the PoPD film and thereby preventing the enzyme leaching. Therefore, it was highly likely that it was the enzyme leaching that accounted for the effective amperometric response decrease over time. Also, the decrease caused by enzyme leaching was big enough to make the influence of other factors such as enzyme inactivation negligible.

4.3.3. Effect of HHP during immobilization on the sensitivity and thermal stability of the L+R fractions or the R fraction AOx biosensors

The electropolymerization of the L+R fractions of AOx was performed at pH 7.0 and at 0.1, 60, 180, and 240 MPa to determine the effect of different high pressure on the thermal stability of AOx biosensors. To determine the effect of the enzyme fractions, the thermostability of the AOx biosensors was tested again using the L+R fractions or the R fraction AOx immobilized at pH 7.0 and at 0.1 or 160 MPa. The pressure 160 MPa was chosen because it was the optimal pressure to increase the stability of the L+R fractions AOx in solution [41]. The results are shown in Table 4.1 and Table 4.2.

4.3.3.1. Sensitivity

Applying high pressure during immobilization had no significant influence ($p > 0.05$) on the sensitivity (Table 4.1, Table 4.2). Enzyme fractions also had no significant influence ($p > 0.05$) on the sensitivity (Table 4.2), suggesting the less stable L fraction AOx was not inactivated during

immobilization. Electrochemical impedance spectroscopy (EIS) was performed on electrodes before and after immobilization to determine the possible changes of the PoPD film formed at different pressures. Examples of the Nyquist plots of the EIS results are shown in the supplemental material Fig. S4.4. No differences were found between the Nyquist plots of the electrodes immobilized at high pressure and at 0.1 MPa, suggesting that applying HHP during immobilization did not change the formation of the PoPD films. It was in accordance with our previous finding that applying HHP during immobilization of GOx did not affect the sensitivity of GOx biosensors [44]. Therefore, the HHP applied during immobilization did not change the permeability of the PoPD films.

The sensitivity of the AOx biosensors immobilized through electropolymerization with PoPD film reported in this research (Table 4.1, Table 4.2) was lower than the sensitivities of the AOx biosensors recently reported by others. Gayda, et al. [22] reported an AOx/horseradish peroxidase biosensor immobilized through adsorption of up to 50 U mL^{-1} AOx onto green synthesized nanoparticle modified graphite electrodes with the sensitivity 14 nA mm^{-2} mM^{-1} to methanol. Stasyuk, et al. [21] reported an AOx biosensor by immobilizing 15 – 35 U mL^{-1} AOx through adsorption onto the bimetallic PtRu nanoparticle covered graphite electrode and then covered by polymers, giving the sensitivity 336 nA mm^{-2} mM^{-1} to ethanol. Soylemez, et al. [52] reported an AOx biosensor by covalent binding the AOx to the (4,7-di(thiophen-2-yl)benzo[c][1,2,5]selenadiazole-*co*-1*H*-pyrrole-3-carboxylic acid) polymer which was electropolymerized on the graphite electrode, having the sensitivity 164 nA mm^{-2} mM^{-1} to ethanol. The high sensitivities presented by others were obtained by using electrodes with large electrochemical surface areas such as porous graphite electrodes modified with nanomaterials. The difference in the sensitivity was also attributed to the different electrode surface areas used for

calculation, i.e., Gayda, et al. [22] used the centrical electrode surface area 7.3 mm^2 to calculate the current density instead of the electrochemical surface area. The platinum wires (1.6 cm long, 0.8 mm diameter) used in our study had a centrical surface area 0.5 mm^2. But the electrochemical surface area was used to calculate the current density. The platinization increased the electrochemical surface area about 4.5 times from 13.2 ± 6.0 mm^2 to 53.0 ± 12.8 mm^2. Therefore, the sensitivity would be approximately 100 times higher if using the centrical surface area instead of the electrochemical surface area.

4.3.3.2. Thermostability

The different pressures applied during immobilization had no significant ($p > 0.05$) influence on the pseudo-first-order rate constant of response loss (Table 4.1, Table 4.2). Therefore, the L+R fractions or the R fraction AOx biosensors immobilized at different pressures had similar thermostability. As described in the section 4.3.2, the decrease in the amperometric responses of the AOx biosensors was most likely due to enzyme leaching rather than enzyme inactivation. Therefore, the high pressures applied during immobilization or using different enzyme fractions did not change the speed of enzyme leaching at 50 °C. The effect of HHP on enzymes could not be assessed since the k did not represent the enzyme inactivation. High pressure was reported to increase the stability of the GOx and AOx in solution [40, 41]. But the stabilizing effect on GOx could not be retained by immobilization after depressurization [44]. Whether the stabilizing effect on AOx could be retained by immobilization remained unclear.

4.3.4. Storage stability of the L+R fractions or the R fraction AOx biosensors

To determine the effect of HHP during electropolymerization on the storage stability of AOx biosensors, the L+R fractions or the R fraction AOx biosensors immobilized at pH 7.0 and at 0.1 or 240 MPa were stored in 0.1 M phosphate buffer (pH 7.5) at room temperature (23 ± 1 °C)

for 15 days. Table 4.4 shows the sensitivity before and after the 15-days storage, and the pseudo-first-order k of the L+R fractions or the R fraction AOx biosensors immobilized at 0.1 or 240 MPa. No significant difference was found between the biosensors using different enzyme fractions, or between the biosensors immobilized at 0.1 or 240 MPa on the sensitivities or the rate constant of response loss. Because the amperometric response decrease was highly likely due to enzyme leaching, the high pressure (240 MPa) applied during immobilization or using different enzyme fractions did not affect the speed of enzyme leaching at room temperature. The average half-life time of the AOx biosensors immobilized by electropolymerization with PoPD films at 0.1 MPa or 240 MPa was 5.3 days with a standard deviation of 1.5 days (n = 12). The average remaining residual amperometric response of the biosensors after storing 15 days at room temperature was 15.3 % with a standard deviation of 7.7 % (n = 12). The storage stability would be higher if there was no enzyme leaching.

The storage stability was not comparable to the reports by others, because in other reports the storage temperature was typically 4 °C or not mentioned. The AOx biosensors immobilized by adsorption onto graphite electrodes retained 50 % activity after 2 or 3 days when using unmodified or green synthesized nanoparticle modified electrodes, respectively (storage temperature not reported) [22]. The AOx biosensors immobilized onto PtRu nanoparticle modified graphite electrodes retained 20 % response after 14 days and had a half-life time 10 days (storage temperature not reported) [21]. The AOx biosensors immobilized through cross-linking with glutaraldehyde onto printed carbon nanotube electrodes had a half-life time 2-3 days while almost completely lost responses after storing at 4 °C for 5 days [53]. The AOx biosensor with the highest storage stability found in the literature was the biosensor where the AOx was immobilized with chitosan on a membrane of eggshell; it retained 87 % of its original response after storing at 4 °C

for three months [19]. It is important to report the storage temperature because biosensors stored at different temperatures have different storage stability. In practical industrial scenarios, the AOx biosensors are intended to work at room temperature or higher temperatures such as fermentation for a period time. Therefore, the storage stability of AOx biosensors at room temperature or even higher temperatures is the piece of information valuable to provide but missing in the literature.

4.3.5. Effect of pH during immobilization and effect of HHP during thermal inactivation of immobilized AOx

As described in the previous sections, the decrease in the amperometric response was most likely attributed to the enzyme leaching. In Table 4.1, 4.2, and 4.4, the immobilization of AOx was performed at pH 7.0 to avoid denaturing AOx whose working pH was from 5.5 to 9. It was reported that the pH during electropolymerization of oPD affected the compactness of the PoPD film where the phenazine-like structure was favored at lower pH while the ring-opened structure was increased at higher pH [30]. Therefore, to determine whether a lower pH could reduce or stop enzyme leaching by forming a more compact PoPD film, the pH 5.2 was also used to immobilize the L+R fractions or the R fraction AOx. We previously also reported the stabilizing effect of HHP against thermal inactivation of immobilized GOx where the thermostability of the GOx biosensors was 20.6 times higher when inactivated at 180 MPa and 70 °C compared to 0.1 MPa and 70 °C [44]. If the lower pH 5.2 could stop enzyme leaching, to test whether high pressure had similar effects on the immobilized AOx, the AOx immobilized at pH 5.2 were inactivated at 50 °C and 0.1 or 160 MPa for up to 10 min. Table 4.3 shows the sensitivity and the pseudo-first-order k of the immobilized AOx inactivated in the high pressure reactor. No significant difference ($p > 0.05$) was found in the pseudo-first-order k of biosensors immobilized at different pH, with different enzyme fractions, or using different inactivation pressures. The examples of the cyclic voltammetry (CV)

plots of the electropolymerization of oPD at pH 7.0 and pH 5.2 can be found in the supplemental material Fig. S4.5. The plots were similar except the oxidation peak at ~0.60 V *vs.* Ag|AgCl when the electropolymerization was carried out at pH 5.2 shifted to ~0.55 V when the electropolymerization was carried out at pH 7.0. In accordance with the report by Losito, et al. [30], this potential shift where a lower oxidation potential was needed in a more basic condition was because of the generation of H^+ ions during the oxidation of oPD into radical cations. It was not able to tell whether the number of phenazine-like structure was increased when immobilized at pH 5.2 based only on the CV plots. Electrospray ionization-tandem mass spectrometry or X-ray photoelectron spectroscopy is needed to characterize the structure of PoPD film [27, 30]. However, these studies are beyond the scope of this study. The k of the L+R fractions AOx biosensor immobilized at pH 7.0 or pH 5.2 was not significantly different, suggesting that the lower pH 5.2 did not result in a PoPD film that could reduce or stop the enzyme leaching. Therefore, neither the pH 5.2 nor pH 7.0 used during electropolymerization was able to fabricate the AOx biosensors where the pseudo-first-order rate constant of response loss was related to the enzyme inactivation. It was possible that the similar stabilizing effect of HHP when inactivating the immobilized GOx occurred when inactivating the immobilized AOx, but the pseudo-first-order k would not change no matter how much more stable of the enzymes became. As described in section 4.3.2, the pseudo-first-order k of enzyme leaching was too high to see the relatively small changes of the inactivation of enzymes. Therefore, the effect of HHP on the immobilized AOx against thermal treatment could not be determined. Using pH lower than 5.2 was possible to form a more compact PoPD film but would worsen the AOx denaturation during immobilization. Therefore, electrochemically generated PoPD is not an adequate immobilization method for AOx.

4.4. Summary

The decrease in the amperometric response of the AOx biosensors at 50 °C or during storage at room temperature was most likely due to the enzyme leaching rather than the inactivation of enzymes. Therefore, it did not allow us to test the hypotheses that the HHP applied during immobilization or during thermal inactivation would increase the stability of AOx biosensors in terms of enzyme stability. Immobilization through electropolymerization increased the thermal stability of the L+R fractions AOx because the pseudo-first-order k of the AOx biosensor was smaller than the pseudo-first-order k_{inact} of the L+R fractions AOx in solution. But the effect of immobilization on the R fraction AOx could not be determined because the pseudo-first-order k of the AOx biosensor was approximately 44 times higher than the pseudo-first-order k_{inact} of the R fraction AOx in solution, also suggesting the decrease in the amperometric response was caused by enzyme leaching out of the immobilization matrix. Indeed, the dimension of the AOx was similar to the thickness of the PoPD film. The lower pH 5.2 instead of pH 7.0 used during electropolymerization did not reduce or stop the enzyme leaching. Therefore, electrochemically generated PoPD is not an adequate immobilization method for AOx. A different immobilization method is needed to investigate the effects of HHP on the stability of AOx biosensors. To test the effectiveness of an immobilization method, it has to be addressed on a case-by-case basis for various enzymes with different properties such as different dimensions of the proteins.

Acknowledgment

This work was supported by the USDA National Institute of Food and Agriculture [grant number 2014-67021-21604/ project accession no. 1001899].

4.5. References

[1] A. Kakoti, A.K. Kumar, P. Goswami, Microsome-bound alcohol oxidase catalyzed production of carbonyl compounds from alcohol substrates, J. Mol. Catal. B: Enzym. 78 (2012) 98-104.

[2] N.G. Patel, S. Meier, K. Cammann, G.C. Chemnitius, Screen-printed biosensors using different alcohol oxidases, Sens. Actuators B: Chem. 75(1) (2001) 101-110.

[3] T. Monteiro, M.G. Almeida, Electrochemical enzyme biosensors revisited: Old solutions for new problems, Crit. Rev. Anal. Chem. 49(1) (2019) 44-66.

[4] Y. Fang, R.P. Ramasamy, Current and prospective methods for plant disease detection, Biosens. 5(3) (2015) 537-561.

[5] R. Monosik, M. Stredansky, J. Tkac, E. Sturdik, Application of enzyme biosensors in analysis of food and beverages, Food Anal. Methods 5(1) (2012) 40-53.

[6] L. Rotariu, F. Lagarde, N. Jaffrezic-Renault, C. Bala, Electrochemical biosensors for fast detection of food contaminants-trends and perspective, Trends Anal. Chem. 79 (2016) 80-87.

[7] L. Barthelmebs, C. Calas-Blanchard, G. Istamboulie, J.-L. Marty, T. Noguer, Biosensors as analytical tools in food fermentation industry, Bio-Farms for Nutraceuticals, Springer2010, pp. 293-307.

[8] J.I. Reyes-De-Corcuera, R. Cavalieri, Biosensors. Encyclopedia of Agricultural, Food Biol. Eng. (2003).

[9] P. Mehrotra, Biosensors and their applications-A review, J. Oral Biol. Craniofacial Res. 6(2) (2016) 153-159.

[10] H.H. Nguyen, S.H. Lee, U.J. Lee, C.D. Fermin, M. Kim, Immobilized enzymes in biosensor applications, Mater. 12(1) (2019) 121.

[11] N.J. Ronkainen, H.B. Halsall, W.R. Heineman, Electrochemical biosensors, Chem. Soc. Rev. 39(5) (2010) 1747-1763.

[12] A.M. Azevedo, D.M.F. Prazeres, J.M.S. Cabral, L.P. Fonseca, Ethanol biosensors based on alcohol oxidase, Biosens. Bioelectron. 21(2) (2005) 235-247.

[13] S. Cinti, M. Basso, D. Moscone, F. Arduini, A paper-based nanomodified electrochemical biosensor for ethanol detection in beers, Anal. Chim. Acta 960 (2017) 123-130.

[14] D. Odacı, S. Timur, A. Telefoncu, Carboxyl esterase-alcohol oxidase based biosensor for the aspartame determination, Food Chem. 84(3) (2004) 493-496.

[15] E.B. Bahadır, M.K. Sezgintürk, Applications of commercial biosensors in clinical, food, environmental, and biothreat/biowarfare analyses, Anal. Biochem. 478 (2015) 107-120.

[16] P. Goswami, S.S.R. Chinnadayyala, M. Chakraborty, A.K. Kumar, A. Kakoti, An overview on alcohol oxidases and their potential applications, Appl. Microbiol. Biotechnol. 97(10) (2013) 4259-4275.

[17] A. Klos-Witkowska, V. Martsenyuk, V. Karpinskyi, Analysis of Stability in Enzyme Biosensor Based on Michaelis-Menten Model with Time Delays, Acta Phys. Pol. 135 (2019) 375-379.

[18] J.I. Reyes-De-Corcuera, H.E. Olstad, R. García-Torres, Stability and stabilization of enzyme biosensors: The key to successful application and commercialization, Annu. Rev. Food Sci. Technol. 9 (2018) 293-322.

[19] G. Wen, Y. Zhang, S. Shuang, C. Dong, M.M. Choi, Application of a biosensor for monitoring of ethanol, Biosens. Bioelectron. 23(1) (2007) 121-129.

[20] S.R. Chinnadayyala, M. Santhosh, N.K. Singh, P. Goswami, Alcohol oxidase protein mediated in-situ synthesized and stabilized gold nanoparticles for developing amperometric alcohol biosensor, Biosens. Bioelectron. 69 (2015) 155-161.

[21] N. Stasyuk, G. Gayda, A. Zakalskiy, O. Zakalska, R. Serkiz, M. Gonchar, Amperometric biosensors based on oxidases and PtRu nanoparticles as artificial peroxidase, Food Chem. 285 (2019) 213-220.

[22] G.Z. Gayda, O.M. Demkiv, N.Y. Stasyuk, R.Y. Serkiz, M.D. Lootsik, A. Errachid, M.V. Gonchar, M. Nisnevitch, Metallic nanoparticles obtained via “green” synthesis as a platform for biosensor construction, Appl. Sci. 9(4) (2019) 720.

[23] A. Sassolas, L.J. Blum, B.D. Leca-Bouvier, Immobilization strategies to develop enzymatic biosensors, Biotechnol. Adv. 30(3) (2012) 489-511.

[24] R.A. Sheldon, S. van Pelt, Enzyme immobilisation in biocatalysis: why, what and how, Chem. Soc. Rev. 42(15) (2013) 6223-6235.

[25] H.H. Nguyen, M. Kim, An overview of techniques in enzyme immobilization, Appl. Sci. Converg. Technol. 26(6) (2017) 157-163.

[26] C.-C. Wu, H.-C. Chang, Estimating the thickness of hydrated ultrathin poly (o-phenylenediamine) film by atomic force microscopy, Anal. Chim. Acta 505(2) (2004) 239-246.

[27] I. Losito, E. De Giglio, N. Cioffi, C. Malitesta, Spectroscopic investigation on polymer films obtained by oxidation of o-phenylenediamine on platinum electrodes at different pHs, J. Mater. Chem. 11(7) (2001) 1812-1817.

[28] S. Cosnier, Biosensors based on electropolymerized films: new trends, Anal. Bioanal. Chem. 377(3) (2003) 507-520.

[29] E. Turkmen, S.Z. Bas, H. Gulce, S. Yildiz, Glucose biosensor based on immobilization of glucose oxidase in electropolymerized poly(o-phenylenediamine) film on platinum nanoparticles-polyvinylferrocenium modified electrode, Electrochim. Acta 123 (2014) 93-102.

[30] I. Losito, F. Palmisano, P.G. Zambonin, o-Phenylenediamine electropolymerization by cyclic voltammetry combined with electrospray ionization-ion trap mass spectrometry, Anal. Chem. 75(19) (2003) 4988-4995.

[31] I.D. Karalemas, C.A. Georgiou, D.S. Papastathopoulos, Construction of a l-lysine biosensor by immobilizing lysine oxidase on a gold-poly(o-phenylenediamine) electrode, Talanta 53(2) (2000) 391-402.

[32] M.J. Lobo Castañón, A.J. Miranda Ordieres, P. Tuñón Blanco, Amperometric detection of ethanol with poly-(o-phenylenediamine)-modified enzyme electrodes, Biosens. Bioelectron. 12(6) (1997) 511-520.

[33] M.J. Eisenmenger, J.I. Reyes-De-Corcuera, High pressure enhancement of enzymes: a review, Enzyme Microb. Technol. 45(5) (2009) 331-347.

[34] H. Vila-Real, A.J. Alfaia, R.S. Phillips, A.R. Calado, M.H.L. Ribeiro, Pressure-enhanced activity and stability of α-l-rhamnosidase and β-d-glucosidase activities expressed by naringinase, J. Mol. Catal. B: Enzym. 65(1) (2010) 102-109.

[35] V.V. Mozhaev, R. Lange, E.V. Kudryashova, C. Balny, Application of high hydrostatic pressure for increasing activity and stability of enzymes, Biotechnol. Bioeng. 52(2) (1996) 320-331.

[36] A. Hédoux, Y. Guinet, L. Paccou, Analysis of the mechanism of lysozyme pressure denaturation from Raman spectroscopy investigations, and comparison with thermal denaturation, J. Phys. Chem. B 115(20) (2011) 6740-6748.

[37] Y. Li, M. Miao, M. Liu, X. Chen, B. Jiang, B. Feng, Enhancing the thermal stability of inulin fructotransferase with high hydrostatic pressure, Int. J. Biol. Macromol. 74 (2015) 171-178.

[38] B.B. Boonyaratanakornkit, C.B. Park, D.S. Clark, Pressure effects on intra- and intermolecular interactions within proteins, Biochim. Biophys. Acta 1595(1) (2002) 235-249.

[39] M.D. Collins, M.L. Quillin, G. Hummer, B.W. Matthews, S.M. Gruner, Structural Rigidity of a Large Cavity-containing Protein Revealed by High-pressure Crystallography, J. Mol. Biol. 367(3) (2007) 752-763.

[40] A. Halalipour, M.R. Duff Jr, E.E. Howell, J.I. Reyes-De-Corcuera, Glucose oxidase stabilization against thermal inactivation using high hydrostatic pressure and hydrophobic modification, Biotechnol. Bioeng. 114(3) (2017) 516-525.

[41] M.I. Buchholz-Afari, A. Halalipour, D. Yang, J.I. Reyes-De-Corcuera, Increased stability of alcohol oxidase under high hydrostatic pressure, J. Food Eng. 246 (2019) 95-101.

[42] A. Halalipour, M.R. Duff Jr, E.E. Howell, J.I. Reyes-De-Corcuera, Effects of high hydrostatic pressure or hydrophobic modification on thermal stability of xanthine oxidase, Enzyme Microb. Technol. 103 (2017) 18-24.

[43] L.S. Wallace, The effect of high hydrostatic pressure on stability of pyruvate oxidase from *aeroccocus species*, University of Georgia Theses and Dissertations (2017) 19-50.

[44] D. Yang, H.E. Olstad, J.I. Reyes-De-Corcuera, Increased thermal stability of a glucose oxidase biosensor under high hydrostatic pressure, Enzyme Microb. Technol. 134 (2020) 109486.

[45] B.-C. Lai, J.-G. Wu, S.-C. Luo, Revisiting Background Signals and the Electrochemical Windows of Au, Pt, and GC Electrodes in Biological Buffers, ACS Appl. Energy Mater. 2(9) (2019) 6808-6816.

[46] Y. Li, T. Li, M. Yao, S. Liu, Metal-free nitrogen-doped hollow carbon spheres synthesized by thermal treatment of poly (o-phenylenediamine) for oxygen reduction reaction in direct methanol fuel cell applications, J. Mater. Chem. 22(21) (2012) 10911-10917.

[47] J. Dumont, G. Fortier, Behavior of glucose oxidase immobilized in various electropolymerized thin films, Biotechnol. Bioeng. 49(5) (1996) 544-552.

[48] J.M. Cregg, K.R. Madden, K.J. Barringer, G.P. Thill, C.A. Stillman, Functional characterization of the two alcohol oxidase genes from the yeast *Pichia pastoris*, Mol. Cell. Biol. 9(3) (1989) 1316.

[49] A. Nezamzadeh-Ejhieh, Z. Salimi, Heterogeneous photodegradation catalysis of o-phenylenediamine using CuO/X zeolite, Appl. Catal. A: Gen. 390(1) (2010) 110-118.

[50] C. Koch, P. Neumann, O. Valerius, I. Feussner, R. Ficner, Crystal structure of alcohol oxidase from *Pichia pastoris*, PLoS One 11(2) (2016).

[51] H.J. Hecht, H.M. Kalisz, J. Hendle, R.D. Schmid, D. Schomburg, Crystal Structure of Glucose Oxidase from *Aspergillus niger* Refined at 2·3 Å Reslution, J. Mol. Biol. 229(1) (1993) 153-172.

[52] S. Soylemez, S. Goker, L. Toppare, A promising enzyme anchoring probe for selective ethanol sensing in beverages, Int. J. Biol. Macromol. 133 (2019) 1228-1235.

[53] H. Yu, X. Luo, W. Shi, P. Sha, A. Volmer, W. Xiao, Y. Cui, A cork-based smart biosensing system for ethanol, IEEE Sens. J. 19(6) (2018) 2313-2319.

Table 4.1. Sensitivity and pseudo-first-order rate constant of response loss (k) of the L+R fractions AOx biosensors immobilized at pressures from 0.1 to 240 MPa. The biosensors were inactivated at 50 °C and 0.1 MPa for an accumulated time of 1, 2, 4, 6, 8, and 10 min. The values are reported as mean ± 95% confidence interval ($n \geq 2$).

Pressure (MPa)	Sensitivity before heating (nA mm^{-2} mM^{-1}) × 10^2	k (min^{-1})	R^2 for k
0.1	9.1 ± 5.4	0.14 ± 0.05	0.94
60	5.4 ± 6.6	0.18 ± 0.06	0.93
180	5.1 ± 6.6	0.12 ± 0.06	0.94
240	2.4 ± 6.6	0.10 ± 0.06	0.94

No significant differences ($p > 0.05$) were found in means of sensitivity or k.

Table 4.2. Sensitivity and pseudo-first-order rate constant of response loss (k) of the L+R fractions or the R fraction AOx biosensors immobilized at 0.1 or 160 MPa. The biosensors were inactivated at 50 °C and 0.1 MPa for an accumulated time of 1, 2, 4, 6, 8, and 10 min. The values are reported as mean ± 95% confidence interval (n = 2).

Pressure (MPa)	Enzyme fraction	Sensitivity before heating (nA mm^{-2} mM^{-1}) × 10^2	k (min^{-1})	R^2 for k
0.1	L+R	8.3 ± 2.2	0.20 ± 0.07	0.92
0.1	R	6.7 ± 2.2	0.17 ± 0.07	0.91
160	L+R	6.4 ± 2.2	0.14 ± 0.07	0.83
160	R	6.2 ± 2.2	0.09 ± 0.07	0.81

No significant differences ($p > 0.05$) were found in means of sensitivity or k between enzyme fractions or pressures.

Table 4.3. Sensitivity and pseudo-first-order rate constant of response loss (k) of the L+R fraction AOx immobilized at pH 7.0 and 0.1 MPa, and the L+R fractions or the R fraction AOx immobilized at pH 5.2 and 0.1 MPa. The biosensors were inactivated at 50 °C and 0.1 or 160 MPa in the high pressure reactor for an accumulated time of 1, 2, 4, 6, 8, and 10 min. The values are reported as mean ± 95% confidence interval (n = 4).

Inactivation pressure (MPa)	Enzyme fraction	Immobilization pH	Sensitivity before heating (nA mm^{-2} mM^{-1}) × 10^2	k (min^{-1})	R^2 for k
0.1	L+R	7.0	11.3 ± 2.5*	0.15 ± 0.04	0.98
160	L+R	7.0		0.10 ± 0.04	0.95
0.1	L+R	5.2	2.5 ± 1.3**	0.12 ± 0.06	0.86
160	L+R	5.2		0.13 ± 0.06	0.82
0.1	R	5.2	4.2 ± 1.3**	0.17 ± 0.06	0.83
160	R	5.2		0.15 ± 0.06	0.84

No significant differences ($p > 0.05$) were found in means of k between pressures, between enzyme fractions, or between immobilization pH.

No significant differences ($p > 0.05$) were found in means of sensitivity when immobilized at pH 5.2.

* Sensitivity tested right after immobilization.

** Sensitivity tested after storing at 4 °C overnight after immobilization.

Table 4.4. Sensitivity on day 1 and day 15 of the storage, and pseudo-first-order rate constant of response loss (k) of the L+R fractions or the R fraction AOx biosensors immobilized at 0.1 or 240 MPa. The biosensors were stored at room temperature (23 ± 1 °C) and 0.1 MPa for 15 days. The amperometric response of each biosensor was measured every day. The values are reported as mean ± 95% confidence interval (n = 3).

Pressure (MPa)	Enzyme fraction	Sensitivity (nA mm^{-2} mM^{-1}) × 10^2 on day 1	Sensitivity (nA mm^{-2} mM^{-1}) × 10^2 on day 15	k (h^{-1}) × 10^3	R^2 for k
0.1	L+R	11.9 ± 4.2	1.0 ± 1.4	7.3 ± 1.8	0.92
0.1	R	5.8 ± 4.2	0.8 ± 1.4	6.0 ± 1.8	0.85
240	L+R	5.4 ± 4.2	1.5 ± 1.4	5.0 ± 1.8	0.75
240	R	10.2 ± 4.2	2.1 ± 1.4	5.4 ± 1.8	0.93

No significant differences ($p > 0.05$) were found in means of sensitivities on day 1 and day 15 between pressures or between enzyme fractions.

No significant differences ($p > 0.05$) were found in means of k between pressures or between enzyme fractions.

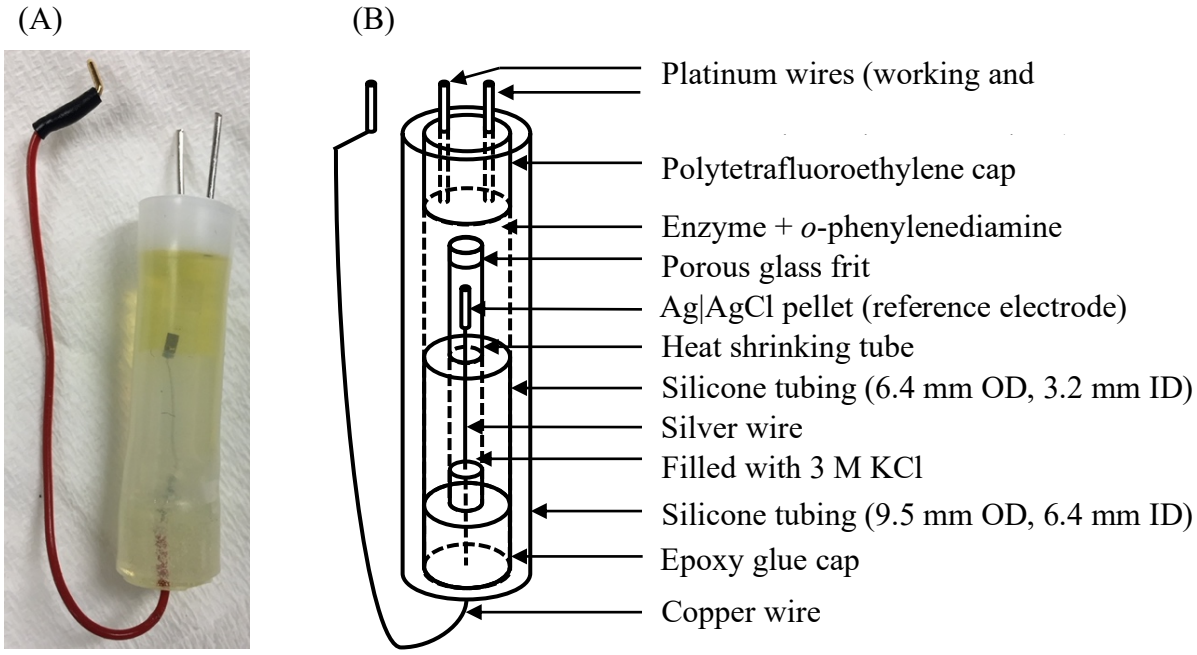

Fig. 4.1. The picture (A) and the schematic diagram (B) of the electrochemical cell designed for high pressure reactor.

Supplemental materials

Table S4.1. Relative current density to the 0.1 M phosphate buffer (pH 7.5) at heating time 10 min. All the AOx biosensors were heated at 50 °C for up to 10 min at 0.1 MPa or 160 MPa. The L+R fractions or the R fraction AOx were immobilized at pH 5.2 or pH 7.0 at ambient pressure. The values are reported as mean ± one standard deviation (n = 4).

Enzyme fraction	Immobilization pH	Inactivation pressure (MPa)	Relative current density at 10 min
L+R	7.0	0.1	61.8 ± 8.9
L+R	7.0	160	54.4 ± 6.2
L+R	5.2	0.1	64.6 ± 11.7
L+R	5.2	160	62.4 ± 13.3
R	5.2	0.1	56.7 ± 7.1
R	5.2	160	68.1 ± 7.9

No significant differences ($p < 0.05$) were found in means of relative current density at 10 min across different treatments.

Table S4.2. The means of coefficient of determination (R^2) for fitting data to zero, first, and second order models describing the relationship of the relative current density and treatment time.

Enzyme fraction	Immobilization pressure (MPa)	Immobilization pH	Inactivation pressure (MPa)	Inactivation temperature (°C)	R^2		
					Zero	First	Second
L+R	0.1	7.0	0.1	50	0.86	0.94	0.96
L+R	80	7.0	0.1	50	0.92	0.93	0.95
L+R	160	7.0	0.1	50	0.91	0.94	0.98
L+R	240	7.0	0.1	50	0.95	0.94	0.94
R	0.1	7.0	0.1	50	0.71	0.91	0.96
R	160	7.0	0.1	50	0.67	0.81	0.95
L+R	0.1	7.0	0.1	23	0.78	0.92	0.83
L+R	240	7.0	0.1	23	0.67	0.75	0.86
R	0.1	7.0	0.1	23	0.69	0.85	0.89
R	240	7.0	0.1	23	0.85	0.96	0.85
L+R	0.1	7.0	160	50	0.92	0.95	0.96
L+R	0.1	5.2	0.1	50	0.75	0.86	0.92
L+R	0.1	5.2	160	50	0.66	0.82	0.92
R	0.1	5.2	0.1	50	0.63	0.83	0.93
R	0.1	5.2	160	50	0.70	0.84	0.92

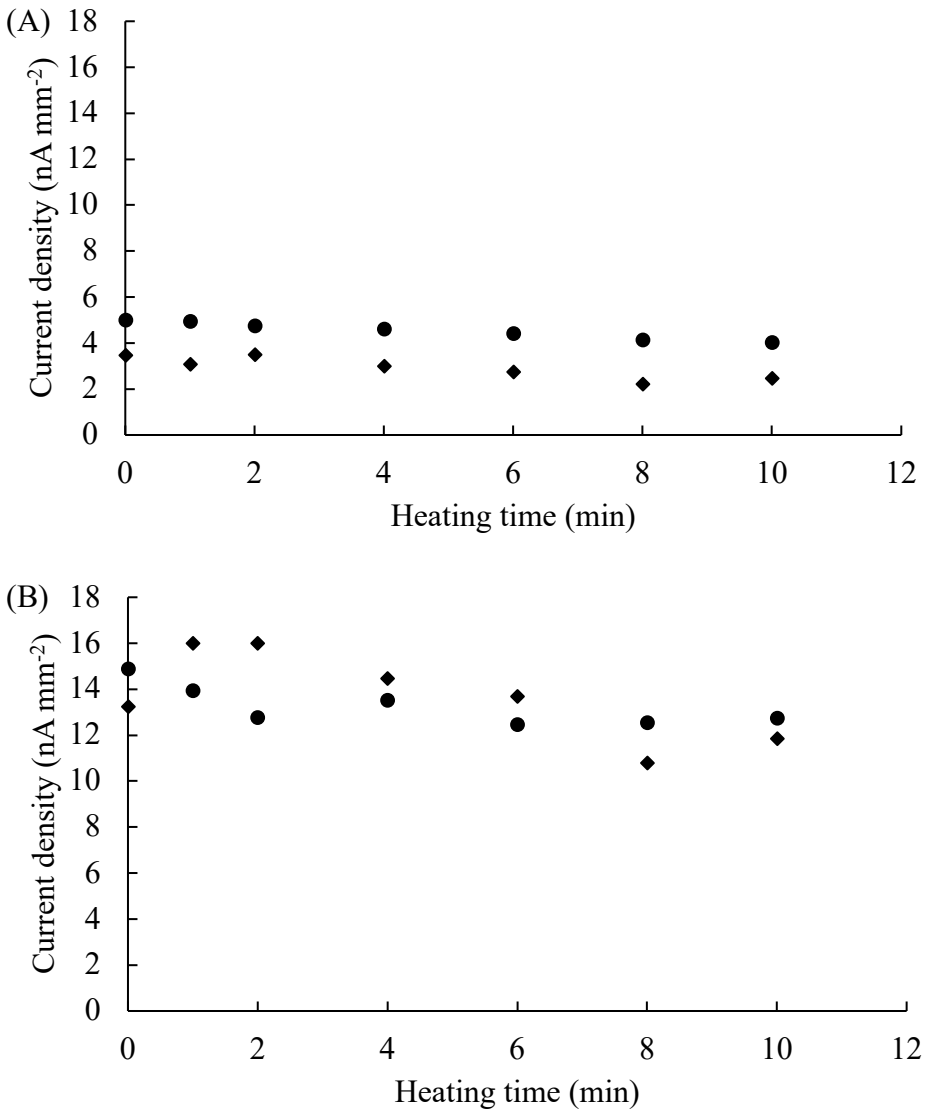

Fig. S4.1. Current density responses of two electrodes electropolymerized with oPD at atmospheric pressure without enzymes to the 0.1 M phosphate buffer (pH 7.5) (A) or H_2O_2 solution (B), after heating at 50 °C in 0.1 M phosphate buffer (pH 7.5) in a water bath for up to 10 min. ◆ and ● represent the two different electrodes.

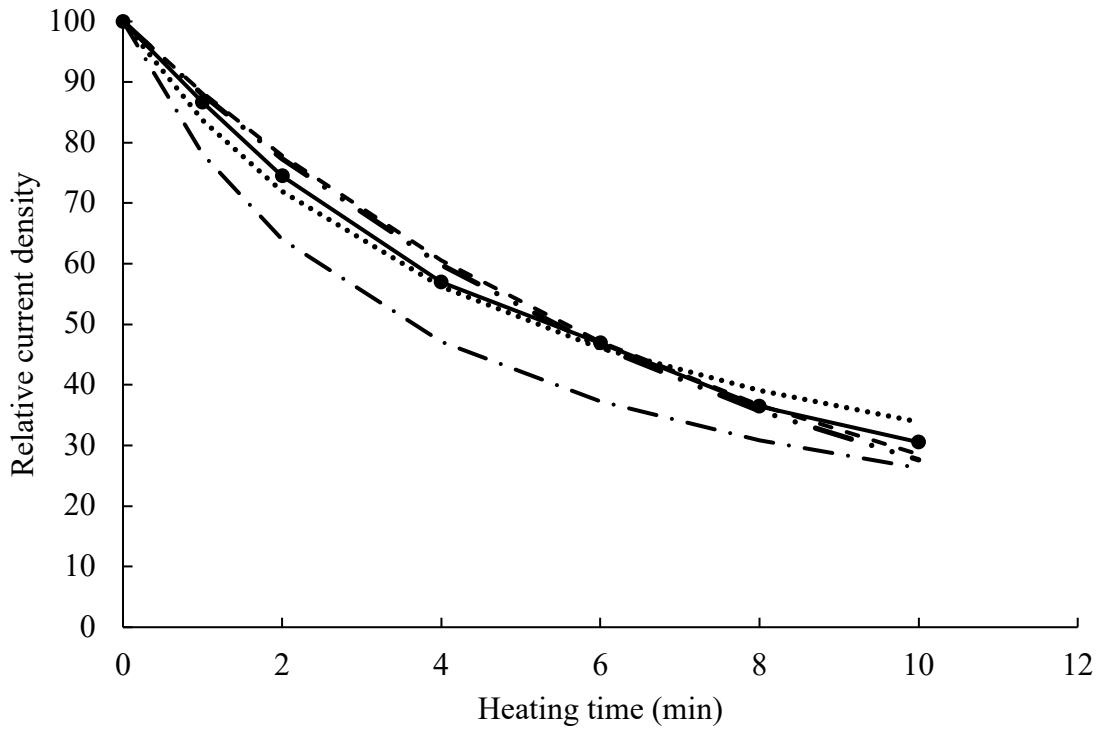

Fig. S4.2. The relative current density change over treatment time of the original data (●), prediction from the linearized pseudo-first-order model (- - -), prediction from the linearized pseudo-second-order model (- • -), prediction from the non-linearized pseudo-first-order model (- • • -), and prediction from the non-linearized pseudo-second-order model (• • •). The AOx was immobilized in PoPD at pH 7.0 and was inactivated at 50 °C and 0.1 MPa.

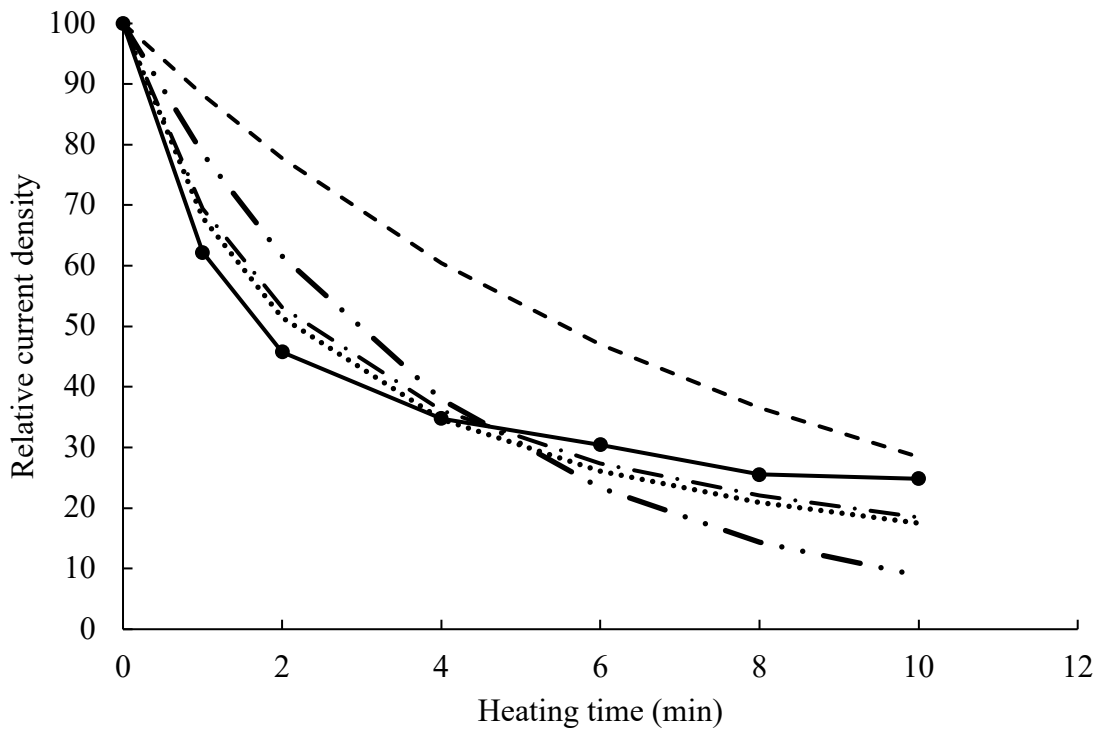

Fig. S4.3. The relative current density change over treatment time of the original data (●), prediction from the linearized pseudo-first-order model (- - -), prediction from the linearized pseudo-second-order model (- • -), prediction from the non-linearized pseudo-first-order model (- • • -), and prediction from the non-linearized pseudo-second-order model (• • •). The AOx was immobilized in PoPD at pH 5.2 and was inactivated at 50 °C and 0.1 MPa.

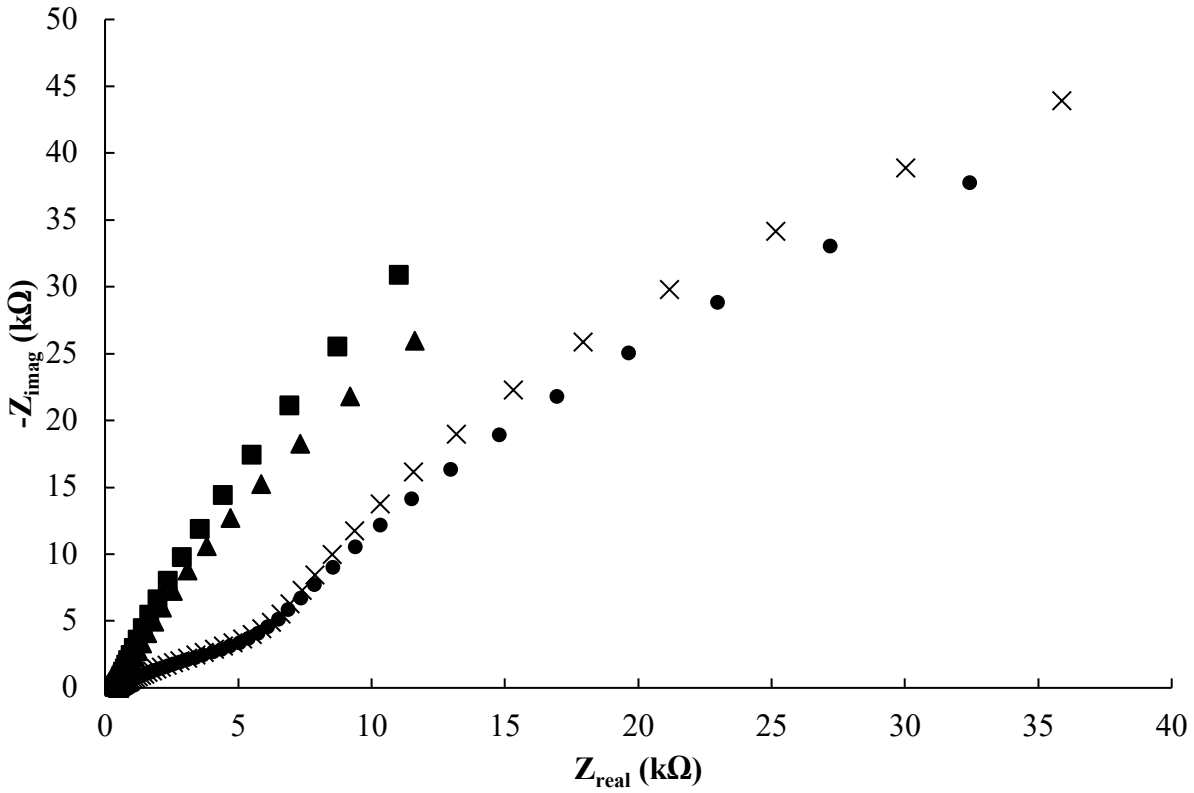

Fig. S4.4. Examples of the Nyquist plots of the EIS results. The EIS was performed on the electrode before (■) and after (●) the immobilization at 0.1 MPa and the electrode before (▲) and after (×) the immobilization at 160 MPa.

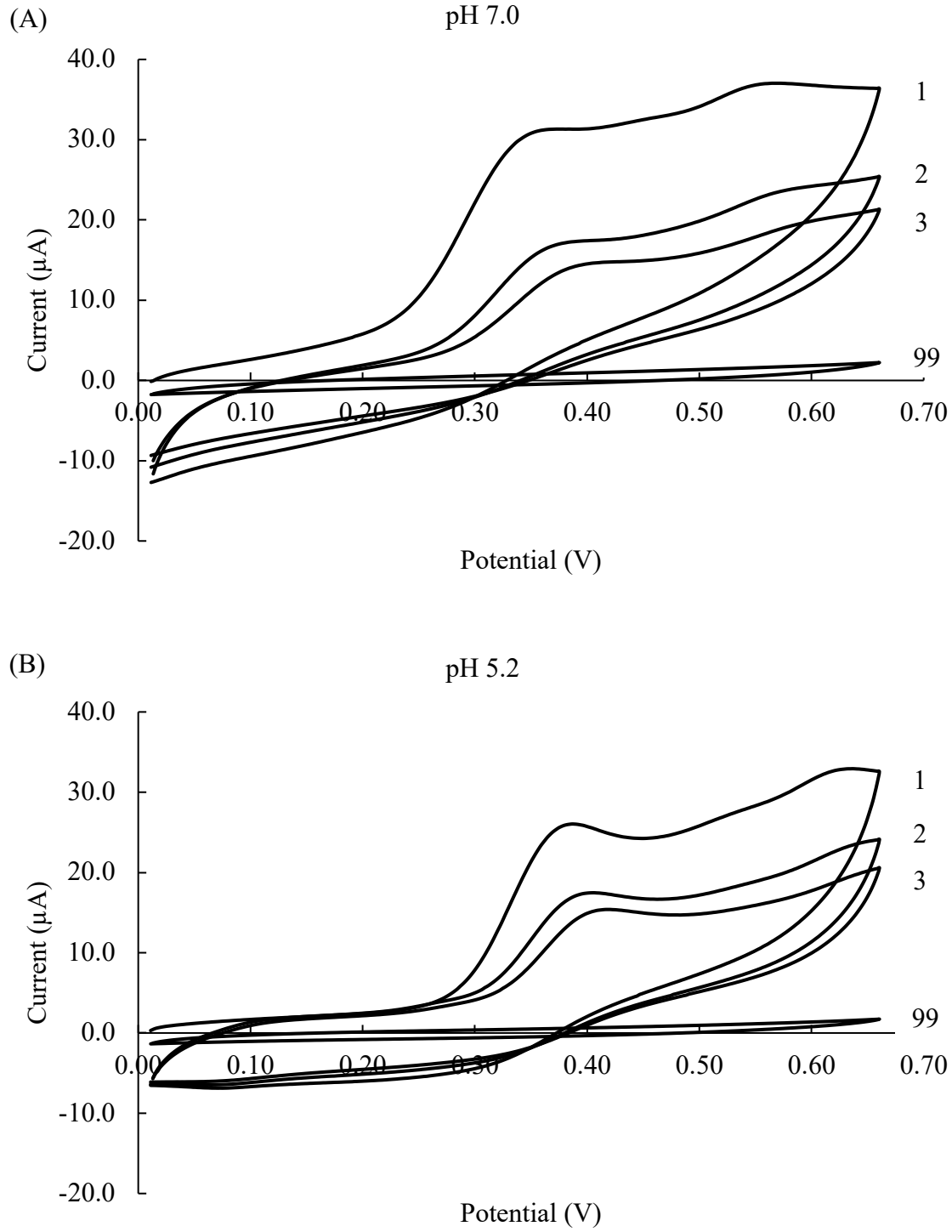

Fig. S4.5. Examples of the cyclic voltammetry plots of the electropolymerization at pH 7.0 (A) or at pH 5.2 (B). The cyclic voltammetry was performed at 100 mV s^{-1} from 0 to 0.65 V *vs.* Ag|AgCl in 3.0 M KCl for 100 cycles. The first three cycles and the cycle 99 were chosen.

CHAPTER 5

SUMMARY AND SUGGESTED FUTURE STUDIES

Our research team is interested in the effects of high hydrostatic pressure (HHP) on a series of oxidases, such as glucose oxidase (GOx), alcohol oxidase (AOx), pyruvate oxidase, galactose oxidase, and xanthine oxidase. We have previously reported the stabilizing effect of HHP on the GOx and AOx in solution, and the increased activity of GOx in solution at HHP (Halalipour et al. 2017; Buchholz-Afari et al. 2019; Halalipour et al. 2020). In this report, the effect of HHP on the immobilized GOx or AOx was studied. The activity of the AOx in solution at HHP was also determined. Therefore, the effects of HHP have been studied on the activity of both the GOx and AOx in solution, on the stability of the two enzymes in solution, and on the stability of the two immobilized enzymes. The native, aniline-modified, or benzoate-modified GOx increased its catalytic activity with HHP at temperatures from 25 to 69.1 °C, and reached the maximum activity at around 180 MPa; the aniline-modified GOx had the reaction rate 11.3 times at 69.1 °C and 180 MPa relative to the rate at 25 °C and 0.1 MPa (Halalipour et al. 2020). The activity of the AOx also increased at HHP and at higher temperatures compared to at 0.1 MPa and 25 °C (Chapter 3). Alcohol oxidase from *P. pastoris* has two enzyme fractions, the labile (L) fraction and the resistant (R) fraction. The R fraction is of more interest because it is ~150 times more stable than the L fraction. The reaction rate of the R fraction AOx at 50 °C was 17.9 ± 3.6 or 17.7 ± 0.8 μM min^{-1} at 80 or 160 MPa, respectively. It was approximately 6 times relative to the reaction rate, 3.2 ± 0.2 μM min^{-1}, at 25 °C and at atmospheric pressure. However, different from GOx whose activity increase was due to both the stabilizing effect and activating effect of HHP, the activity increase

of the R fraction AOx at HHP was only attributed to the stabilization of HHP against thermal inactivation. As for the stability of the two enzymes in solution, the thermostability of GOx was increased at most 50 times when the GOx was inactivated at 240 MPa and 74.5 °C compared to the enzymes inactivated at atmospheric pressure at the same temperature (Halalipour et al. 2017); the thermostability of the L fraction AOx was increased up to 14 times when inactivating the AOx in solution at 160 MPa and 49.4 °C compared to the ones inactivated at ambient pressure at the same temperature (Buchholz-Afari et al. 2019). Immobilization alone increased the stability of GOx. Immobilization of GOx in electrochemically generated poly-*o*-phenylenediamine (PoPD) nano-films increased the thermostability by up to 20.6 times at 70 °C and atmospheric pressure relative to the GOx in solution under the same conditions (Chapter 2). The thermostability of the immobilized GOx was further increased at HHP. Immobilized GOx inactivated at 70 °C and 180 MPa was 87.6 times more stable than GOx in solution inactivated at 70 °C and atmospheric pressure. The stability increase of the immobilized GOx at HHP was higher than the sum of the stabilizing effect of HHP on GOx in solution and the stabilizing effect of immobilization, suggesting a synergistic stabilizing effect of HHP and immobilization against thermal inactivation. However, applying HHP during immobilization had no effect on the stability of GOx biosensors, indicating the stabilization effect of HHP could not be retained by immobilization after depressurization. Immobilization through electropolymerization also increased the thermal stability of the L+R fractions AOx (Chapter 4). However, the pseudo-first-order rate constant of response loss of the AOx biosensor was approximately 44 times higher than the pseudo-first-order rate constant of inactivation of the R fraction AOx in solution, suggesting the decrease in the effective amperometric response was caused by enzyme leaching out of the immobilization matrix. Indeed, the dimension of the AOx was similar to the thickness of the PoPD film. Therefore, the

exact stabilizing effect of immobilization on the two enzyme fractions was not able to be determined. The effect of HHP on the stability of the AOx biosensors in terms of the stability of AOx could not be determined, either. The pseudo-first-order rate constant of response loss of the AOx biosensors induced by enzyme leaching was big enough to make any possible stabilizing effect of HHP on the enzymes negligible. The lower pH 5.2 instead of pH 7.0 used during electropolymerization did not reduce or stop the enzyme leaching. A pH lower than 5.2 was able to form a more compact PoPD film, but it would worsen the denaturation of the AOx during immobilization. Therefore, electrochemically generated PoPD is not an adequate immobilization material for AOx. A different immobilization method is needed to study the effect of HHP on the stability of the immobilized AOx.

The findings in this report contributed to our understanding of the effects of HHP on the activity and the stability of GOx or AOx, and on the stability of GOx or AOx biosensors. However, they brought up more questions. Below are some suggested future studies. 1). The first suggested study is to modify the current immobilization method to get a thicker PoPD film or find another immobilization method to assess the effect of HHP on the AOx biosensor. If a new immobilization method is used, another entrapment method is preferred because there is no chemical interaction to the enzymes and the enzyme activity remains unchanged. 2). From Chapter 2 it was concluded that the stabilizing effect of HHP cannot be retained after depressurization by immobilization in PoPD at HHP. However, it is still unknown whether the PoPD film formed at HHP is the same as the one formed at 0.1 MPa. Moreover, whether using pH 5.2 during immobilization results in a more compact PoPD film than using pH 7.0 needs to be verified. Therefore, it is worth studying the structure of the PoPD film using the electrospray ionization-tandem mass spectrometry or X-ray photoelectron spectroscopy. 3). The activity of both GOx and AOx increased at HHP.

However, for GOx it was the combined effect of HHP stabilization and activation. For AOx, it was only the stabilization effect of HHP against thermal inactivation. The difference may be attributed to the different conformation of the two enzymes at HHP. Therefore, it is worth studying a) the changes of the flexibility and hydrophobicity of the amino acid around the active sides at HHP; b) the effects of altering the interdomain interactions at HHP to the enzyme activity; c) the accessibility of the active sides at HHP for the two enzymes using the methods such as high pressure NMR spectroscopy or high pressure X-ray crystallography. 4). The mechanism of enzyme stabilization by HHP remains unclear. a) The non-rigid cavities in the proteins can be compressed at HHP and contribute to the increased stability before reaching to the pressure where water is penetrated inside the cavity resulting in protein unfolding. It is worth studying the changes of the cavities of different oxidases as gradually applying HHP till reaching the point of denaturation. The number, surface area, or volume of the cavities in different enzymes needs to be considered its possible correlation to the optimal pressure for stabilization. b) It is also worth studying the possible relationship between the number of subunits (interdomain interactions) or the size of proteins to the stabilizing effect of HHP. 5). Even though the immobilization cannot retain the stabilizing effect of HHP on GOx, it is worth studying whether the GOx goes back to its original conformation or into a different conformation but having the same stability. Therefore, the comparison of the conformation of GOx before and after immobilization at HHP by NMR spectroscopy or X-ray crystallography needs to be studied. 6). Our research team is interested in a series of oxidases and have studied the stabilizing effect of HHP on the soluble enzymes. Just like GOx and AOx, it is worth studying the activity of pyruvate oxidase, galactose oxidase, and xanthine oxidases at HHP and also the effect of HHP on the stability of the enzyme biosensors.

References

Buchholz-Afari MI, Halalipour A, Yang D, Reyes-De-Corcuera JI. 2019. Increased stability of alcohol oxidase under high hydrostatic pressure. Journal of food engineering. 246:95-101.

Halalipour A, Duff Jr MR, Howell EE, Reyes-De-Corcuera JI. 2020. Catalytic activity and stabilization of phenyl-modified glucose oxidase at high hydrostatic pressure. Enzyme and Microbial Technology.109538.

Halalipour A, Duff Jr MR, Howell EE, Reyes-De-Corcuera JI. 2017. Glucose oxidase stabilization against thermal inactivation using high hydrostatic pressure and hydrophobic modification. Biotechnology and Bioengineering. 114(3):516-525.